SAPIENZA
UNIVERSITÀ DI ROMA

Harnessing Electrobioremediation for Sustainable Groundwater Decontamination: Mechanisms, Applications and Efficacy

Department of Chemical Engineering Materials Environment

PhD Thesis in Chemical Processes for Industry and Environment

(XXXVII Cycle)

Marco Resitano

Matricola 1610136

Tutor

Dr. Federico Aulenta

2024-2025

Contents

Page

Chapter I – Introduction

I.1 Introduction

Groundwater is a vital natural resource, constituting approximately 30% of the world's freshwater supply. In many arid regions, groundwater serves as the sole source of water, underpinning agriculture, industry, and domestic water needs. As urbanization intensifies and agricultural practices expand, the vulnerability of groundwater to contamination has become increasingly evident. Contaminants, ranging from agricultural nitrates to industrial solvents, percolate through soil and aquifers, reaching depths that challenge natural remediation processes. Addressing this contamination is crucial not only for water security but also for public health and ecological sustainability (Malik et al., 2023; Mineo, 2023; Ravindiran et al., 2023; Sadia et al., 2023; Xie et al., 2024). The migration of contaminants within groundwater systems depends on a complex interplay of hydrogeological, chemical, and biological factors. Physical processes, such as advection and dispersion, contribute to the transport of pollutants from their source to surrounding areas (You et al., 2020). In addition, chemical reactions, including adsorption and ion exchange, determine the contaminants' fate within the aquifer (Locatelli et al., 2019). Biological degradation, where microorganisms break down contaminants, serves as a natural attenuation process in some cases (Alvarez and Illman, 2005). Understanding these mechanisms is critical to designing effective remediation techniques. In recent years, the contamination of groundwater has far-reaching implications beyond just environmental impacts. Contaminated groundwater, often undetected until it poses acute health risks, affects millions of people globally (Malik et al., 2023). For example, nitrate pollution from agricultural fertilizers can lead to "blue baby syndrome" in infants and other chronic health problems in adults (Majumdar, 2003). Heavy metals and industrial solvents contribute to elevated cancer risks, while microbial contamination leads to widespread infectious diseases (Pradhan et al., 2023; Sinha and Prasad, 2020). Economically, groundwater pollution imposes significant costs related to medical expenses, loss of agricultural productivity, and remediation efforts (Reddy and Behera, 2006). The sources of groundwater contaminants are as varied as they are pervasive. Agricultural activities, while

essential for food production, introduce vast quantities of nutrients (notably nitrogen and phosphorus) into groundwater systems (Fernández-López et al., 2023; Malik et al., 2023). Industrial operations, including waste disposal and mining activities, have contributed numerous synthetic chemicals such as trichloroethylene (TCE) and heavy metals like arsenic and lead (Ravindiran et al., 2023). Recently, attention has also shifted to emerging contaminants such as pharmaceuticals, personal care products, and microplastics, which enter groundwater through wastewater and runoff, and pose uncertain risks to ecosystems and human health (Pradhan et al., 2023). In Europe, the most frequently detected groundwater contaminants are chlorinated hydrocarbons (CHCs), mineral oil, polycyclic aromatic hydrocarbons (PAHs), heavy metals, phenols, cyanides, aromatic hydrocarbons (BTEX: benzene, toluene, ethyl benzene, and xylene). Their relative distribution in is reported in **Figure I-1**.

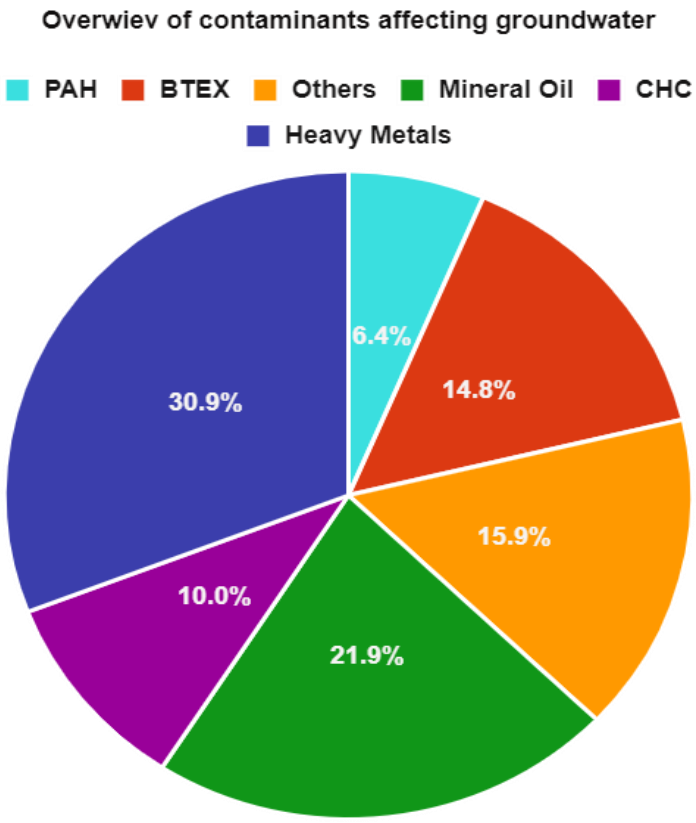

Figure I-1 *The distribution of the contaminants in groundwater* (Panagos et al., 2013)

The persistent threats these contaminants pose to human, animal, and ecosystem health, call for urgent remedies (Motlagh et al., 2020; Pradhan et al., 2023; Sinha and Prasad, 2020). The technologies to remove contaminants from a polluted site can be broadly grouped into two main categories and can be applied individually or in synergy: physicochemical and biological technologies (Alvarez and Illman, 2005). Physicochemical technologies can include physical removal (i.e. excavation of soil and sediment or groundwater pumping), washing by co-solvents or surfactants, thermal desorption, electrokinetic movement of contaminants and oxidation or reduction via chemical agents (Alvarez and Illman, 2005; Yasri and Gunasekaran, 2017). Biological technologies (or Bioremediation) are increasingly being considered since they exploit the vast metabolic diversity of naturally occurring microorganisms to degrade organic contaminants by using the pollutant as a source of energy and carbon (Alvarez and Illman, 2005). Bioremediation relies on the ability of microorganisms to degrade contaminants, or at least to transform them into less harmful compounds. The goal of bioremediation is to stimulate the removal of contaminants by overcoming the limitations to microbial metabolism that would otherwise prevent contaminant removal. The most common approach involves the stimulation of the indigenous microorganisms by acting on the factors that are limiting their metabolism, as for example adding electron acceptors or nutrients (Biostimulation)(Sarkar et al., 2016). Another strategy, that is often applied when the native populations do not have the required metabolic abilities to remove the contaminants, is the addition of selected strains or consortia, to improve the degradation ability of the microbial community (Bioaugmentation)(El Fantroussi and Agathos, 2005). Biological processes are often less expensive compared to physicochemical methods and allows the complete mineralization of the pollutants. However, they frequently require more time to achieve full remediation (Daghio et al., 2017).

Both physical-chemical and biological treatments can be applied *in-situ* or *ex-situ*. The *ex-situ* processes involve the extraction of the contaminated matrix (soil or groundwater) and the treatment in aboveground facilities and plants, while the *in-situ* treatments involve the treatment directly into the site, targeting either the

contaminant plume or the contamination source without extraction. *In-situ* treatments offer potential advantages such as lower operating costs (due to the lower request for energy), lower environmental impact, and the absence (or minimization) of effluents to be treated and discharged. Moreover, they usually allow achieving an effective degradation of contaminants rather than a simple phase transfer (Majone et al., 2015). *In-situ* microbially-mediated reactions have been successfully used for the reduction and/or oxidation of petroleum derived contaminants (Alvarez and Illman, 2005). Despite their promise, a major challenge of bioremediation processes, is their requirements for a thorough site-specific, chemical, geochemical, hydrogeological, and microbiological characterization (that is often more detailed and expensive than for a physicochemical treatment), in order to assess the actual viability of the approach and apply the best available technological options (Tyagi et al., 2011).

In this context, it is relevant to define if the process is aerobic (oxygen as terminal electron acceptor) or anaerobic (nitrate, sulphate or iron as terminal electron acceptor). One of the factors that mostly influence the biodegradation of organic compounds is the availability of terminal electron acceptors; for this reason, a common approach is to supply electron acceptors to stimulate the degradation of organic compounds (Alvarez and Illman, 2005). Aerobic metabolism is stimulated by adding oxygen to the contaminated matrix (e.g. by air sparging)(Farhadian et al., 2008), which has the benefit of faster rates of hydrocarbon removal compared to anaerobic bioremediation strategies (Weelink et al., 2010). Furthermore, even though the oxidation of hydrocarbons can occur in anaerobic environments (Weelink et al., 2010), oxygen is an important reactant for hydrocarbon breakdown (Baldwin et al., 2009). The oxygen addition strategy suffers of a number of limitations such as: (I) the high energy consumption associated with aeration, (II) the low efficiency of oxygen utilization due to the rapid consumption by reduced mineral substances such as Fe(II) and HS^-, usually abundant in contaminated matrices (Tuxen et al., 2006)(III) the undesired stripping of volatile contaminants, and (IV) the high growth yield of aerobic microorganisms which may cause clogging problems near air/oxygen injection points.

Anaerobic microbial metabolism can be effectively enhanced by adding sulphate or nitrate (Coates et al., 1996; Vaiopoulou et al., 2005). Moreover, the addition of chelators, which solubilize Fe^{3+}, or the addition of soluble electron shuttles (e.g. humic substances) can promote anaerobic metabolisms (Clark et al., 2012; Lovley, 2008; Lovley and Woodward, 1996). The main drawback of the strategies mentioned above is that the supplemented reagents can be rapidly consumed and migrate naturally away from the contaminated area. Continuous amendment with the depleted reagents or electron acceptors is therefore required, and this increases the cost of the remediation (Zhang et al., 2010). In *in-situ* bioremediation, anaerobic biodegradation plays a more important role than the aerobic counterpart, in fact anaerobic processes are sometimes the only possible solution to remove pollutants (Holliger et al., 1997) as it is often difficult to inject oxygen into the contaminated matrix. Recently, Microbial Electrochemical Technologies (METs) have been suggested as an alternative strategy to overcome some of the limitations of the current bioremediation technologies of soil and water (H. Wang et al., 2015).

I.2 Microbial electrochemical technologies (METs)

Microbial Electrochemical Technologies are systems in which microorganisms catalyze oxidation or reduction reactions using solid-state electrodes, suitably deployed in the contaminated matrix, as virtually inexhaustible electron acceptors or donors, respectively (Zhang et al., 2013, 2010). Specific bacteria, often referred to as exoelectrogens, have the ability to transfer electrons outside the cell to insoluble electron acceptors (Logan and Rabaey, 2012). Electrons can be transferred to the anode by electron mediators or shuttles (Rabaey et al., 2005, 2004), by direct membrane associated electron transfer (Bond and Lovley, 2003), or by so-called nanowires (Lovley, 2011, 2008) produced by the bacteria. The two main archetypes of METs are the Microbial Fuel Cells (MFCs) and the Microbial Electrolysis Cells (MECs). MFCs can be used to generate power; in these systems the electrons produced during the oxidation of the organic matter (or other reduced chemical species) are employed to generate electric current (

Logan et al., 2006). In the cathodic compartment of a MFC, an electrochemical reduction reaction takes place (e.g. oxygen reduction).

By contrast, MECs function with addition of external power to drive the desired, otherwise energetically unfavourable, reaction (Rozendal et al., 2006). A microbial anode in combination with a biological or chemical cathode can be implemented to achieve H_2 production.

This kind of system requires about 3 times less potential difference compared to a conventional chemical electrolysis cell, in which the reactions at the electrodes are not mediated by microorganisms (Rozendal et al., 2006). When operating a MEC, there are two electrical control strategies: (I) operation at a fixed potential (Rozendal et al., 2006) or (II) operation at a fixed current (Andersen et al., 2013). Operation at a fixed potential has the advantage that a desired reaction can be driven, or favourable conditions for a certain (bio)catalyst can be created.

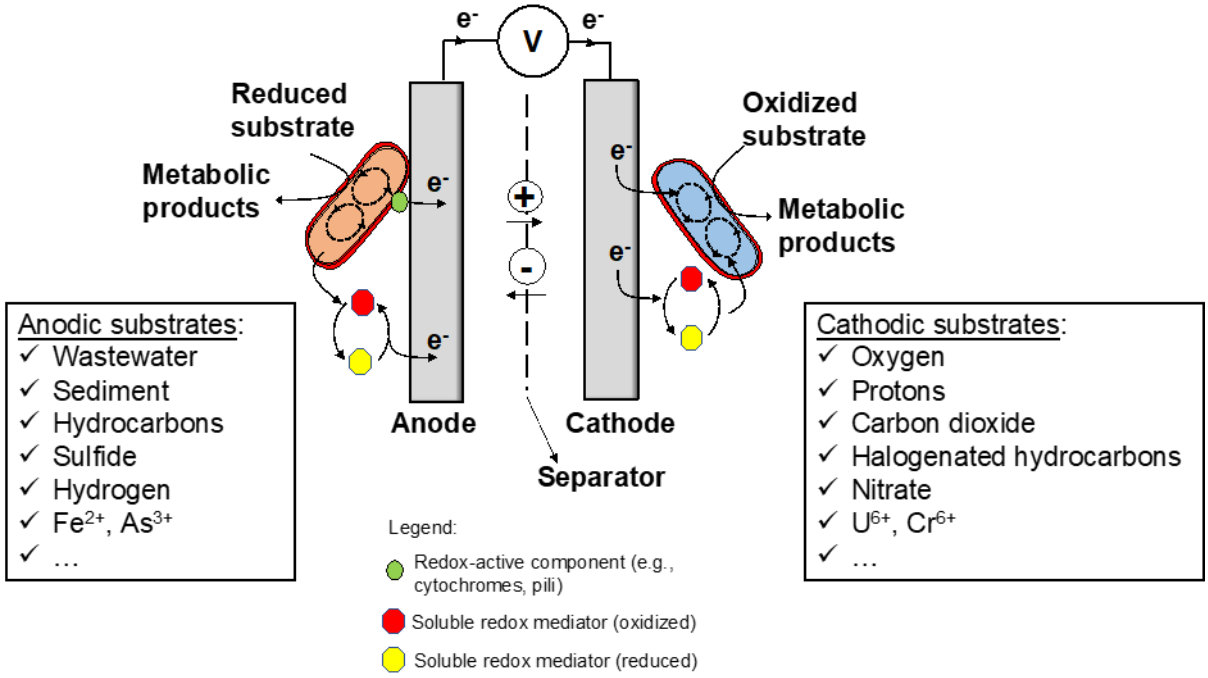

Figure I-2 *Schematic overview of microbially-catalyzed reactions taking place at the anode and at the cathode of a microbial electrochemical systems.*

I.3 Bioremediation applications of METs

Approximately twenty years ago, research on microbial extracellular electron transfer started to gain significant traction (Bond and Lovley, 2003; Rabaey et al.,

2009). The initial breakthrough technology was the microbial fuel cell, generating power from organic waste or sediments (Logan, 2009; Logan et al., 2006). However, it soon became apparent that the influence of microbial electrochemical technologies (METs) extends far beyond this, impacting numerous other domains of industrial and environmental biotechnology for example allowing processes such as groundwater bioremediation to be driven by solid-state electron donors and acceptors in a highly flexible and controllable manner (Aulenta et al., 2010; Daghio et al., 2017; Feng et al., 2023; Leitão et al., 2015; Wang et al., 2020). Unlike conventional bioremediation approaches that only provide one redox condition, METs can provide simultaneously reducing (at the cathode) and oxidizing (at the anode) conditions. This process can even be integrated within a single treatment sequence, thus enabling the complete degradation (and detoxification) of contaminants with specific characteristics as well as complex mixtures thereof (Cruz Viggi et al., 2022; Resitano et al., 2024; Tucci et al., 2023). The most noticeable feature of METs for in situ bioremediation is that the electrodes can be deployed within the contaminated matrix (i.e., soil, sediment, or groundwater). The electrodes can therein serve as virtually inexhaustible electron acceptors or donors for contaminants degradation (or removal via precipitation as in the case of metals), thus eliminating the need for the external, continual injection of chemical amendments. Another key feature of MET is that the “energy level” of the electron donor/acceptor can be set to the desired value with an external potentiostat (to control individual electrode’s potential in a three electrode configuration) or a power source (to control the potential difference between the anode and cathode in a two electrode configuration), hence providing a unique tool for increasing, manipulating, and/or fine-tuning the rate and/or the selectivity of the target reaction(s) (Daghio et al., 2017; Wang et al., 2020). Furthermore, it is worth noting that since the electrode(s) may also serve as a support for microbial growth, METs facilitate the co-localization of the electron donor/acceptor and the degrading microorganisms. Since many organic contaminants (e.g., petroleum hydrocarbons, emerging organic pollutants like pharmaceuticals) can be adsorbed on the surface of carbon-based electrodes,

they tend to concentrate in a highly reactive zone where also the biocatalysts occur, and the electron donor/acceptor are simultaneously present. Over the past few years, electrobioremediation has attracted considerable interest in the scientific community and several lab-scale studies have been published which have provided robust indications that MET can be employed for enhancing the biodegradation of a wide range of organic and inorganic soil and groundwater pollutants (Li and Yu, 2015; Saxena et al., 2020; Wang et al., 2020).

I.4 Cathodic electrobioremediation

The possibility of using (bio)cathodes in MET represents a promising and sustainable approach for groundwater remediation, as microbial processes occurring at the cathode (biocathode) can be exploited to facilitate the removal of several, ubiquitous pollutants, including organic contaminants (e.g., chlorinated solvents), heavy metals, and nitrates, alone or in combination (Ucar et al., 2017). As for chlorinated organic compounds, their conversion into less chlorinated intermediates through reductive dechlorination (RD), carried out by organohalide-respiring bacteria (OHRB), is often limited by the slow metabolism of OHRB and the lack of sufficient external electron donors in groundwater (Aulenta et al., 2006). In a recent study (Chen et al., 2023), direct electron transfer (DET) between *Axonexus* and *Desulfovibrio*/cathode and indirect electron transfer (IET) via riboflavin for *Dehalococcoides* were shown to significantly enhance trichloroethene (TCE) dechlorination in MET biocathodes. A previous study (Chen et al., 2019) reported TCE sequential hydrogenolysis, with its main conversion into less harmful cis-1,2-dichloroethene, and ethene as a minor product, in a 2-chamber bioelectrochemical reactor. Bio-cathodic TCE dechlorination to ethene in paddy soil was enhanced when a pure *D. mccartyi NIT01* culture was added (Meng et al., 2022). As reported previously (Cecconet et al., 2018), biocathodes may offer advantages for the removal of heavy metals such as chromium and vanadium, including no need for chemical additives and the use of bacteria for microbial catalysis. However, most of the studies focus on *ex-situ* applications, with *in-situ* treatments requiring further exploration: Wu et al.

(Wu et al., 2015) developed a Cr(VI)-reducing biocathode by reversing an anodic exoelectrogenic biofilm, achieving higher microbial density than traditional biocathodes; Beretta et al. (Beretta et al., 2020) initially developed bio-anodes in a microbial fuel cell (MFC), then used them as cathodes in microbial electrolysis cell (MEC), observing high Cr(VI) removal efficiency (93%) at −0.300 V vs. SHE. Among reducible inorganic contaminants, nitrate derived from agricultural-related activities is one of the most widespread pollutants (Puggioni et al., 2021). As groundwater is usually characterised by low organic carbon concentration, autotrophic denitrification represents the key metabolism for successful nitrate removal using MET, where a solid-state, virtually inexhaustible electrode can provide the required electrons. Cecconet et al. (Cecconet et al., 2019) simulated the in-situ application of MET to achieve autotrophic denitrification. Ceballos-Escalera et al. (Ceballos-Escalera et al., 2024) designed a compact tubular bioelectrochemical reactor, suitable for decentralized applications in rural areas for simultaneous nitrate removal and groundwater disinfection. The system was capable of high nitrate removal rates (up to 5.0 ± 0.3 kgNO_3/m^3d), and *in-situ* generation of free chlorine at the anode allowed effective water disinfection.

I.5 Anodic electrobioremediation

The microbially-catalyzed anodic oxidation of organic compounds in MET was initially used to reduce the Chemical Oxygen Demand (COD) and Biochemical Oxygen Demand (BOD) in domestic wastewater, while simultaneously producing energy (Logan and Rabaey, 2012). More recently, MET technologies were employed to stimulate the anaerobic oxidation of petroleum hydrocarbons (Daghio et al., 2017). In these systems, the anode collects electrons produced from the oxidation of organic contaminants. The anode electrode can be buried in anoxic benthic sediment or a contaminated aquifer and connected to a cathode in the overlying water. The anode can be pre-inoculated or naturally colonized by resident microbiota capable of electron transfer. Electrons from the anaerobic oxidation of contaminants flow through a connection to the cathode in the aerobic water column, where oxygen reduction reaction (ORR) takes place. Clearly, this

configuration does not allow for power harvesting or activity monitoring. Earlier studies reported using complex mixtures of highly contaminated refinery wastewater and diesel-contaminated groundwater as electron donors in MFCs (Morris et al., 2009; Morris and Jin, 2007) coupling hydrocarbon removal with power production. When using an anode as an electron acceptor, Diesel Range Organics (DRO) removal reached 82%, compared to 31% in the open circuit control. Both alkanes and aromatic hydrocarbons were degraded in BES. The degradation of polycyclic aromatic hydrocarbons (PAHs) was also reported in several studies. PAHs are persistent organic pollutants known for their carcinogenic, mutagenic, and teratogenic properties (Patel et al., 2020). They are primarily found in soils (such as coal and tar deposits) and are produced by the thermal decomposition of organic matter. In one study, sediment/soil-based MFCs were used to assess PAH degradation in polluted soils. The system enhanced the removal rates of anthracene, phenanthrene, and pyrene while generating electricity (12 mW/m^2) (Yu et al., 2017). Although electricity production is a minor aspect of the technology, it serves as a valuable real-time indicator of degradation.

I.6 DIET-based electrobioremediation

The discovery of direct interspecies electron transfer (DIET) among microbial cells has brought attention to new and exciting strategies of microbial cooperation in energy-limited anaerobic ecosystems (Summers et al., 2010). Specifically, when grown under selective conditions, *Geobacter metallireducens* and *Geobacter sulfurreducens* (two iron-reducing bacteria known for their ability to exchange electrons with extracellular, insoluble electron acceptors or donors) were found to form electro-conductive microbial aggregates. In these aggregates, electrons were transferred from *G. metallireducens* to *G. sulfurreducens* during the syntrophic degradation of ethanol, likely facilitated by c-type cytochromes.

This disruptive discovery challenged the established paradigm that electron exchange within mixed microbial communities occurs only through diffusion of soluble molecules like H_2 or formate (Stams and Plugge, 2009). Experimental

findings and theoretical calculations have pointed out that DIET is a significantly faster and more effective energy transfer mechanism compared to interspecies H_2 transfer (Viggi et al., 2014). This leads to the intriguing hypothesis that DIET may be more widespread in natural environments than previously recognized.

Interestingly, further studies reported that adding even small amounts of nano-sized magnetite nanoparticles (<50 mgFe/L) could trigger DIET with negligible lag-phase in syntrophic microbial communities and *Geobacter* species (Kato et al., 2012). It was suggested that conductive magnetite particles attached to microbes served as abiotic electron conduits, in contrast to biological electron conduits like cytochromes, pilins, and pilin-like proteins, connecting redox reactions catalyzed by different microbial species (Liu et al., 2015). More recently, a variety of conductive or semi-conductive minerals and materials such as pyrite, biochar, and graphite were found to substitute for biological connectors to promote and facilitate cell-to-cell DIET (Cheng and Call, 2016).

Overall, while DIET is now recognized as a key metabolic route in the context of anaerobic digestion, its relevance in the fields of biogeochemistry and bioremediation remains largely unexplored, despite a few significant publications highlighting its likely importance (Aulenta et al., 2021).

I.7 Parameters affecting the MET performances

Different parameters can affect the efficiency of MET, among these the electrode materials, applied potential, the presence of redox mediator, the radius of influence and the reactor configuration are of great interest in remediation applications.

I.7.1 Electrode materials

The nature of the electrode can affect the performances of a MET, in particular it should comply with the following properties:

(I) high physical and chemical stability, (II) high electrical conductivity, (III) catalytic activity and selectivity for the target compounds, and (IV) low cost/life ratio. It is of relevant importance to choose an appropriate material because it

could affect the selectivity and efficiency of the hydrocarbon removal process (Anglada et al., 2009). The material also affects the Oxygen Evolution Reaction (OER) overpotential; anodes with low OER overpotential, such as graphite or platinum, are characterized by a high electrochemical activity towards the OER and low chemical reactivity toward oxidation of organics. Thereafter, low current densities are applied at such anodes to drive pollutant oxidation; at higher current densities, current efficiency is expected to decrease due to the production of oxygen. In contrast, anodes with a high OER overpotential, such as a DSAs (Dimensionally Stable Anodes), higher current densities can be applied without the concern that current efficiency is reduced due to occurrence of the OER. Oxygen evolution is a process that could affect the electro-bioremediation both by stimulating the activation of hydrocarbons, or by acting as a side reaction delivering electrons to the anode which are not linked to the oxidation of the contaminant, decreasing the efficiency. Adsorption of hydrocarbons on carbon and organic phases in soil and sediment is known to reduce their bioavailability, however adsorption on the electrode surface does not appear to negatively affect biodegradation of hydrocarbon contaminants. Studies showed that contaminants adsorbed onto the electrode could still be metabolized (Rakoczy et al., 2013; Zhang et al., 2010).

I.7.2 Redox potential

The anode in a MET is the final electron acceptor in microbial metabolism. The energy gain for the microorganisms is higher using electron acceptors with a more positive potential; therefore it is reasonable to hypothesize that a more positive anodic potential can enhance hydrocarbons oxidation. However, results correlating anodic potential to bioelectrochemical oxidation of organic substrates are controversial and do not confirm this expectation. With easily biodegradable substrates (e.g. acetate) a positive correlation between anode potential and current production was observed, but other studies have shown the opposite trend (Aelterman et al., 2008; Wagner et al., 2010). One of the mechanisms to transfer electrons to the electrode involve the presence of redox mediators that

could be produced by the microorganisms (e.g. flavins and phenazines) or that can be artificially provided (e.g. methyl-viologens and quinones). The presence of redox mediators can influence the metabolism, in fact electrodes in METs may serve to recycle the natural mediators, which can be re-oxidized at the anode, providing a continuous source of electron acceptors for the degradative microorganisms. Nevertheless, artificial mediators can be toxic and inhibitory to microbial activity; mediator-free METs are preferable during bioremediation because they could diffuse away from the reaction area and interact with other processes therefore decreasing the efficiency (Daghio et al., 2017).

I.7.3 Radius of influence of the electrode

The extension of the radius of influence of an electrode is one of the most important aspects to address before applying BES-based technologies for the bioremediation of soil and sediments. The reported studies clearly indicate that several factors may affect the radius of influence in field applications (e.g. electrode design, water content, soil type, mass transport) and these parameters may have to be evaluated in site specific conditions in order to obtain the best treatment efficiency (Daghio et al., 2017).

I.7.4 Reactor configuration

All bioremediation processes are influenced by the physical and chemical conditions of the contaminated matrix (e.g., soil, groundwater), especially for *in-situ* bioremediation. The biodegradation performances are significantly affected by matrix pH, salinity, temperature, nutrient content, soil water content and soil Permeability (Leahy and Colwell, 1990). Specifically, for BESs the contaminated matrix typically requires water saturation for proton transfer from the anode to the cathode. In addition, background nutrient content, especially N and P, would be required to be at levels that support anaerobic microbial activity. The MET best configuration can change depending on the applications. Sometimes the performances of these systems could be limited because of the large distance between the anode and cathode, which results in high resistance loss. Column

or tubular configurations alleviated such problems and have also been shown to be more effective for the same types of contaminants. A typical column reactor can be constructed by wrapping an assembly of anode, separator, and cathode layers around a perforated tube. Such configuration greatly improved the compactness of the reactor, reduced intrinsic loss, and can be potentially integrated with current infrastructures such as monitoring wells or piezometers (Yuan et al., 2010). For remediation of aqueous contaminants, enclosed systems have been tested in different operational patterns, such as flow through, recirculation, and multi-chamber integration. Dual-chamber reactors are widely used in lab scale studies, because separation of the anode and cathode by a membrane allows simple identification of reaction pathways for a specific contaminant. So far, most studies were conducted in lab scale, but several groups have successfully demonstrated MET remediation in pilot scale (H. Wang et al., 2015). Despite the different advantages and the scientific interest, field scale bioelectrochemical systems have not yet been tested and verified under fully representative conditions and concerns have also been raised regarding their actual scalability. To overcome these limitations, several alternative configurations are presently being considered (e.g. involving concentric electrodes), whereby the spacing between electrodes is kept as small as possible without adversely affecting process performance. More scale-up studies are expected, and there are several key factors that need to be considered for real-world applications. For example, compared with METs for wastewater treatment, the *in-situ* field applications for soil and groundwater remediation require more flexible configurations to adapt to different depths, soil matrix types and other physical/chemical parameters. In addition, different contaminants generally coexist in soil, sediment, or groundwater, which may require integrated remediation strategy. So far, most studies focused on removing one contaminant or mixed contaminants of the same type (electron donor or acceptor), so more studies are needed to tackle co-existing yet different types of chemicals.

I.8 Aims of the Thesis

Microbial electrochemical technologies (MET) represent promising tools for the *in-situ* bioremediation of groundwater contaminated by a wide range of pollutants, such as petroleum hydrocarbons (PH) and heavy metals. These technologies provide continuous supply of electron donors or acceptors directly within the subsurface environment, thus enhancing microbial degradation processes. However, the mechanisms linking the degradation of contaminants to current generation are still not fully understood, limiting the development of robust and scalable systems for field applications. Furthermore, most studies focused on the treatment of single contaminants under laboratory conditions, whereas real environmental contexts typically involve multiple co-contaminants requiring more integrated remediation strategies.

In this context, the main objective of this Ph.D thesis was to develop and assess the effectiveness of innovative bioelectrochemical reactor configurations for the in-*situ* bioremediation of complex groundwater contaminated by organic and inorganic compounds. The research investigates how reactor design, electrode materials, and operating conditions influence contaminant removal efficiency, with also a focus on understanding the microbial processes involved in pollutant degradation.

In **Chapter II**, the thesis presents a further development and assessment of a recently developed bioelectrochemical reactor configuration, referred to as the "Bioelectric well" (**Fig.I-3**) specifically designed for the *in-situ* treatment of groundwater contaminated by organic pollutants. Indeed, in a previous study the viability of such system to treat a synthetic groundwater containing toluene was demonstrated. This chapter further examined factor and conditions affecting the anodic toluene oxidation by a mixed microbial community and the corresponding electricity generation pattern. Interestingly, the electrogenic anaerobic biodegradation of toluene was found to occur via a syntrophic pathway involving both hydrocarbon-degrading bacteria and electroactive microorganisms. The study provides insights into the coupling between microbial oxidation of toluene

and electron transfer processes at the anode, analyzing how current generation correlates with contaminant degradation.

Chapter III builds on this concept, extending for the first time the application of the “bioelectric well” technology to the treatment of mixed contamination scenarios. In this chapter, the reactor is exploited for the simultaneous degradation of toluene and trichloroethene (TCE), a common co-contaminant in groundwater. Notably, the research demonstrated how the bioelectric well supports simultaneously both oxidative and reductive degradation pathways, with toluene being oxidized at the anode and TCE being reductively dechlorinated at the cathode, via abiotic hydrogen generation. The results highlight the potential of this system for treating complex mixtures of pollutants in a single-stage process. In **Chapter IV**, the thesis explores the simultaneous removal of toluene and chloroform (CF) in a continuous-flow bioelectrochemical reactor, addressing, again, the challenge of co-contamination with organic pollutants requiring different degradation pathways. This study investigates how the bioelectrochemical system facilitates the concurrent biodegradation of these two compounds while analyzing the impact of competitive inhibition when additional substrates, such as acetate, are introduced. The findings suggest that METs can be effectively employed in scenarios involving multiple contaminants, although further optimization is required to maximize removal rates under mixed contaminant conditions.

Chapter V expands the application of METs to the treatment of both organic and metal contaminants. Here, the thesis investigates the removal of toluene and copper using a single-chamber bioelectrochemical cell. The oxidation of toluene at the anode drives the reduction and precipitation of copper at the cathode, resulting in the complete removal of both contaminants. This chapter illustrates the versatility of METs in simultaneously addressing organic and inorganic pollutants, showing how they can be employed for also for *in-situ* remediation of complex groundwater scenarios.

In **Chapter VI,** a novel approach combining nitrate electro-bioremediation with ultrafiltration technology is presented. The objective of this research was to

develop a system where conductive membranes serve as both electrodes and filtration media, allowing for the simultaneous filtration of water and biodegradation of contaminants directly on the membrane surface. This configuration enhances the efficiency of the bioremediation process by reducing membrane fouling and co-localizing contaminants and microorganisms at the membrane, facilitating more effective degradation. The integration of these conductive membranes enables the application of an electric potential to drive the nitrate reduction while simultaneously filtering out suspended particles and other contaminants. This dual functionality provides a significant advantage over traditional systems, where membrane fouling often limits operational lifespan and efficiency. The use of this integrated system reduces the need for frequent membrane cleaning and maintenance, making the technology more sustainable and applicable to large-scale water treatment operations. The results demonstrated a significant nitrate removal efficiency, showcasing the potential of this integrated approach for advanced water remediation applications. This latter research was conducted during a research stay at The Laboratory of Chemical and Environmental Engineering (LEQUIA), of the University of Girona (UdG), under the supervision of Prof. Sebastià Puig. The findings from this study lay the groundwork for future research aimed at scaling up this innovative technology for broader environmental applications.

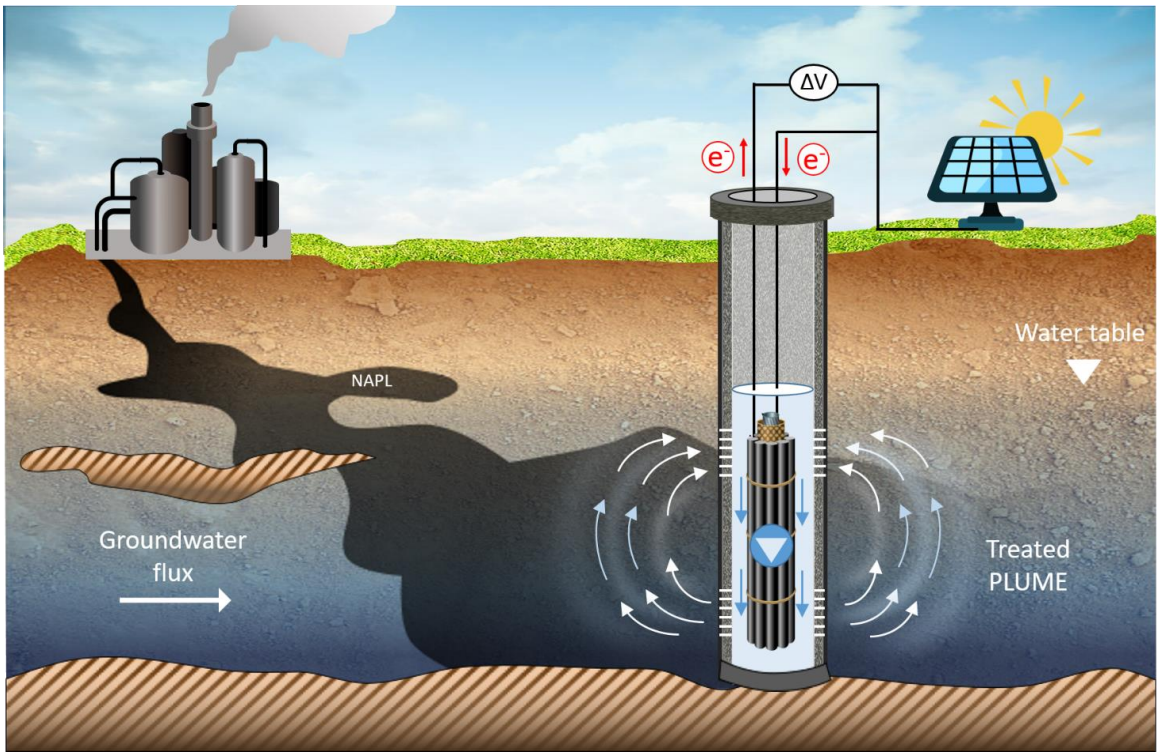

Figure I-3 *Illustration of the prototype named "Bioelectric Well" operated in-situ*

Chapter II

Syntrophy drives the microbial electrochemical oxidation of toluene in a continuous-flow “bioelectric well”

Adapted From:

Tucci, M., Milani, A., Resitano, M., Viggi, C.C., Giampaoli, O., Miccheli, A., Crognale, S., Matturro, B., Rossetti, S., Harnisch, F., Aulenta, F., 2022. Syntrophy drives the microbial electrochemical oxidation of toluene in a continuous-flow ‘bioelectric well’. J. Environ. Chem. Eng. 10, 107799. https://doi.org/10.1016/j.jece.2022.107799

II.1 Introduction

The presence of petroleum hydrocarbons (PHs) in groundwater is mostly caused by accidental spills and industrial discharges, and it represents a critical threat to human health and the ecosystem (Weelink et al., 2010). Due to their high mobility and water solubility, benzene, toluene, ethylbenzene and xylenes (BTEX) are particularly dangerous when dispersed in the environment (Akmirza et al., 2017), often amounting up to 90% of the dissolved pollutants in groundwater contamination plumes (Suarez and Rifai, 2002). This aspect, combined with the toxicity, demands for the implementation of effective remediation (Bolden et al., 2015). In this regard, bioremediation is considered an effective strategy: it takes advantage of the capability of naturally occurring microorganism to use pollutants as substrates and convert them into harmless or less dangerous products (Okoh et al., 2020). In subsurface environments, however, bioremediation is often limited by the scarcity of bioavailable electron acceptors or donors, negatively affecting the removal rates (Modin and Aulenta, 2017). To overcome this problem, several remediation techniques have emerged, which mainly involve the injection of electron acceptors (*e.g*. oxygen) or donors (*e.g.* lactate) into the contaminated aquifer to enhance the metabolism of the degrading microbial communities (Farhadian et al., 2008). Microbial electrochemical technologies (METs) are emerging as a viable alternative to this approach, by supplying a virtually inexhaustible electron acceptor or donor directly in the subsurface environment in the form of a solid electrode (Cecconet et al., 2020). In this way, several drawbacks linked to traditional bioremediation strategies can be avoided, such as: (a) quick consumption or migration of the amendment solution; (b) contaminant plume shift or dilution caused by the injection; (c) uncontrolled biomass growth near injection points and (d) accumulation of unwanted metabolites derived from the amendment (He and Su, 2015). For this reason, METs can result in a more sustainable and cost-effective technology. However, only few studies have addressed the use METs for the anaerobic oxidation of BTEX (Yang et al., 2020), and in order to design effective prototypes for field applications, a deeper understanding of the removal mechanism is necessary.

Herein, we studied the degradation of toluene as model BTEX using a prototype of MET called “bioelectric well”. In previous works this prototype has been successfully tested for the removal of phenol, toluene or a mixture of BTEX in continuous-flow mode (Espinoza-Tofalos et al., 2020; Enza Palma et al., 2019, 2018b). It consists of a membrane-less tubular bioelectrochemical reactor where anode and cathode are placed concentrically and in close proximity to each other in order to minimize ohmic losses. Importantly, due to the cylindrical shape and close inter-electrode spacing even upon scale-up, the bioelectric well could be directly installed inside groundwater wells or piezometers for *in-situ* treatment of PH. In this work we analyzed the performances of the system in several operational conditions, such as different contaminant loads, open circuit *vs.* polarized, continuous mode *vs*. batch mode, etc., in order to identify the main factors that influence the degradation process and its possible limitations. Furthermore, we monitored the concentration of metabolites in the liquid phase of the reactor and conducted microbiological analyses to have a deeper understanding of the microbial interactions responsible for degradation of toluene.

II.2 Experimental section

II.2.1 Chemicals and electrode potentials

All chemicals were of analytical grade and were supplied from Merck KGaA (Darmstadt, Germany). De-ionized water (Millipore, Darmstadt, Germany) was used to prepare the microbial medium, and all other solutions. All potentials provided in this article refer to the standard hydrogen electrode (SHE).

II.2.2 Reactor setup and operations

The bioelectric well was constructed as described elsewhere (Tucci et al., 2021). A cylindrical anode made of 8 contiguous graphite rods (purity: 99.995%, length: 30 cm, ø: 0.6 cm; Sigma-Aldrich, Italy) and a stainless-steel mesh cathode (dimensions: 3 x 30 cm; type 304, Alpha Aesar, USA) were concentrically placed

in a 250 mL glass cylinder (**Fig. II-1**). Anode and cathode were kept physically separated by a polyethylene mesh (ø: 1cm, length 30cm; Fig. 1B), which still allowed hydraulic connection. Titanium wires (ø: 0.81mm Alfa Aesar, USA) were used to connect anode and cathode to an external circuit. The anode was continuously polarized at +0.2 V vs. SHE by an IVIUMnSTAT potentiostat (IVIUM Technologies, The Netherlands), and an Ag/AgCl electrode (+0.198 V vs. SHE; AMEL, Italy) was used as reference electrode. The inoculum consisted of 0.25 L of contaminated groundwater obtained from a petrochemical site in Italy. The reactor was continuously fed with mineral medium (**Tab. II-1**).

Table II-1 *– Composition of the mineral medium used for the study*

Minerals	
Compound	**Concentration (g/L)**
NH_4Cl	0.5
$MgCl_2 \times 6H_2O$	0.1
$CaCl_2 \times 2H_2O$	0.05
K_2HPO_4	0.4
Trace metals	
Compound	**Concentration (mg/L)**
Nitrilotriacetic acid	4.5
$FeSO_4 \times 7H_2O$	0.556
$MnSO_4 \times H_2O$	0.086
$CoCl_2 \times 6H_2O$	0.17
$ZnSO_4 \times 7H_2O$	0.21
H_3BO_3	0.019
$NiCl_2$	0.02
Na_2MoO_4	0.01
Vitamins	
Compound	**Concentration (mg/L)**
Biotin (B7)	0.02
Folic acid (B9)	0.02
Pyridoxine (B6)	0.1
Thiamine (B1)	0.05
Riboflavin (B2)	0.05

Nicotinic acid (B3)	0.05
Pantothenic acid (B5)	0.05
Cyanocobalamin (B12)	0.002
4-aminobenzoic acid (B10)	0.05

Prior to use, the medium inlet was sparged with pure nitrogen gas to eliminate oxygen. Then the medium was spiked with toluene at a different concentration for each feeding cycle, ranging from about 1 to 40 mg L^{-1} (**Tab. II-3**). The inlet was then stored in 5 L collapsible Tedlar® gas bags. The medium was pumped into the reactor through a port situated at the bottom of the cylinder (flow rate: 0.63 L d^{-1}, HRT 11 h) using a peristaltic pump (120S, Watson Marlow, Falmouth, UK), while the treated effluent exited from a port near the upper end by passive overflow. The inlet and at the outlet of the reactor were equipped with flow-through sampling cells (volume: 25 mL). In order to avoid the formation of concentration gradients of substrate, products and biomass, the liquid phase of the reactor was constantly recycled with another peristaltic pump (flow rate: 192 mL min^{-1}; model: 323, Watson Marlow, Falmouth, UK; **Fig. II-1**). All the tubings were made of Viton® (Sigma-Aldrich, Italy), which keeps volatilization losses and organic contaminant adsorption to a minimum. At the end of the experiment the electrodes were disconnected from the potentiostat and the reactor was operated at open circuit potential (OCP) as a control condition. Furthermore, in a follow-up experiment the reactor was operated in OCP and in batch mode to analyze the possible accumulation of degradation intermediates. Throughout the whole study, the system was kept at room temperature (*i.e.,* 24 ± 3°C).

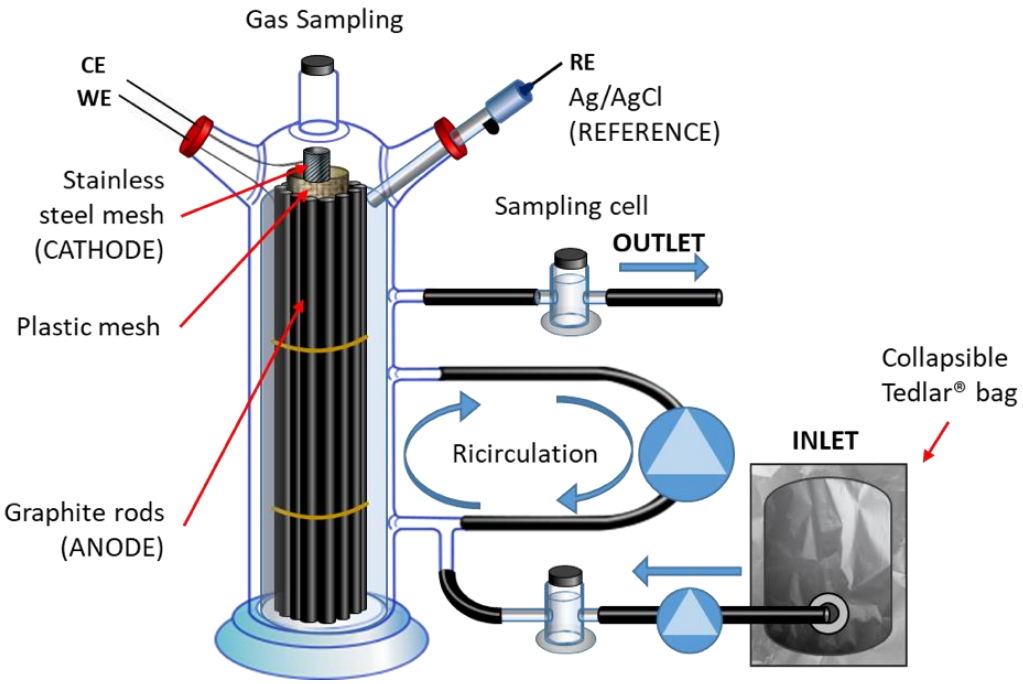

Figure II-1 *- Schematic representation of the bioelectrochemical reactor "bioelectric well" when operated in continuous-flow mode: 3D sketch of cylindrical reactor and peripherals*

II.2.3 Cyclic voltammetries

Cyclic voltammetries (CVs) were conducted on the bioanode at scan rates of 1 mV/s within the potential range between -0.4 and 0.8 V vs. SHE using an IVIUMnSTAT potentiostat (IVIUM Technologies, The Netherlands). The stainless-steel cathode was used as counter electrode, while as an Ag/AgCl electrode (+0.198 V vs. SHE; AMEL, Italy) served as reference.

II.2.4 Gas analyses

Gaseous samples were analyzed in terms of O_2, H_2 and CH_4 using a gas-chromatograph (Agilent 8860, GC system USA) equipped with a thermal conductivity detector (TCD). The concentration of toluene was measured by injecting gaseous samples into gas-chromatograph (Agilent 8860, GC system USA) equipped with a flame ionization detector (FID). Gas-phase concentrations were converted into liquid-phase concentrations using tabulated Henry's Law constants (Sander, 2015). The GC methods, calibration ranges and LOD of analytical methods are reported in the **Table II-2**.

Table II-2 *– Description of analytical methods employed for the quantification of toluene and H_2, CH_4, O_2 gases*

Toluene analysis			
GC system	Agilent 8860 with FID detector		
Column	Agilent DB-624 GC fused silica (60m x 0.53 mm inner diameter, 0.3 μm thickness)		
Operational parameters	GC method: Carrier gas: nitrogen 7 mL/min; Injection Temp: 250 °C; Interface Temp: 300 °C; Oven Temp Program: 100°C for 1.0 min, then ramp 20°C/min up to 150°C, hold for 1 min		
Calibration range	0 – 29 ppm		
LOD	0.3 ppm		
LOQ	1 ppm		
Gas analysis			
GC system	Agilent 8860 with TCD detector		
Column	Agilent Carboxen 1000 stainless steel packed (3.05 m x 0.32cm, OD, 2 mm ID, Carboxen-1000 packing, mesh size 60/80, pre-conditioned)		
Operational parameters	GC method: Carrier gas: Nitrogen 10 mL/min; Injection Temp: 200 °C; Interface Temp: 300 °C; Oven Temp Program: 100°C for 10.0 min		
Gas	H_2	CH_4	O_2
Calibration range (ppm)	23 – 69	1.5 – 6.1	65 - 392
LOD	0.3 ppm	0.3 ppm	0.3 ppm
LOQ	1 ppm	1 ppm	1 ppm

II.2.5 ^{1}H-NMR analyses of liquid samples

The liquid samples collected during the batch phase operated in OCP mode were analyzed via Proton Nuclear Magnetic Resonance (^{1}H-NMR) spectroscopy. Initially, 350 microliters of each sample were added to 350 microliters of trimethylsilyl propionic-2,2,3,3-d4 acid (TSP)- D2O 2mM solution (final concentration of 1mM). This mixture of each sample was then vortexed and transferred into precision tubes. After that, ^{1}H-NMR spectra were acquired at 298 K using a JEOL JNM-ECZR spectrometer (JEOL Ltd, Tokyo, Japan) equipped with a magnet operating at 14.09 Tesla and at 600.17 MHz for 1H frequency. All the spectra were recorded with 64k points and 128 scans, setting spectral width to 9.03 KHz (15 ppm), with and irradiation attenuator of 48 dB, a pre-saturation pulse length of 2.00 s, relaxation delay of 5.72 s, for an acquisition time of 5.81

s. The identification step was achieved by two-dimensional experiments ^{1}H-^{1}H Homonuclear Total Correlation Spectroscopy (TOCSY), ^{1}H-^{13}C Heteronuclear Single Quantum Correlation (HSQC) on selected samples and confirmed by literature comparison. TOCSY experiments were recorded at 298 K with a spectral width of 15 ppm in both dimensions, using 8k × 256 data points matrix, repetition time of 3.00 s and 80 scans, with a mixing time of 80.00 ms. HSQC experiments were acquired with a spectral width of 9.03 KHz (15 ppm) in proton dimension and 30 KHz (200 ppm) in the carbon dimension, using 8k × 256 data points matrix for the proton and the carbon dimensions, respectively, with a repetition delay of 2 s and 96 scans. One-dimensional NMR spectra were processed and quantified by using the ACD Lab 1D-NMR Manager ver. 12.0 software (Advanced Chemistry Development, Inc., Toronto, ON, Canada); 2D-NMR spectra were processed by using JEOL Delta v5.3.1 software (JEOL Ltd, Tokyo, Japan). All the NMR spectra were manually phased, baseline corrected and referenced to the chemical shift of the TSP methyl resonance at δ = 0.00. The quantification of metabolites was obtained by comparing the integrals of their diagnostic resonances with the internal standard TSP integral and normalized for their number of protons, and then multiplied for two, in order to consider the dilution factor. Final concentration was expressed as mM.

II.2.6 High-Throughput rRNA Gene Sequencing and Bioinformatic Analysis

The contaminated groundwater used to inoculate the reactor (T_0: 45 mL) and liquid sample (T_f: 10 mL) taken at the end of the operation were filtered through polycarbonate membranes (pore size 0.2 mm, 47 mm diameter, Nuclepore) and immediately stored at -20°C. In addition, the biofilm grown on the graphite rods was also collected at the end of the operation for subsequent microbiological analyses. The DNeasy PowerSoil Pro Kit (QIAGEN - Germantown, MD) was used for the DNA extraction. The genomic DNA was utilized as template for the amplification of the V1-V3 region of 16S rRNA gene of *Bacteria* (27F 5'-AGAGTTTGATCCTGGCTCAG-3'; 534R 5'-ATTACCGCGGCTGCTGG-3') and the region V3–V5 of 16S rRNA gene of *Archaea* (340F 5'-

CCCTAHGGGGYGCASCA-3'; 915R 5'-GWGCYCCCCCGYCAATTC-3') following the procedure for library preparation and sequencing described in (S. Crognale et al., 2019). The samples were paired end sequenced (2x301bp) on a MiSeq platform (Illumina) using a MiSeq Reagent kit v3, 600 cycles (Illumina, USA) following the standard guidelines for preparing and loading samples. Phix control library was spiked at a concentration of 20%. Bioinformatics elaborations were performed using QIIME2 v. 2018.2 (Bolyen et al., 2019) following the procedure reported elsewhere (Crognale et al., 2021). High-throughput sequencing of the V1-V3 and V3-V5 regions of the bacterial and archaeal 16S rRNA gene yielded a total of 32,274 and 60,744 sequence reads after quality control and bioinformatic processing that resolved into 579 and 81 ASVs, respectively. Dataset are available through the Sequence Read Archive (SRA) under accession PRJNA785770. Sequencing results were used for the calculation of biodiversity indices for each sample by using PAST software (PALAEONTOLOGICAL STATISTICS, ver. 2.17) (Hammer et al., 2001).

II.2.7 Droplet Digital PCR quantification of key-functional genes

The QX200™ Droplet Digital™ PCR System (Bio-Rad, Pleasanton, CA) was used in order to quantify the functional genes involved in anaerobic degradation of petroleum hydrocarbons. The ddPCR reaction mixture consisted of 11 µL of 2× ddPCR EvaGreen supermix (Bio-Rad, Italy), 1 µL of each primer (at 7.5µM concentration), 6 µL of nuclease-free water, and 3 µL of sample DNA. The reaction mixture was mixed with droplet generation oil (20 µL mixture + 70 µL oil) via microfluidics in the Droplet Generator (Bio-Rad, Italy). Following droplet generation, the water-in-oil droplets were transferred to a standard 96-well PCR plate, which was heat sealed with foil plate seal (Bio-Rad) and placed on a Bio-Rad CFX96 thermocycler (ramping speed at 2 °C s^{-1}) for PCR amplification using the following conditions: 5 min at 95°C, followed by 39 cycles of 30 s at 95°C and 1 min at 55-60°C according to the primer pair, followed by 5 min hold at 4°C and 5 min at 95°C. Upon completion of PCR, the plate was transferred to a Droplet Reader (Bio-Rad) for automatic measurement of fluorescence in each droplet in

each well (approximately 2 min per well). The benzylsuccinate synthase (bssA), involved in toluene degradation, was targeted using 7772f – 8546r primer pair (Winderl et al., 2007). The primer pairs bcrCf-bcrCr and bzdNf-bzdnR were used for the amplification of the benzoyl CoA reductases class I (bcrC, bzdN) (Kuntze et al., 2011); while the benzoyl CoA reductase class II (bamB) was amplified using bamBf – bamBr primers (Löffler et al., 2011)

II.2.8 Calculations

The removal rate of toluene *r* (mg L^{-1} d^{-1}) was calculated using the following equation:

$$r_{Tol} = \frac{\Delta Tol}{V_r} Q \quad (1)$$

where *ΔTol* (mg L^{-1}) is the difference between the concentration of toluene measured in the influent (Tol_{In}) and the concentration measured in the effluent (Tol_{out}), V_r (L) is the empty volume of the reactor and *Q* (L d^{-1}) is the flow rate of the influent.

The relative toluene removal $q_{Tol\%}$ was calculated as follows:

$$q_{Tol\%} = \frac{\Delta Tol}{C_{Tol(in)}} \times 100 \quad (2)$$

To calculate electron equivalents per day (mmol d^{-1}) generated by the complete oxidation of toluene (meq_{Tol}), the following equation was used:

$$meq_{Tol} = \frac{\Delta Tol}{MW_{Tol}} \times f_{Tol} \times Q \quad (3)$$

where MW_{Tol} is the toluene molecular weight (92.14 g mol^{-1}) and f_{Tol} represents the number of mmol of electrons released from the complete oxidation of 1 mmol of toluene according to the following stoichiometric equation:

$$C_7H_8 + 14\ H_2O = 7\ CO_2 + 36\ H^+ + 36\ e^- \quad (4)$$

Therefore, the value of f_{Tol} is 36.

Analogously, the electron equivalents per day (mmol d^{-1}) needed for methane production (meq_{Met}) were calculated using the following equation:

$$meq_{Met} = Met_{Out} \times f_{Met} \times Q \quad (5)$$

Where Met_{Out} (mmol L^{-1}) is the concentration of methane measured at in the effluent and f_{Met} represents the number of mmol of electrons necessary for the

conversion of 1 mmol of CO_2 to methane, according to equation (6), which is equal to 8.

$$CO_2 + 8\ H^+ + 8\ e^- = CH_4 + 2\ H_2O \quad (6)$$

The columbic efficiency (*CE*) was calculated as the ratio between charge that is the integral of the electric current over time and the theoretical charge deriving from the oxidation of removed toluene, according to the following equation:

$$CE(\%) = \frac{\int i(t) \times dt \times 60 \times 60 \times 24}{(meq_{Tol}) \times F} \times 100 \quad (7)$$

where *i* is the measured current (mA), *dt* is the time (s), *F* is the Faraday's constant (96485.3 C mol^{-1}), meq_{Tol} is the amount of electron equivalents of toluene removed per day (mmol d^{-1}).

The cathode capture efficiency (*CCE*) of the methane generation was calculated as follows:

$$CCE(\%) = \frac{(meq_{Met}) \times F}{\int i(t) \times dt \times 60 \times 60 \times 24} \times 100 \quad (8)$$

where meq_{Met} represents the millimoles of electron equivalents needed for the production of methane.

II.3 Results and discussion

II.3.1 Reactor performance

The bioelectric well was operated in continuous-flow mode for about 50 days, and six different runs were performed at different influent toluene concentrations. For each run, current, concentration of toluene in the influent and effluent and methane generation were measured. Moreover, the coulombic efficiency (*CE*) and the cathode capture efficiency (*CCE*) were calculated. **Figure II-2** exemplifies the calculation (cycle III, influent toluene concentration: 5.5 ± 1 mg L^{-1}) and the average values for all experimental runs are reported in **table II-3**.

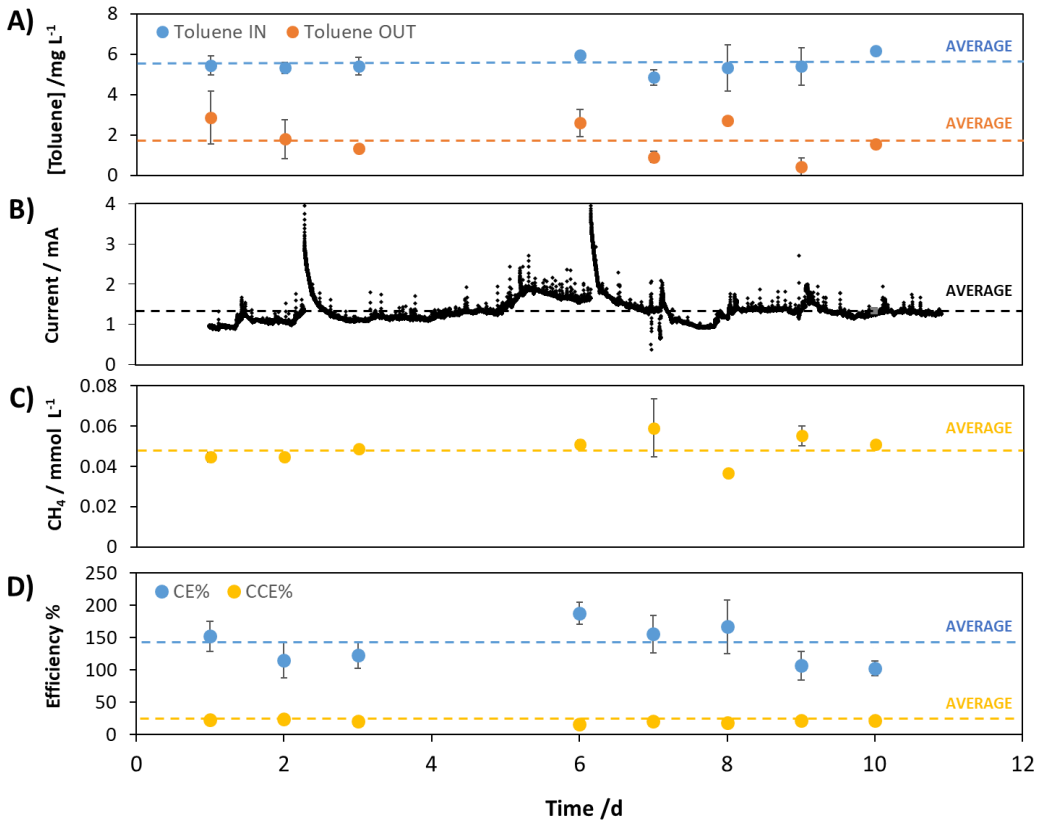

Figure II-2 *– Trends of A) toluene concentrations in the influent and effluent of the reactor, B) current generation, C) methane produced, D) coulombic efficiency (CE) and cathode capture efficiency (CCE) for the third experimental run of the reactor (Inlet toluene concentration 5.5mg/L).*

The highest achieved toluene removal rate (r_{Tol}) was 71 ± 13 mg L^{-1} d^{-1}, with an average degradation of the influent contaminant load of about 70%. The *CE* was highly dependent on the influent toluene concentration with broad variations. In run V the *CE* value is as high as 2275 ± 735 %, which is because a significant current was generated, even if the influent concentration of toluene was very low (*i.e*. 0.9 ± 0.7 mg L^{-1}). This aspect of an "impossible" *CE* will be further discussed in the following paragraphs. The methane generation, together with the carbon capture efficiency, decreased throughout the experiment.

Table II-3 *– Average values of performance indicators during each experimental run (see calculation section).*

Run	Duration (d)	Tol_{in} (mg L^{-1})	Tol_{out} (mg L^{-1})	r_{Tol} (mg L^{-1} d^{-1})	q_{Tol} (%)	Current (mA)	Met_{out} (mmol L^{-1})	*CE* (%)	*CCE* (%)
I	8	17.0 ± 1.6	3.9 ± 0.3	28 ± 3	76 ± 3	1.86 ± 0.04	0.18 ± 0.02	55 ± 7	56 ± 5
II	8	23.7±2.9	10.4 ± 1.6	29 ± 4	56 ± 3	1.94 ± 0.03	0.10 ± 0.01	56 ± 7	30 ± 3
III	15	5.5±0.1	1.8 ± 0.3	8 ± 1	68 ± 6	1.33 ± 0.09	0.049 ± 0.002	134 ± 10	21 ± 1
IV	9	9.0±1.2	4.0 ± 0.4	11 ± 2	55 ± 3	1.58 ± 0.06	0.06 ± 0.01	123 ± 2	23 ± 5
V	7	0.9±0.7	0.2 ± 0.1	2 ± 1	76 ± 7	1.06 ± 0.07	0.03 ± 0.02	**2275 ± 753**	11 ±6
VI	4	39.7±8.8	7.1±3.4	71 ± 13	85 ± 5	2.44 ± 0.45	0.03 ± 0.01	30 ± 9	8 ± 1
OCP	8	26.4 ± 0.6	10.5 ± 1.0	35 ± 3	60 ± 5	/	0.06 ± 0.01	/	/

Figure II-3 shows cyclic voltammograms (CV) recorded during different operational runs. No redox peaks were observed on the blank (abiotic) electrode either in the absence (black line) or in the presence of toluene. The CV of the biofilm anode in presence of toluene (inlet toluene concentration: 1 mg L^{-1}, red line) shows a clear signal with an oxidation peak at 0.22 V vs. SHE. This strongly suggests the colonization of the electrode surface by a biofilm comprising of electroactive microorganisms, metabolically linked to toluene degradation. When the toluene concentration was increased (inlet toluene concentration: 40 mg L^{-1}, yellow line), a corresponding rise of the oxidative current is apparent, showing a clear catalytic wave, with a maximum current density of ca. 9.3 µA cm^{-2}.

By calculating the first derivative $\Delta i/\Delta E$ of the CVs of the bioanode in the presence of toluene, the formal potential (E_f) of the redox sites involved in toluene oxidation is gained. The average E_f obtained for all feeding cycles is 0.03 ± 0.02 V *vs.* SHE. This value is slightly higher than the ones reported in literature for *Geobacter*-dominated anodic biofilms, which is between -0.1and 0.15 V vs. SHE (Patil et al., 2012; Riedl et al., 2019; Scarabotti et al., 2021).

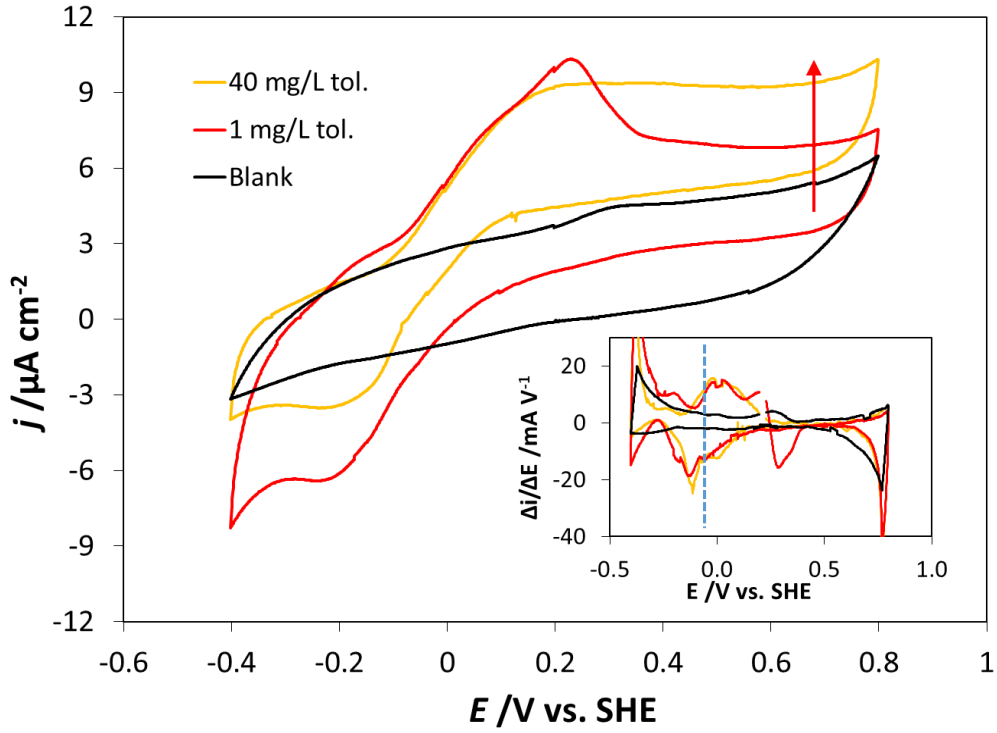

Figure II-3 *– Cyclic voltammograms conducted on the electrode without biofilm (abiotic control) and on the bioelectrode at two different concentrations of toluene (scan rate: 1mV/s). The inset shows the first derivative of the voltammograms Δi/ΔE: the blue arrows point to the peaks which correspond to the formal potentials of the extracellular electron transfer of the bioelectrode.*

II.3.2 Impact of toluene load

The concentration of toluene in the influent had a significant impact on the reactor performance. As depicted in **figure II-4A**, toluene removal rate displayed a linear dependency on the inlet toluene concentration, whereas current generation shows a non-linear relationship. Specifically, the current increase is linear at low influent toluene concentrations, while for concentrations higher than 10 mg L^{-1} the curve shows a saturation behaviour (**Fig. II-4B**). This aspect is further confirmed by the CV analysis (using CV data collected during the different runs), when plotting the value of current (at 0.7 V vs. SHE during the anodic scan of the CV) as a function of toluene concentration (**Fig. II-4C**). Obviously, the mismatch between toluene removal and current generation trends has a major impact on the *CE*, which shows an inverse correlation with the toluene load, dropping from 134% at 5 mg L^{-1} down to 30% at 40 mg L^{-1} inlet concentration, respectively (**Fig.**

II-4D). This phenomenon seems to indicate that, at high concentrations of toluene, another route of toluene removal, which is not linked to electric current generation, becomes predominant. Along this this, it is possible that toluene is degraded under methanogenic conditions. To test this hypothesis, we conducted a run of the reactor under OCP conditions (**Fig. II-5**), in order to quantify the contribution of the methanogenic pathway on toluene removal, upon blocking the microbial electrochemical oxidation.

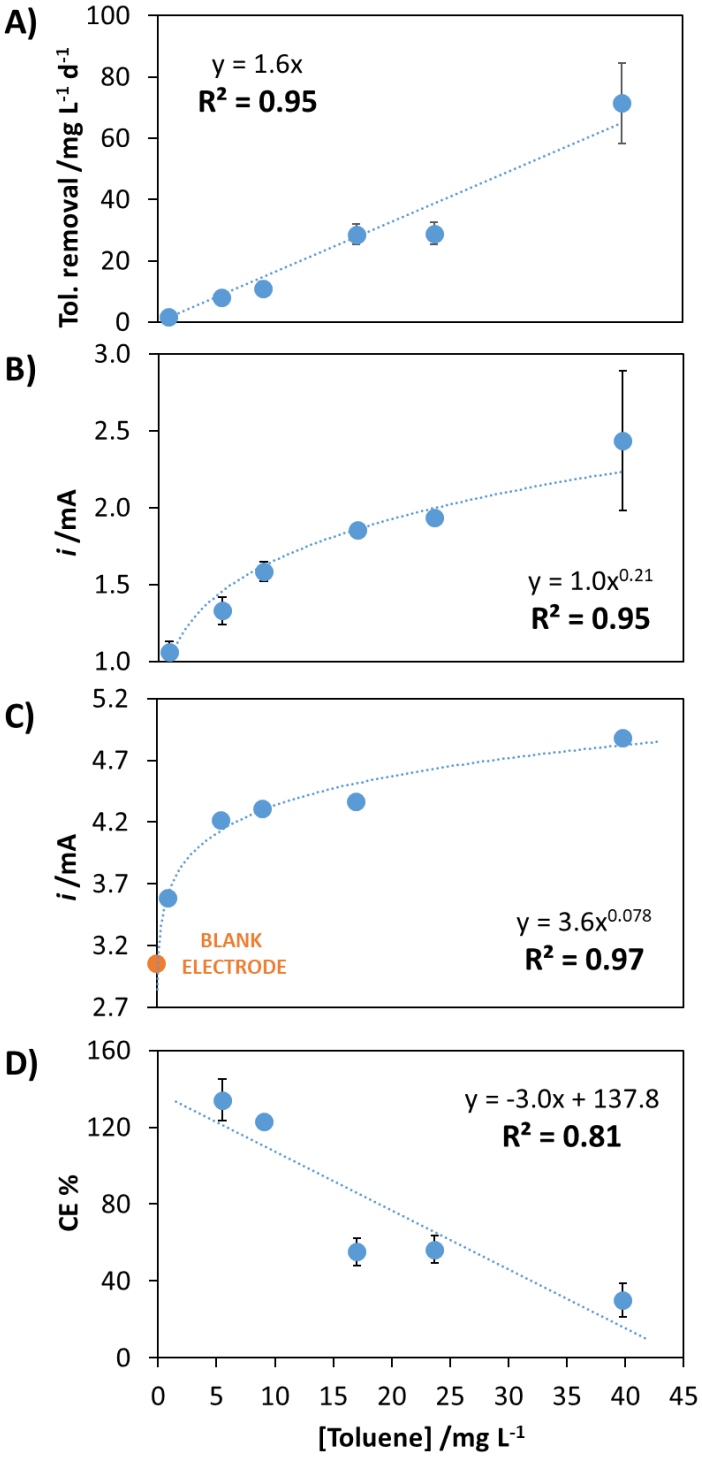

Figure II-4 *– Influence of the toluene concentration on A) toluene removal, B) current generation C) oxidative current obtained during CVs, in correspondence to an anodic potential of 0.7 V vs. SHE, and D) coulombic efficiency.*

However, the obtained results indicate that methane generation accounts only for a minor share of the removed toluene (**Fig. II-5**). Indeed, the methane conversion efficiency (i.e., the percentage of the removed toluene which was recovered as methane) was as low as 7.7%. Thus methanogenic toluene degradation cannot explain the observed uncoupling between current generation and toluene removal.

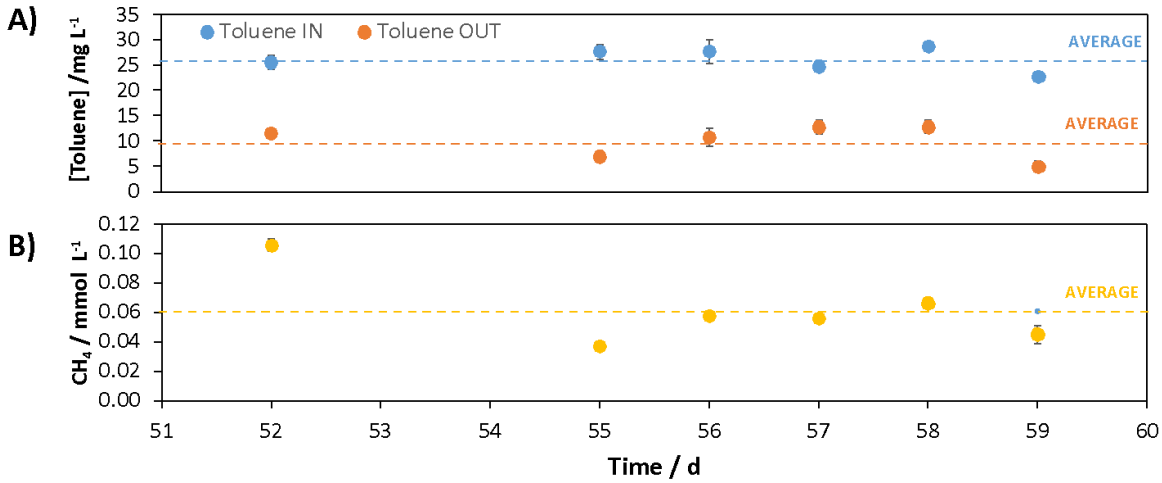

Figure II-5 *- Trends of toluene (A) concentrations in the influent and effluent of the reactor and methane (B) produced for the reactor operated in OCP mode.*

II.3.3 Deciphering microbial syntrophy

Considering the previous results, we speculated that the degradation of toluene involves two different steps: first toluene is converted into metabolic intermediates without the involvement of the electroactive microorganisms, subsequently these intermediates are oxidized by the electroactive bacteria in the anodic biofilm. This hypothesis was tested by performing another open circuit experiment with the reactor being operated, this time, in batch mode so as to magnify the possible accumulation of metabolic intermediates.

To this aim, the reactor was emptied to remove all metabolites and microorganisms present in the planktonic phase and then completely filled with fresh medium spiked with 10 mg L^{-1} toluene. Cyclic voltammograms were performed, at given time intervals, during the experiment to monitor the bioelectrocatalytic activity, while the abundance of metabolites (i.e., molecules

which are directly converted into electric current by the electroactive biofilm) was quantified using NMR.

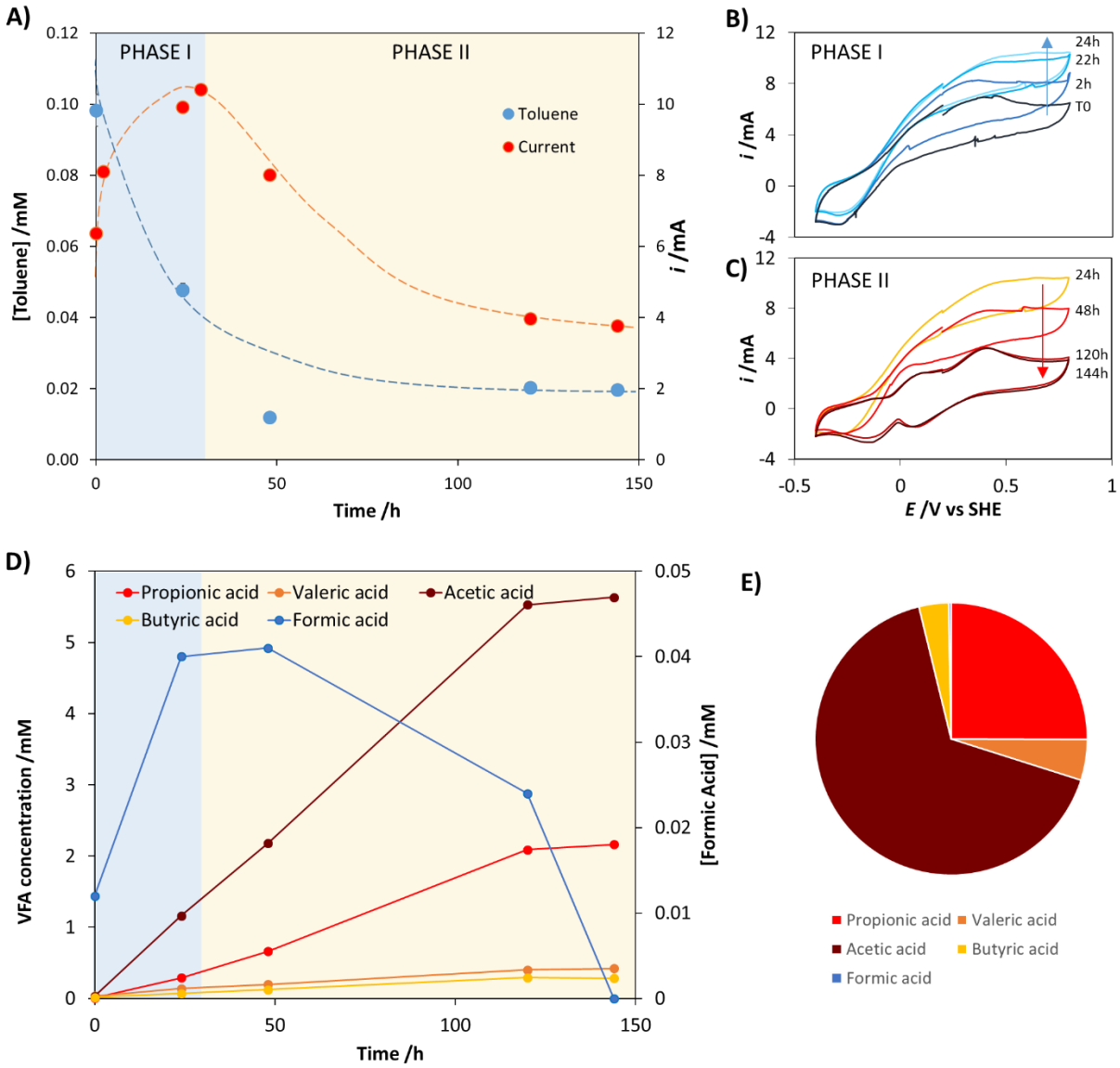

Figure II-6 *– A) Trend of the toluene concentration and the oxidative current recorded at 0.7V vs. SHE during cyclic voltammograms while the reactor was operated in batch mode in OCP. B) Cyclic voltammograms recorded at different times during the step of intermediate accumulation. C) Cyclic voltammograms recorded at different times during the step of intermediate depletion. D) Trend of VFA and formic acid concentration, as determined by NMR. E) VFA composition after 150 h.*

In **figure II-6** it is possible to see how, while the toluene concentration rapidly decreases, the oxidative current obtained during CVs increases, reaching a peak

after about 29 h (phase I). After that the current starts decreasing again (phase II). These results show that the microbial electrochemical activity is linked to the abundance of certain metabolites stemming from toluene degradation. They also seem to confirm that bioelectrochemical toluene degradation requires a syntrophic or cooperative interaction between different microbial populations: initially toluene is rapidly converted into metabolic intermediates (*i.e.* VFAs, including formate and also likely H_2), then the intermediates are further oxidized by electroactive bacteria present on the anode or, to a minor extent, in a methanogenic pathway in the bulk of the reactor. Therefore, VFAs are likely employed as electron carriers in a sort of metabolite cross-feeding. Indeed, VFAs are well-known substrates for electroactive microorganisms (Jin et al., 2016; Kiely et al., 2011; Rosales-Sierra et al., 2017; Zhang et al., 2019). It can be noticed how the accumulation process in phase I is much faster than the degradation process in phase II, which explains the different behaviour of toluene removal and current generation, which was mainly observed during the reactor's runs at high concentrations of toluene and under polarization. This mechanism can also explain why in run V the current was still relatively high even in absence of toluene: the metabolic intermediates present in the bulk or stored within the biofilm were still available for oxidation by the bioanode.

II.3.4 Microbial community features

The key functional genes involved in the anaerobic degradation of petroleum hydrocarbons were quantified using ddPCR assays. In particular, in the contaminated groundwater (T_0_bulk) the biomarkers of benzoyl-CoA desaturation (genes *bcrC, bzdN, bamB*) in the central pathway for the conversion of benzylsuccinate into acetyl-CoA (Boll et al., 2014; Fuchs et al., 2011) were present in the range 9.2 ^{3} gene copies L^{-1} and 3.7 x 10^4 gene copies L^{-1} (**Fig. II-7**), showing a high biodegradation potential. In line with the performances of the reactor, the abundances of the functional genes involved in toluene degradation (e.g., *bssA, brcC, bzdN, bamB*) were substantially higher in the liquid effluent sampled at the end of the reactor operation than in the groundwater used as

inoculum. In particular, an enrichment of the benzylsuccinate synthase (*bssA*), a biomarker gene of anaerobic toluene degrading bacteria that use fumarate addition pathway was observed (Von Netzer et al., 2016), with values ranged from 0 (b.d.l.) to 1.0 x 10^6 gene copies L^{-1}. Also, in line with the toluene degradation data, the abundance of functional genes encoding for the ATP-dependent class I (*brcC, bzdN*) and the ATP-independent class II (*bamB*) benzoyl CoA reductases were higher in the bulk at the end of the reactor operation rather than in the inoculum. In detail, the *bamB* gene accounted for 5.7 x 10^4 gene copies L^{-1}, *bcrC* for 1.9 x 10^7 gene copies L^{-1}, and *bzdN* for 2.2 x 10^5 gene copies L^{-1}. The key-functional genes involved in the anaerobic toluene degradation pathway were highly abundant also in the biofilm grown on graphite rods (**Fig. II-7**), suggesting an electroactive microbial community highly involved in this process. In particular, the *bcrC* showed the highest abundance (1.2 x 10^7 gene copies per cm^2 graphite), followed by *bssA* (3.7 x 10^4 gene copies per cm^2 graphite), *bamB* (9.0 x 10^3 gene copies per cm^2 graphite), and *bzdN* (3.3 x 10^3 gene copies per cm^2 graphite).

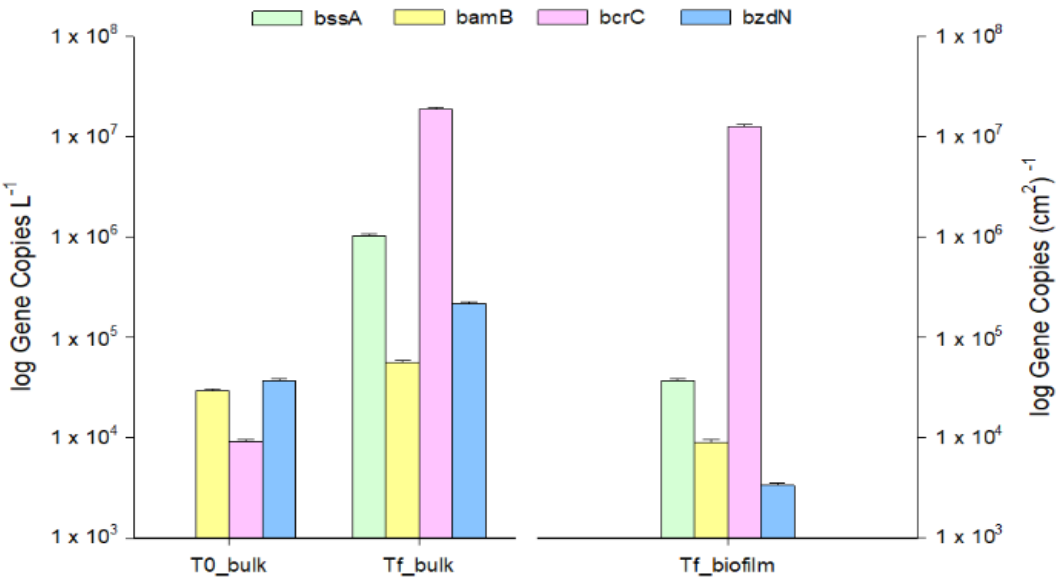

Figure II-7 *- Abundance of key-functional genes involved in anaerobic toluene degradation estimated by ddPCR in the liquid effluent of the reactor (T_0 and T_f) and biofilm grown on graphite rods. Data are reported in Log scale.*

The microbial community analysis by means of high-throughput sequencing revealed a high diversity in both bacterial (Simpson index: 0.93, Shannon: 3.37) and archaeal (Simpson index: 0.85, Shannon: 2.12) composition in the groundwater used as inoculum of the reactor. The bacterial microbiome of the liquid phase was mainly characterized by the presence of *Betaproteobacteriales* affiliated with *Undibacterium* (12.7% of total reads), *Curvibacter* (7.3%), *Ralstonia* (4.6%), and *Rhodoferax* (3.3%) genera, followed by 18.4% of reads affiliated with family *Spirochaetaceae* (phylum *Spirochaetes*) (**Fig. II-8a**). The phyla *Actinobacteria, Chloroflexi, Bacteroidetes*, and *Firmicutes* represented up to 34.8% of total reads. The archaeal portion of microbial community was mainly composed by *Methanocella* (16.2%), *Methanoregula* (21.4%), and *Candidatus Methanoperedens* (11.3%), followed by not identified members of *Micrarchaeia* (21.4) and *Woesearchaeia* (9.2%) classes (**Fig. II-8b**).

At the end of the operation, a different microbial community composition was observed in the effluent. In particular, the large majority of the bacterial reads recovered by the sequencing were affiliated with the families *Propionibacteriaceae* (52.7%), *Rhodocyclaceae* (18.5%), *Rhizobiaceae* (12.0%), and *Burkholderiaceae* (2.6%). Among these families, the presence of genera *Mesorhizobium* and *Zooglea*, together with identified members of *Rhodocyclaceae* suggested high potentialities of bulk reactor microbiome in hydrocarbon degradation (Bacosa et al., 2020; Táncsics et al., 2020, 2018; Weelink et al., 2007). Furthermore, in line with the observed production of acetic and propionic acids (Goodfellow et al., 2012), a large occurrence of *Propionicicella* (52.4%, **Fig. II-8a**) was observed. The archaeal microbiome was strongly selected (Simpson index 0.07, Shannon 0.19) and mainly represented by *Methanobacterium* (96.6% of total reads) (**Fig.II-8b**). The relative abundance of this hydrogenotrophic methanogen is in line with the CH_4 production observed in this study and consistent with previous reports on archaeal communities in methanogenic bioelectrochemical reactors (Cheng et al., 2009; Sasaki et al., 2011; Siegert et al., 2014; Van Eerten-Jansen et al., 2013).

The microbial community in the anodic biofilm grown on graphite rods provided direct evidence for the enrichment of electroactive bacteria. The classes *Anaerolineae* and *Clostridia* represented the main taxa colonizing the biofilm. Within these classes, *Anaerolineaceae*, a well-known electroactive bacterial family (Feng et al., 2020; Roustazadeh Sheikhyousefi et al., 2017; Xu et al., 2016), represented up to 34.1% of total reads (**Fig. II-8a**). Furthemore, the occurrence of several reads affiliated with genera *Geobacter and Desulfovibrio* are in line with previous evidences of these typical electroactive microorganisms in electrode biofilms (Hou et al., 2021; Lovley, 2011). Regarding the archaeal microbiome, also in the case of biofilm, *Methanobacterium* dominated the archaeal community representing up to 90.3% of archaeal reads (**Fig. II-8b**).

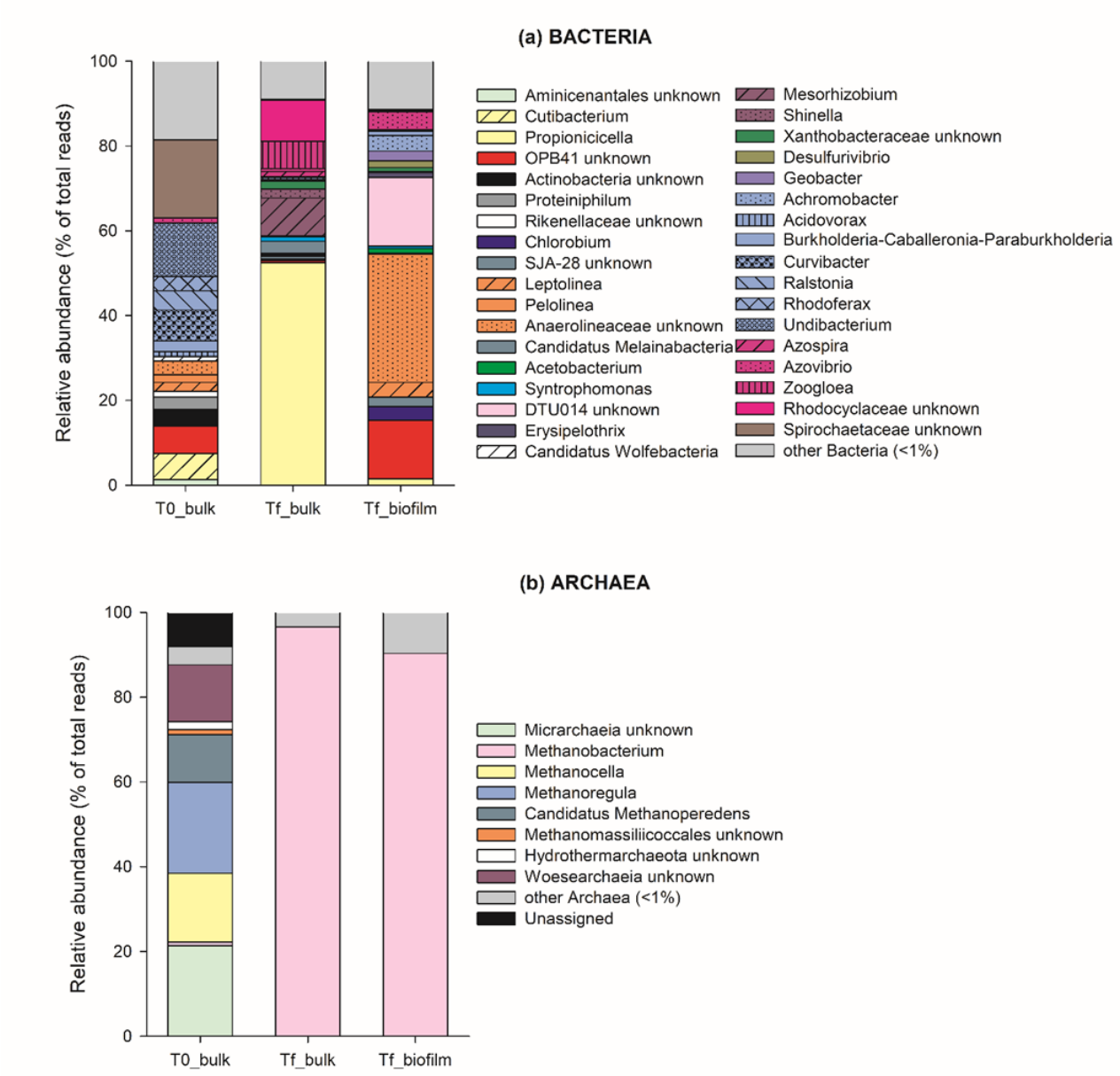

Figure II-8 *- Relative abundance (% of total reads) of bacterial and archaeal genera (≥1% in at least one sample) in the liquid effluent of the reactor sampled at the beginning (T_0) and at the end (T_f) of the experiment) and biofilm grown on graphite rods (Tf-biofilm).*

Microbiological data obtained in this study suggested a close interplay and synergy between suspended (bulk) and immobilized (biofilm) biomass, in line with reactor performance (**Fig. II-9**). Indeed, according to previous reports (Bacosa et al., 2020; Táncsics et al., 2020, 2018; Weelink et al., 2007) the hydrocarbon degraders *Rhodocyclaceae* and *Rhizobiaceae* present in the bulk could drive the

degradation of toluene leading to the production of key intermediates useful for the subsequent fermentative processes, most likely operated by *Propionicicella* members (Goodfellow et al., 2012). Progressively, the VFAs as well as H_2 produced by fermentation can be used by electroactive bacteria, namely *Geobacter*, *Desulfovibrio* and *Anaerolinaceae*, for generating CO_2 and H^+ (Laczi et al., 2020; Liang et al., 2016, 2015; Rossmassler et al., 2019). At the same time, the hydrogenotrophic methanogen *Methanobacterium* can be considered responsible for the minor methane production observed in the reactor (Cheng et al., 2009; Sasaki et al., 2011; Siegert et al., 2014; Van Eerten-Jansen et al., 2013). The microbiome described in the present study strongly supported the previous idea of a syntrophic interaction between hydrocarbon degrading bacteria, fermenters and electroactive microorganisms in bioelectrochemical systems (Gieg et al., 2014; Laczi et al., 2020). Anyway, the metabolite or electron transfer between hydrocarbon degraders and methanogenic archaea is complex and not well-understood so far (Embree et al., 2014; Gieg et al., 2014; Laczi et al., 2020).

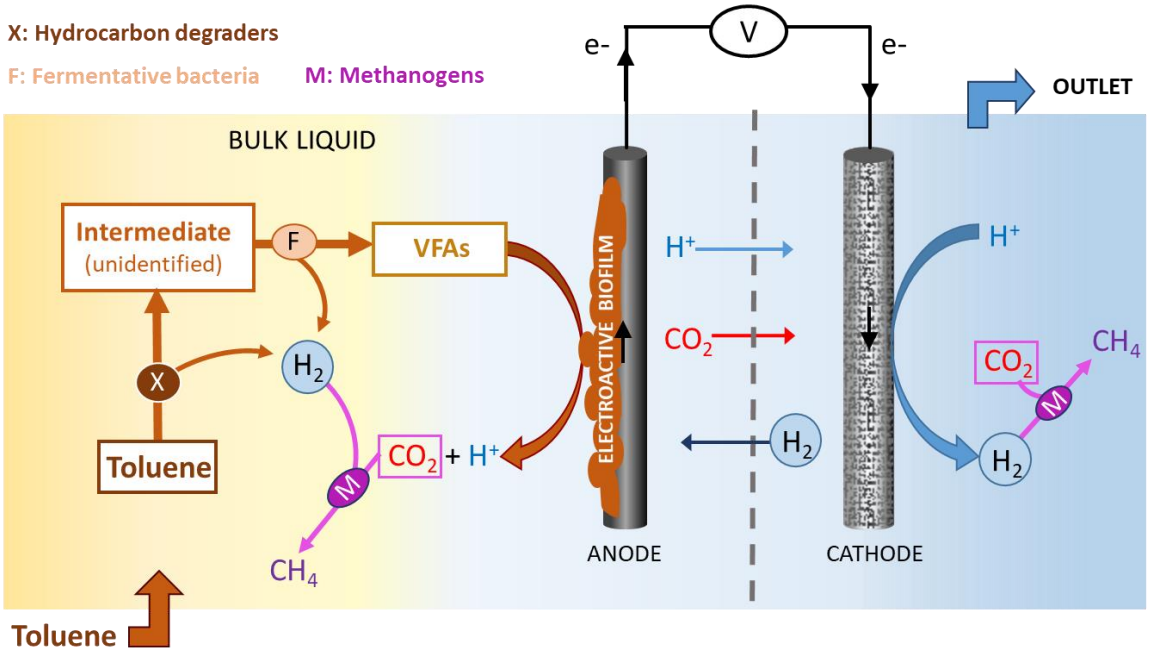

Figure II-9 *– Proposed mechanism for the bioelectrochemical degradation of toluene in the reactor while polarized and operated in continuous-flow.*

II.4 Conclusions

This study shows that the degradation of toluene to CO_2 in a bioelectrochemical system known as the “bioelectric well” is based on a syntrophic interaction between different groups of microorganisms. The degradation process involves at least two steps with different rates: in the first and faster step toluene is broken down to metabolic intermediates like VFAs by microbes able to open the aromatic ring (most probably following an initial fumarate addition). Secondly in a slower step VFAs are competitively consumed by either the electroactive biofilm on the anode or the methanogens in the bulk liquid. This mechanism explains why for higher toluene concentration the removal is linearly correlated with the toluene load, while the current generation tends to a plateau, causing a decrease of the columbic efficiency. Indeed, the metabolic intermediates accumulate in the reactor or are stored in the biofilm, causing current generation even in absence of the only carbon source (*i.e*. toluene). These findings highlight the importance of a diverse microbial environment for the successful bioelectrochemical degradation of recalcitrant pollutants such as aromatic petroleum hydrocarbons. This study further paves the way for the successful design and implementation of bioelectrochemical technologies applicable either *in-situ* or *on site*. Future research should focus on fine-tuning the reactor architecture and microbial and operational characteristic of the bioelectric well in order to optimize the removal efficiency and rate, especially in real environments.

Chapter III

Coupling of bioelectrochemical toluene oxidation and trichloroethene reductive dechlorination for single-stage treatment of groundwater containing multiple contaminants

Adapted from:

Viggi, C.C., Tucci, M., Resitano, M., Crognale, S., Franca, M.L. Di, Rossetti, S., Aulenta, F., 2022. Coupling of bioelectrochemical toluene oxidation and trichloroethene reductive dechlorination for single-stage treatment of groundwater containing multiple contaminants. Environ. Sci. Ecotechnology 11, 100171. https://doi.org/10.1016/J.ESE.2022.100171

III.1 Introduction

Petroleum hydrocarbons (PH) and chlorinated aliphatic hydrocarbons (CAH) are among the most frequent and harmful soil and groundwater contaminants (Majone et al., 2015). Their occurrence in subsurface environments, typically caused by accidental spills, leakage from underground storage tanks, as well as improper manufacturing or disposal practices, poses severe environmental and health concerns due to the relevant toxicity and recalcitrance of such compounds (Lhotský et al., 2017). In the last decades, the ever-increasing knowledge gathered on the ability of microorganisms to degrade or transform pollutants into harmless end-products and on their degradative metabolic pathways has spurred the interest towards the application of bioremediation approaches for the cleanup of contaminated sites (Alvarez and Illman, 2005; Megharaj et al., 2011; Sadañoski et al., 2020; Wu et al., 2017). These are typically based on the manipulation of environmental conditions through for instance the control of the redox potential, and/or the supplementation of electron donors or acceptors (Davoodi et al., 2020). A challenging problem related with the bioremediation of sites containing a mixture of PH and CAH is, however, the fact that these contaminants are degraded via distinctive oxidative and reductive pathways, thus requiring different amendments and redox conditions (Aulenta et al., 2006, 2005; Rabus et al., 2016; Vogt et al., 2016). In particular, the (aerobic or anaerobic) oxidative biodegradation of PH can be typically stimulated by providing naturally occurring microbial communities with an otherwise limiting electron acceptor (e.g., oxygen, nitrate, sulphate). By contrast, CAH are preferably biodegraded via a reductive pathway, often referred to as reductive dechlorination (RD) in which the chlorinated contaminant serves as a respiratory electron acceptor in the energy metabolism of so-called organohalide-respiring bacteria (OHRB) (Atashgahi et al., 2016; Aulenta et al., 2016). Among them, *Dehalococcoides mccartyi* is the only one capable of dechlorinating CAH to harmless ethene through the catalytic activity of the reductive dehalogenases (i.e., *tceA*, *bvcA*, *vcrA*) directly responsible for the RD process (Ritalahti et al., 2006). Thus, the RD of CAH can be stimulated by providing autochthonous OHRB with suitable

electron donors (i.e., H_2 or fermentable substrates). Clearly, to minimize the establishment of competitive reactions which may adversely affect the rate and efficiency of the bioremediation process, the supply of the electron acceptor (to drive the oxidation of PH) and the supply of the electron donor (to drive the RD of CAH) need to be kept separated in space or time, thereby complicating the design, operation, and control of the whole bioremediation process. In principle, a possibility exists that PH may serve as electron donors in the RD of CAH, thus simplifying the overall treatment of PH and CAH mixtures. However, this chance is greatly limited by the fact that the majority of OHRB (*e.g. Dehalococcoides mccartyi,* the only one capable of dechlorinating chloroethenes all the way to harmless ethane) are restricted to using H_2 as the sole electron donor (Löffler et al., 2013). Hence, a single stage biotreatment of PH and CAH, although of potentially great practical and economical value, would require the establishment of a close syntrophic cooperation among PH- and CAH-degrading microorganisms which is seldom observed both in the field and in laboratory experiments. In recent years, microbial electrochemical technologies (METs) have emerged as a novel and highly versatile platform for the treatment of soils and groundwater contaminated by either PH or CAH (Daghio et al., 2018; H. Wang et al., 2015). METs employ electro-active microorganisms to electro-catalyze oxidation or reduction reactions using solid-state electrodes as virtually inexhaustible electron acceptors or donors, respectively. In previous studies, METs have been successfully employed to stimulate the oxidative treatment of groundwater containing PH such as benzene, toluene, xylenes, and ethyl-benzene (BTEX) (Espinoza-Tofalos et al., 2020; Marzocchi et al., 2020; E. Palma et al., 2019; Enza Palma et al., 2018b), as well as the reductive dechlorination of a variety of CAH including perchloroethene (PCE), trichloroethene (TCE), and 1,2,-dichloroethane (1,2-DCA) (Aulenta et al., 2008b, 2008a; Lai et al., 2017; Leitão et al., 2015; Verdini et al., 2015). However, none of these studies have attempted to treat simultaneously PH and CAH at the anode and cathode of the same MET to achieve a single-stage treatment of commingled PH/CAH groundwater. Here, we explored for the first time the possibility of using a

“bioelectric well”, a previously developed MET specifically designed for *in-situ* treatment of contaminated groundwater (Enza Palma et al., 2018b), for the bioremediation of a synthetic groundwater containing a mixture of toluene (model PH) and TCE (model CAH). Results demonstrated that the electric current deriving from the microbially-driven oxidation of toluene at the anode generates H_2 at the cathode which, in turn can sustain the RD of TCE to less-chlorinated or eventually non-chlorinated end-products.

III.2 Experimental Section

III.2.1 Reactor setup and operations

The bioelectrochemical reactor used in the present study consisted of a 250 mL-glass cylinder filled with river sand to simulate a real groundwater environment and increase the surface area where microorganisms can adhere, and housing 8 contiguous graphite rods (purity: 99.995%, length: 30 cm, ø: 0.6 cm; Sigma-Aldrich, Italy) and a concentric stainless-steel mesh cathode (dimensions: 3 x 30 cm; type 304, Alpha Aesar, USA) (Figure 1A). Anode and cathode were kept physically separated by a polyethylene mesh (ø: 1cm, length 30 cm; Figure 1B), which still allowed hydraulic connection between the anodic and cathodic zones. An Ag/AgCl reference electrode (+198 mV versus the standard hydrogen electrode, SHE) was placed on top of the cylinder to control, by means of an IVIUMnSTAT potentiostat (IVIUM Technologies, The Netherlands), the potential of the anode at the desired value (i.e., +200 mV *vs*. SHE). Titanium wires (ø: 0.81mm Alfa Aesar, USA) were used to connect anode and cathode to the potentiostat. At the start of the study the reactor was inoculated with 0.2 L of groundwater from a toluene-contaminated site in Italy (Tucci et al., 2021) and with 50 mL of a TCE-to ethene dechlorinating enrichment culture (Masut et al., 2021). Throughout the study, the reactor was continuously fed with a synthetic groundwater consisting of an anaerobic mineral medium spiked with toluene and TCE (Sigma-Aldrich, Italy) at the desired concentrations (**Tab.III-1**). The medium contained the following components: NH_4Cl (0.5 g/L), $MgCl_2 \cdot 6H_2O$ (0.1 g/L),

K_2HPO_4 (0.4 g/L), and $CaCl_2 \cdot 2H_2O$ (0.05 g/L), 2 mL/L of a trace metal solution (Balch et al., 1979), 2 mL/L of vitamin solution (Zeikus, 1977)(**Tab II-1**). The electrical conductivity of the medium was 4.8 mS/cm, hence within the range of values typically reported for highly contaminated groundwater (i.e., 0.67 to 7.98 mS/cm) (Naudet et al., 2004). During operation, the synthetic groundwater was maintained in a 5 L collapsible Tedlar® bag and entered the reactor through a port situated at the bottom of the cylinder (flow rate: 0.75 L/d, HRT 9.3 h), while the treated effluent exited from a port positioned near the upper end (**Fig. III-1**). The inlet and the outlet of the reactor were equipped with flow-through, vigorously stirred, sampling cells (volume: 25 mL). All the tubes were made of Viton® (Sigma-Aldrich, Italy), which keeps volatilization losses and organic contaminant adsorption to a minimum. Throughout the whole study, the system was kept at room temperature (i.e., 24 ± 3°C).

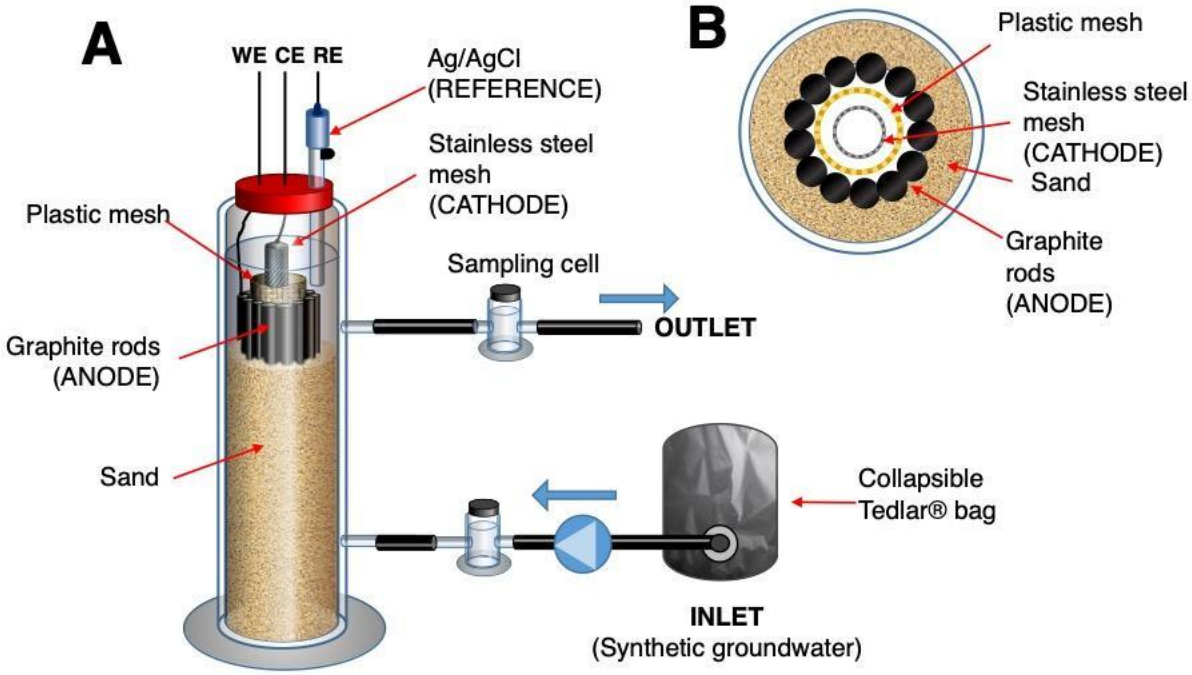

Figure III-1. *Schematic drawing of the continuous flow bioelectrochemical reactor (A); cross-sectional view of the bioelectrochemical reactor displaying the relative position of electrodes.*

Table III-1. *Main operating conditions applied during the different experimental runs*

	Run I	**Run II**	**Run III**	**Run IV**
Operational period (days)	0-10	11-24	25-38	39-53
Anode polarization (V *vs.* SHE)	+0.2	+0.2	+0.2	OCP
HRT (h)	9.3	9.3	9.3	9.3
Average influent Toluene conc. (μmol/L)	170±6	161±7	82±8	119±3
Average influent TCE conc. (μmol/L)	170±15	-	110±9	157±6

III.2.2 Gas analyses

Gaseous samples, taken from the sampling cells using gastight syringes, were analyzed in terms of O_2, H_2 and CH_4 using a gas-chromatograph (Agilent 8860, GC system USA) equipped with a thermal conductivity detector (TCD). The concentration of toluene, TCE, cis-dichloroethene (cis-DCE), vinyl chloride (VC) and ethene (ETH), were measured by injecting gaseous samples into gas-chromatograph (Agilent 8860, GC system USA) equipped with a flame ionization detector (FID). Gas-phase concentrations were converted into liquid-phase concentrations using tabulated Henry's Law constants (Sander, 2015). The GC methods, calibration ranges and LOD of analytical methods are reported in **Table II-2**.

III.2.3 High-Throughput bacterial and archaeal 16S rRNA Gene Sequencing

Sample of effluent at the beginning of the experiment T_0: 1 L) and at the end of Run III (15 mL) were filtered through polycarbonate membranes (pore size 0.2 mm, 47 mm diameter, Nuclepore) and immediately stored at -20°C. Genomic DNA was extracted with the DNeasy PowerSoil Pro Kit (QIAGEN - Germantown, MD) and utilized as template for the amplification of the V1-V3 region of 16S rRNA gene of *Bacteria* (27F 5'-AGAGTTTGATCCTGGCTCAG-3'; 534R 5'-ATTACCGCGGCTGCTGG-3') and the region V3–V5 of 16S rRNA gene of *Archaea* (340F 5'-CCCTAHGGGGYGCASCA-3'; 915R 5'-GWGCYCCCCCGYCAATTC-3') following the procedure for library preparation

and sequencing described in Crognale et al., (2019). The paired end sequencing (2x301bp) was performed on a MiSeq platform (Illumina) using a MiSeq Reagent kit v3, 600 cycles (Illumina, USA) following the standard guidelines for preparing and loading samples. Phix control library was spiked at a concentration of 20%. Bioinformatics analyses were carried out using QIIME2 v. 2018.2 (Bolyen et al., 2019) following the procedure previously reported (Crognale et al., 2021). High-throughput sequencing of the V1-V3 and V3-V5 regions of the bacterial and archaeal 16S rRNA gene yielded a total of 20,438 and 30,988 sequence reads after quality control and bioinformatic processing that resolved into 318 and 15 ASVs, respectively. Datasets are available through the Sequence Read Archive (SRA) under accession PRJNA799244.

III.2.4 Droplet Digital PCR quantification of key-functional genes

The QX200™ Droplet Digital™ PCR System (ddPCR™, Bio-Rad, USA) was used to perform absolute quantification of the functional genes involved in the anaerobic degradation of PH and CAH. For the estimation of PH related genes, such as benzylsuccinate synthase (*bssA* gene) and benzoyl CoA reductases class I (*bcrC, bzdN*) and class II (*bamB*), the ddPCR reaction mixture consisted of 11 µL of 2× ddPCR EvaGreen supermix (Bio-Rad, USA), 1 µL of each primer (at 7.5 µM concentration), 6 µL of nuclease-free water, and 3 µL of sample DNA. For the quantification of the reductive dehalogenase genes *tceA*, *bvcA* and *vcrA*, the PCR reaction mixtures were prepared in a 22 µL total volume for each sample, including ddPCR Supermix for Probes® (Bio-Rad, USA), 3 µL of DNA as a template, 900 nM of each primer and 300 nM of TaqMan probe. The set of primer and probes used are summarized in Table S1. Droplets were generated using an eight-channel DG8 cartridge and cartridge holder (Bio-Rad, USA). 20 µL of PCR reaction mixture were combined with 70 µL of droplet generation oil and placed in QX200 Droplet Generator (Bio-Rad, USA). Following droplet generation, 40 µL of water-in-oil droplets were transferred to a standard 96-well PCR plate, which was heat sealed with foil plate using the PX1™ PCR plate sealer (Bio-Rad, USA) and amplified with the T100 thermal cycler (Bio-Rad,

USA). PCR cycle parameters for PH-related genes were as follows: 5 min at 95°C, followed by 39 cycles of 30 s at 95°C and 1 min at 55-60°C according to the primer pair (ramping speed at 2°C/s), followed by 5 min hold at 4°C and 5 min at 95°C. Whereas the PCR cycling conditions for the *tceA, bvcA* and *vcrA* genes were: 10 min at 95° C, 39 cycles for 30 sec at 94°C and 1 min at 60°C (ramping rate set to 2 °C/s), 10 min at 98°C, ending at 4°C. Upon completion of PCR, the plate was transferred to QX200 Droplet Reader (Bio-Rad, USA) to detect positive and negative fluorescent droplets for calculation of the targeted gene concentrations. Data were analyzed using QuantaSoft Software® (Bio-Rad, USA) and quantitative data were reported as gene copy numbers per volume of sample (95% confidence intervals).

III.2.5 Calculations

The removal rate of toluene and TCE q (μmol/L d) were calculated using the following equation:

$$q = \frac{C_{in} - C_{out}}{V_r} Q \qquad (1)$$

where C_{in} and C_{out} (μmol/L d) are the toluene or TCE liquid phase concentrations measured in the influent and the effluent, V_r (L) is the empty volume of the reactor and Q (L/ d) is the volumetric flow rate.

Similarly, the formation rate of TCE reductive dechlorination products q_{RD} (μeq/L d) was calculated as:

$$q_{RD} = \frac{C_{out,DCE} \times 2 + C_{out,VC} \times 4 + C_{out,ETH} \times 6}{V_r} Q \qquad (2)$$

Where $C_{out,DCE}$, $C_{out,VC}$, and $C_{out,ETH}$ (μmol/L d) are the measured liquid phase concentration of dechlorination products and 2, 4, or 6 are the number of moles of electrons required for the formation of 1 mol of cis-DCE, VC, ethene from TCE, respectively (Aulenta et al., 2011).

The toluene or TCE removal $_{\%}$ were calculated as follows:

$$\eta_{\%} = \frac{C_{in} - C_{out}}{C_{in}} \times 100 \quad (3)$$

The columbic efficiency (*CE*) was calculated as the ratio between charge that is the integral of the electric current over time and the theoretical charge deriving from the oxidation of removed toluene, according to the following equation:

$$CE(\%) = \frac{\int i(t) \times dt \times 60 \times 60 \times 24}{(\Delta_{Tol} \times f_{Tol}) \times F} \times 100 \quad (4)$$

where *i* is the measured current (mA), *F* is the Faraday's constant and Δ_{Tol} is the amounts of removed toluene per day (mmol/d), f_{Tol} represents the number of mmol of electrons released from the complete oxidation of 1 mmol of toluene.
The apparent activation energy of the current-producing, toluene degradation rate was estimated as reported elsewhere (Liu et al., 2011). In brief, as electric current is proportional to toluene degradation rate, which is in turn proportional to the rate constant, then in a narrow temperature range (15-25 °C), it is possible to represent the data by the following Arrhenius equation:

$$\ln k = \ln A - Ea/RT \quad (5)$$

where k is the rate constant, Ea (J/mol) the apparent activation energy, R the gas constant (J/mol K), T (K) the temperature, and A the preexponential factor.

III.3 Results and discussion

III.3.1 Performance of the continuous flow bioelectrochemical reactor

The continuous flow bioelectrochemical reactor was operated for a period of 53 days (i.e., corresponding to nearly 140 HRT) under different operating conditions, as summarized in **Table III-1**.

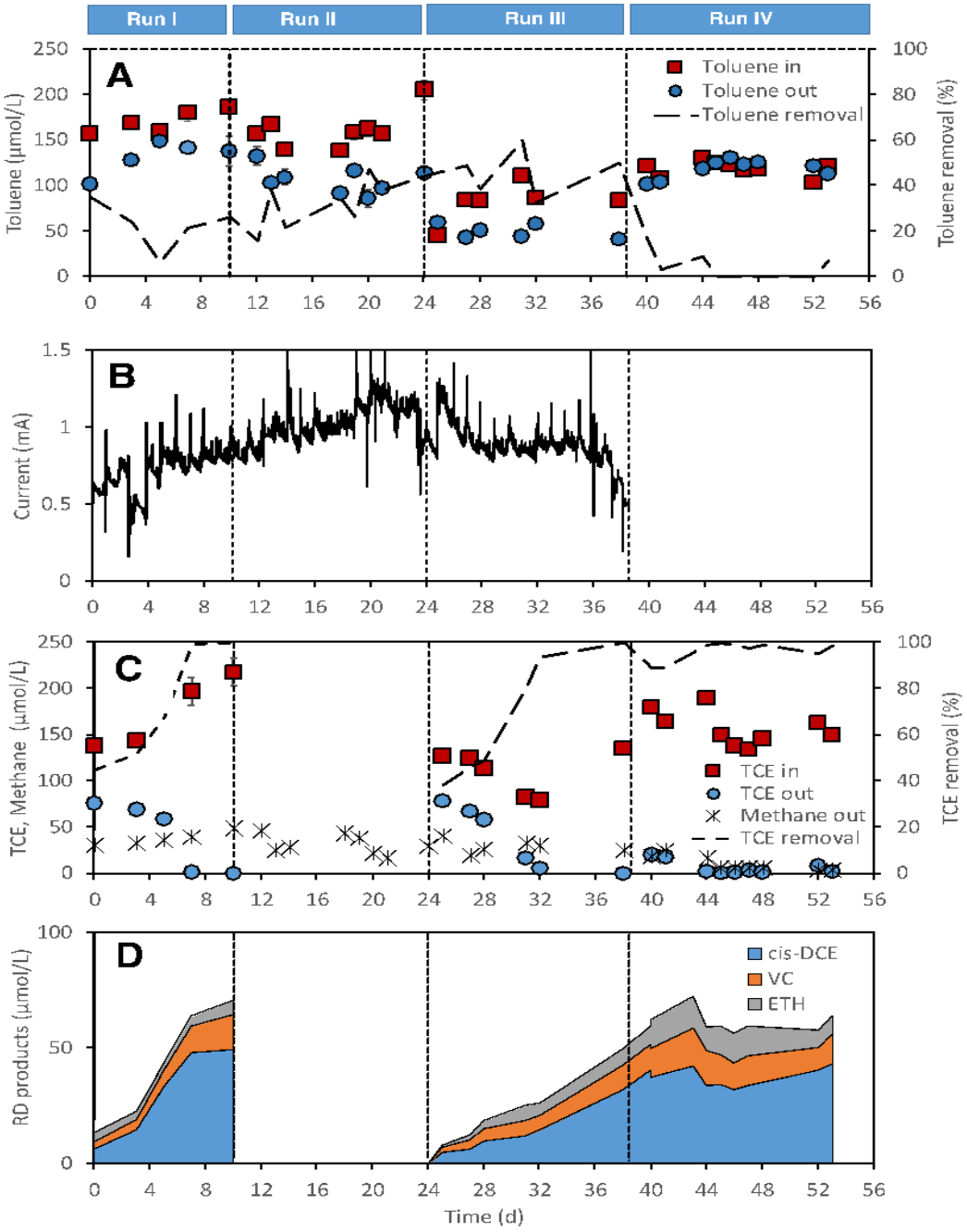

Figure III-2. *Performance parameters of the continuous flow bioelectrochemical reactor under the different experimental Runs. Time-course of influent and effluent toluene concentration and toluene removal efficiency (A); electric current generated from toluene oxidation (B); influent and effluent TCE concentration and effluent methane concentration (C); concentration of TCE reductive dechlorination products (D).*

During Run I, the feed solution contained a mixture of toluene (170±6 μmol/L) and TCE (170±15 μmol/L) as co-contaminants, while the anode of the reactor was poised at +0.2 V *vs*. SHE. On average, during this run, 23±5% of the influent toluene was removed (**Fig. III-2A**). Toluene removal was accompanied by electric current generation, which gradually increased from around 0.55 mA to 0.85 mA, throughout the run (**Fig. III-2B**). The resulting average coulombic efficiency was 40±4 %, thus likely indicating that other biotic (e.g., methanogenic biodegradation) or abiotic (e.g., adsorption and/or volatilization) processes also contributed to the observed toluene removal. Interestingly, TCE removal (**Fig. III-2C**) also increased over time (up to nearly 100% by day 7), as well as the sum of reductive dechlorination products (**Fig. III-2D**), mainly consisting of cis-DCE (50%, on an electron equivalent basis), VC (30%) and ETH (20%), thus mirroring the observed trend of the electric current. Methane was also detected in the effluent of the reactor at an average concentration of 38±3 μmol/L. In principle, methane production could derive both from the syntrophic conversion of toluene (Edwards and Grbić-Galić, 1994), a metabolic process in competition with electric current generation, or from the biological reduction of carbon dioxide fuelled by cathodic H_2. Throughout the whole experimental period, the pH of the influent and effluent of reactor were typically in the range 6.5-7 and were statistically indistinguishable. This reflects the fact that the (proton-releasing) anodic reaction and the (proton-consuming) cathodic reaction occurred in the same reaction environment, hence preventing the establishment of pH gradients.

During Run II, TCE was omitted from the synthetic groundwater and the reactor was fed with toluene as the only organic contaminant. This change resulted in a slight increase in toluene removal which averaged 33±4 % (**Fig. III-3A**), in electric current generation which steadily increased up to nearly 1.2 mA (**Fig. III-3B**), and in the average coulombic efficiency which accounted for 58±7 %. This latter value clearly indicates that electric current generation was the primary biological mechanism underlying toluene removal. Taken as a whole, these findings point to a slight inhibitory effect of TCE on the conversion of toluene into electric

current, which can at least partially explain the lower toluene degradation rates observed in the present study compared to previous investigations in which, however, toluene was supplied as the only organic contaminant (E. Palma et al., 2018; Tucci et al., 2021). During Run III, the influent toluene concentration was halved (82±8 μmol/L) and the influent TCE concentration was reduced by 35%. (**Fig. III-2**). This resulted in a decrease of the average toluene removal rate (**Fig. III-3A**) and of the produced electric current (**Fig. III-3B**), hence confirming the existing correlation between these two parameters. Analogously to what observed during Run I, also during Run III the removal of TCE (and the corresponding formation of RD products) steadily increased over time until reaching, by the end of the run, values comparable to those observed during Run I (**Fig. III-3C**). Collectively, this finding suggests that TCE dechlorination was apparently not limited by electron donor (H_2 or electrons) availability, in agreement with the stoichiometry of the involved reactions which indicates that the complete electrogenic biodegradation of 1 mol of toluene (equation 5) would provide sufficient H_2 (equation 6) to drive the complete reduction of 6 mol of TCE to ethene (equation 7).

$$C_7H_8 + 14H_2O \rightarrow 7CO_2 + 36H^+ + 36e^- C_7H_8 + 14H_2O \rightarrow 7CO_2 + 36H^+ + 36e^- \quad (5)$$

$$36e^- + 36H^+ \rightarrow 18H_2 36e^- + 36H^+ \rightarrow 18H_2 \quad (6)$$

$$6C_2HCl_3 + 18H_2 \rightarrow 6C_2H_4 + 18HCl 6C_2HCl_3 + 18H_2 \rightarrow 6C_2H_4 + 18HCl \quad (7)$$

During the last operational run, toluene and TCE were simultaneously fed to the bioelectrochemical reactor which, however, was maintained at open circuit potential (OCP). Notably, upon removal of anode polarization, toluene biodegradation ceased almost immediately, and the effluent concentration rapidly equalled the influent concentration (**Fig. III-2A**). Upon interruption of the anodic polarization, the RD of TCE ceased to increase and stabilized at values similar to those observed during the previous runs. Most probably, during the whole Run III, the reductive dechlorination of TCE was fuelled by electrons deriving from the

endogenous decay of the biomass present within the bioreactor (e.g., the anodic biofilm grown on toluene). Although such a metabolic activity is clearly meant to decline over time and therefore cannot be sustained over a long-term, it may still be important in buffering TCE dechlorination during periods in which electrode polarization is temporarily dismissed.

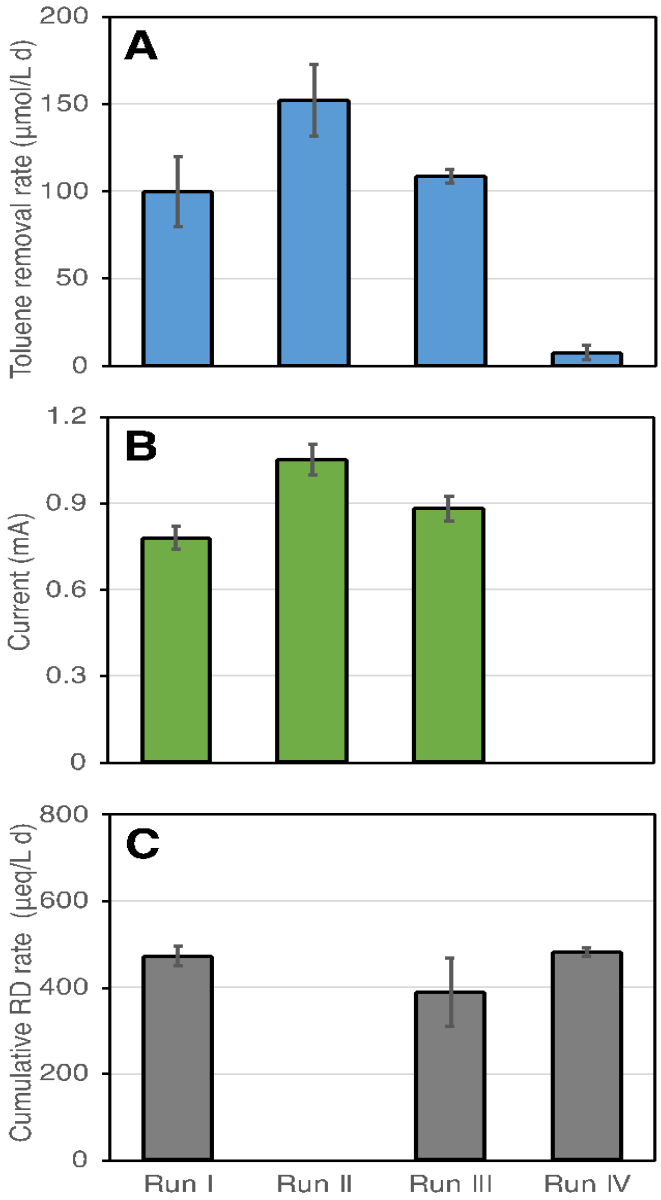

Figure III-3. *Average toluene removal rate (A), electric current generation (B), and cumulative reductive dechlorination rate (C) during the different experimental runs. As for the reductive dechlorination rate, reported values refer to the last data points of each run when a nearly stable activity was achieved. The error bar indicates the standard error of the mean.*

III.3.2 Mass-transport limitations

The observed inhibitory effect of TCE on the electrogenic toluene degradation was not sufficient to explain the substantially lower (around 3-fold) performance of the bioelectrochemical reactor, particularly in terms of toluene removal and electric current generation, relative to previous studies, notwithstanding the fact that the same inoculum and identical anodes were employed no such citation. In that previous case, however, the bioelectrochemical reactor was equipped with an internal recycle of the liquid phase to minimize the establishment of substrate/products concentration gradients and was not filled with sand, as in the present case. Hence, to verify whether the performance of the reactor was controlled by mass-transport limitations triggered by the adopted changes in the reactor configuration, we analyzed the existing correlations between the electric current and the ambient temperature (**Fig. III-4A**). In brief, as the electric current is proportional to the rate of toluene oxidation which is in turn proportional to the rate constant of the reaction, experimental data collected during Run III were plotted in Arrhenius form (ln *i* vs. 1/T) to determine the “apparent” activation energy of the reaction (i.e., the current response of the system to temperature variations; **Fig. III-4B**). Although, to the best of our knowledge, no other values of the activation energy are available in the literature for the electrogenic toluene oxidation reaction, the herein obtained value of 25.9 ± 0.3 kJ/mol is substantially lower with respect to values reported for other bioelectrocatalytic reactions, or for (bio)chemical reactions in general, which typically fall within the range (40–80 kJ/mol) (Bailey, 1980; Liu et al., 2011; Villano et al., 2011). Collectively, this result provides a strong line of evidence that the electric current deriving from the microbially-driven toluene oxidation was in turn rate-limited by mass-transport of the substrate (or products) rather than by the intrinsic kinetics of the bioelectrocatalytic reaction.

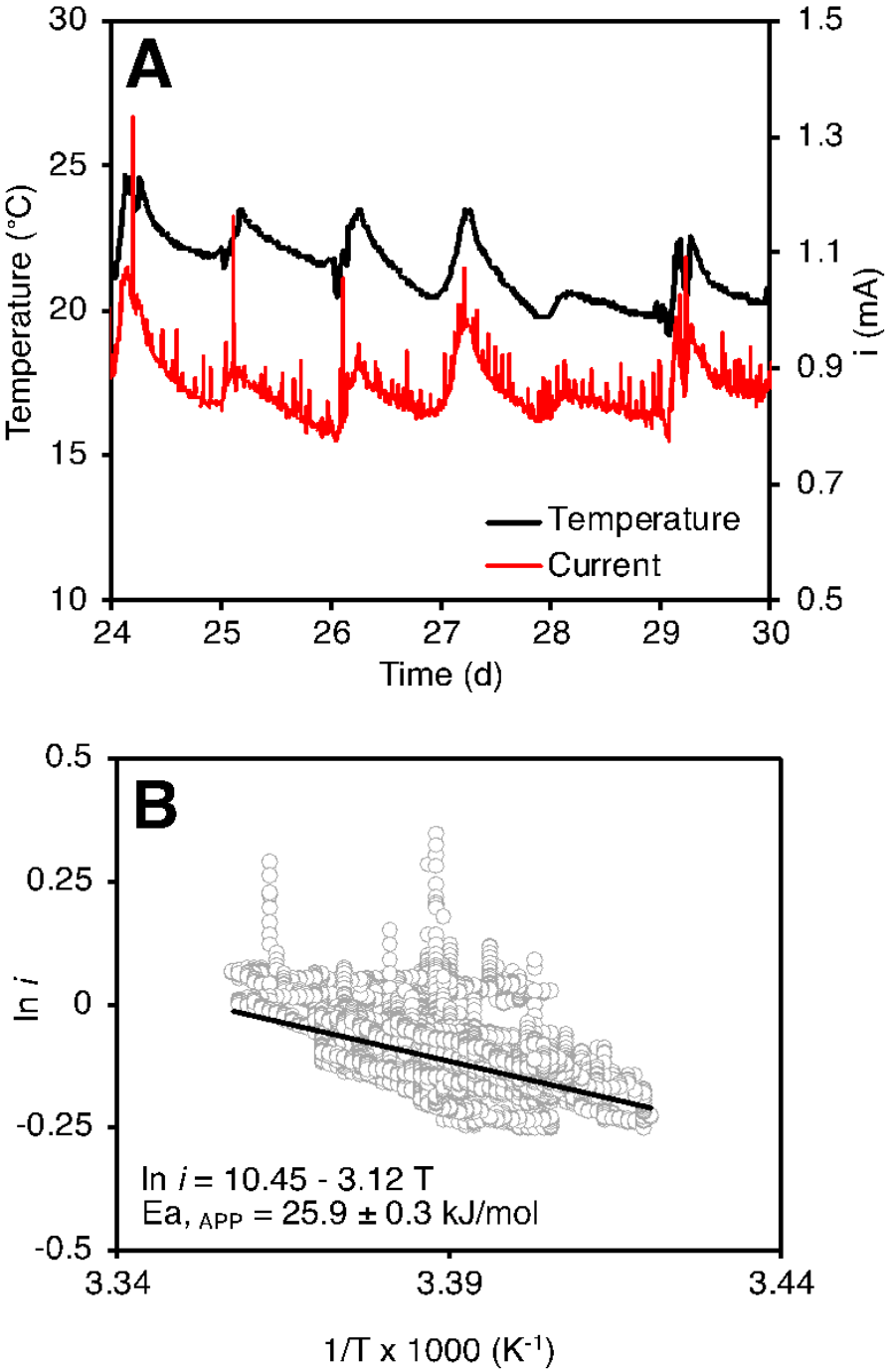

***Figure III-4**. Fluctuations of electric current and ambient temperature relative to the period of Run 3 from day 24 to day 30 (A). Dependence of electric current on temperature: Arrhenius plot (B).*

III.3.3 Microbial community characterization

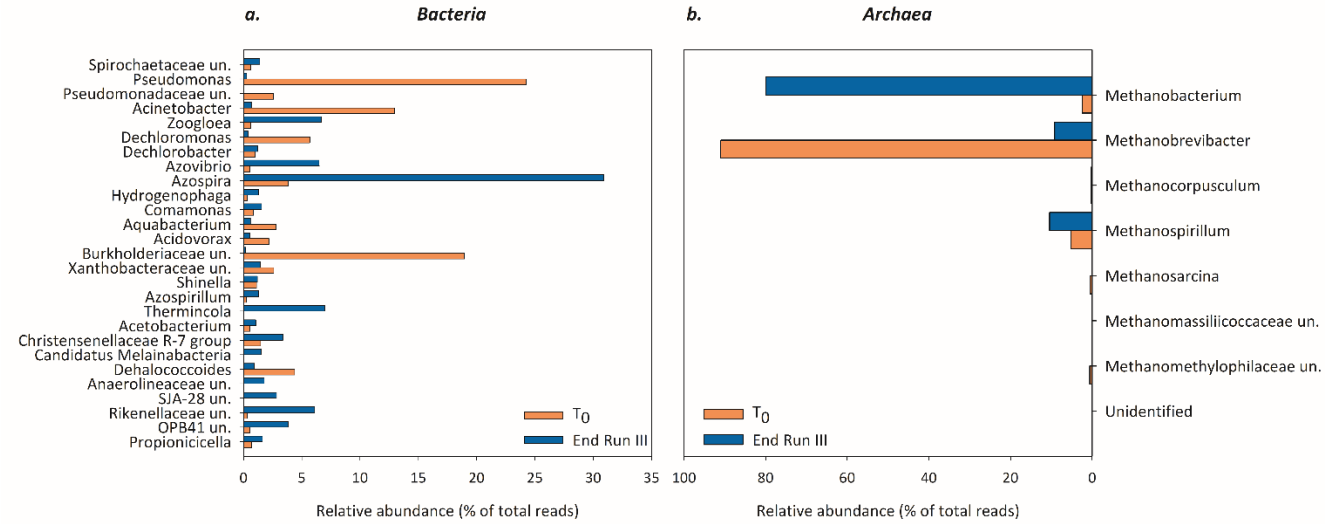

***Figure III-5**. Microbial characterization at genus-level of bacterial (A) (only genera >1% of total reads in at least one sample are depicted) and archaeal (B) communities within the bioelectrochemical reactor estimated by high-throughput sequencing.*

The biomolecular characterization revealed slight differences among microbial communities at the beginning of the experiment and at the end of Run III within the bioelectrochemical reactor. The results obtained with the high-throughput sequencing of bacterial and archaeal 16S rRNA gene suggested an initial high potential in PH degradation and TCE-RD. Indeed, the microbiome at T_0 is mainly composed by genera *Pseudomonas* (24.2% of total reads), *Acinetobacter* (13.0%), *Dechloromonas* (5.7%), *Dehalococcoides* (4.4%), *Dechlorobacter* (1.0%), and unidentified members of *Burkholderiaceae* family (19.0%) (**Fig. III-5a**). The presence of these genera was often reported in previous studies for their capability to degrade petroleum hydrocarbon and to reduce chlorinated compounds (Crampon et al., 2018). The archaeal microbiome was mostly composed by genus *Methanobrevibacter* (91.0%), followed to minor extent by *Methanospirillum* (5.2%) and *Methanobacterium* (2.4%) (**Fig. III-5a**).

The characterization at the end of Run III revealed a bacterial community mainly represented by genera *Azospira* (30.9%), *Thermincola* (7.0%), *Zooglea* (6.7%), and *Azovibrio* (6.5%). Overall, AVSs affiliated with *Rhodocyclaceae* family represented 45.5% of the total sequences. Notably, its members are commonly

found in polluted environments and are typically associated with the anaerobic biodegradation of a wide range of aromatic hydrocarbons. The presence of genera *Thermincola* and *Zooglea* can be related to the toluene degradation observed in the bioelectrochemical reactor. These genera are, indeed, reported to be active degraders of petroleum hydrocarbons (Táncsics et al., 2020; Toth et al., 2021). The presence of *Azovibrio*, a microaerophilic, N_2 fixing bacterium, capable of using oxygen, nitrate or even perchlorate as terminal electron acceptor, have been previously demonstrated to boost bioremediation processes in oil-contaminated soils (Sarkar et al., 2016; Yang et al., 2014). Members of genus *Dechloromonas*, together with the closely related *Azospira,* are considered to represent the predominant perchlorate-reducing bacteria in the environment and have been found to be ubiquitous (Chakraborty et al., 2005; Coates et al., 1999; Weelink et al., 2010). Several strains of *Dechloromonas* have been studied for their capability to degrade benzene, toluene, ethylbenzene, and xylene compounds both aerobically and anaerobically with perchlorate or chlorate as a suitable electron acceptor (Chakraborty et al., 2005). Furthermore, in line with low CH_4 production herein measured and with previous evidence in methanogenic bioelectrochemical reactors (Cheng et al., 2009; Sasaki et al., 2011; Siegert et al., 2014; Van Eerten-Jansen et al., 2013), archaeal microbiome was mostly represented by hydrogenotrophic methanogens affiliated with genera *Methanobacterium* (79.9%), *Methanospirillum* (10.4%), and *Methanobrevibacter* (9.2%) (Fig.5b). In line with sequencing output and process data, the abundance of key-functional genes involved in PH-degradation (i.e., *bssA, brcC, bzdN, bamB*) and TCE-reductive dechlorination (i.e., *tceA*, *vcrA*, *bvcA*) were quantified in the samples at T_0 and at the end of run III (**Fig. III-6**). In detail, the abundance of benzylsuccinate synthase (*bssA*), the biomarker gene of anaerobic toluene degrading bacteria that use fumarate addition pathway (Von Netzer et al., 2016), showed similar values between the beginning of the experiment and the end of run III (on average 2.1 x 10^5 gene copies/L; **Fig. III-6a**), consistently with the toluene degradation rate observed in the reactor. Furthermore, the abundance of *bcrC* and *bzdN* genes, encoding for the ATP-dependent class I benzoyl CoA

reductases (Boll et al., 2014; Fuchs et al., 2011), decreased from 4.4 x 10^7 to 1.8 x 10^6 and from 1.4 x 10^5 to 4.0 x 10^4 gene copies/L, respectively (**Fig. III-6a**). A slight increasing trend was, instead, observed for the ATP-independent class II (*bamB*) benzoyl CoA reductases counting 6.2 x 10^4 gene copies/L in the sample at T_0 and 1.8 x 10^5 gene copies/L at the end of run III (**Fig. III-6a**)

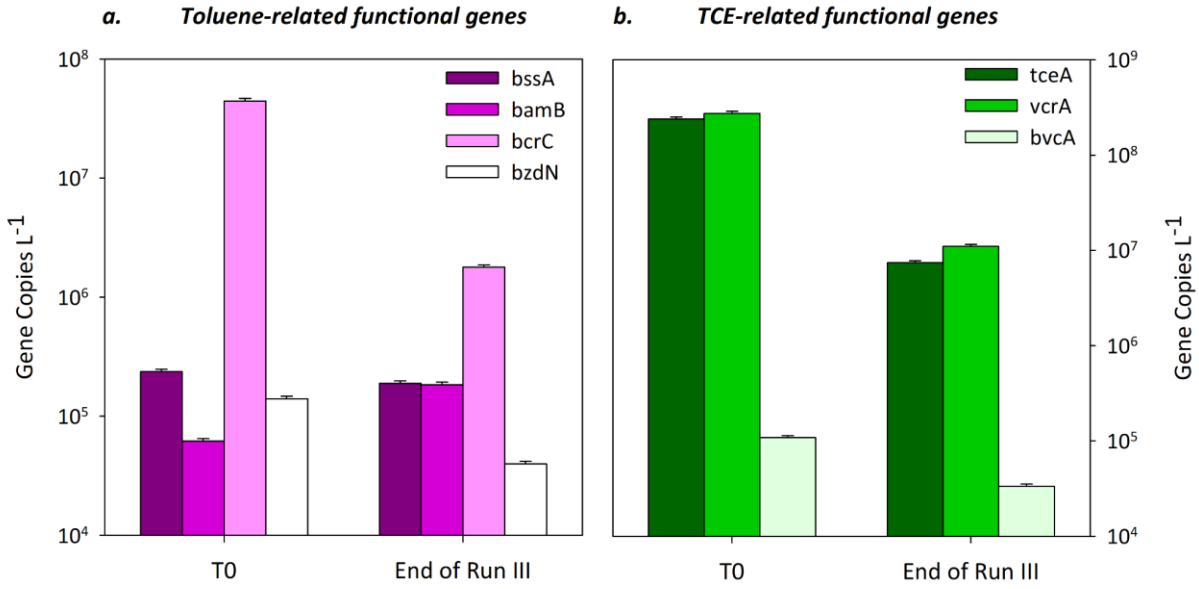

***Figure III-6**. Abundance of key-functional genes involved in anaerobic toluene degradation (a) and TCE reductive dechlorination (b) estimated by ddPCR in the effluent of the reactor at the beginning of the experiment (T0) and at the end of run III. Data are reported in Log scale.*

In addition, at the beginning of the experiment, *tceA* (2.4 x 10^8 gene copies/L) and *vcrA* (2.7 x 10^8 gene copies/L) were the most abundant reductive dehalogenase genes found, while *bvcA* (1.1 x 10^5 gene copies/L) was detected at minor extent (**Fig. III-6b**). In line with the decrement of the cumulative RD rate observed at the end of the run III, all the reductive dehalogenase genes analysed decreased at least by one order of magnitude and accounted for 7.4 x 10^6, 1.1 x 10^7 and 3.3 x 10^4 gene copies/L of *tceA*, *vcrA,* and *bvcA*, respectively (**Fig. III-6b**). Overall, differences in terms of microbial composition and abundance of key-functional genes were observed at the end of run III in comparison with T_0, most likely due to the various experimental conditions tested. However, even though these variations affected the microbial communities, a microbiome highly

involved in the simultaneous toluene degradation and TCE-reductive dechlorination was strongly established. In fact, the microbiological results fully supported the PH-degradation and TCE-reductive dechlorination rates observed in this study.

III.4 Conclusions

This study demonstrated, for the first time, the possibility to treat a (synthetic) groundwater containing a mixture of toluene and TCE using a single stage bioelectrochemical system which exploited a graphite anode (for toluene oxidation) and a stainless-steel cathode (for TCE reduction) positioned in the same reaction environment. The electric current (up to nearly 1 mA) resulting from the microbially-catalyzed oxidation of toluene (with a maximum observed removal rate of 150 μmol/L d), with a polarized anode (+0.2 V vs. SHE) serving as terminal electron acceptor. The hydrogen produced (abiotically) at the cathode sustained, in the bulk of the reactor, the partial dechlorination of TCE to less-chlorinated intermediates (i.e., cis-DCE, VC, and ETH), at a maximum rate of 500 μeq/L d. Toluene degradation and current generation were, however, found to be rate-limited by external mass transport phenomena. Further studies, focusing on the identification of alternative packing materials and on the application of different hydrodynamic regimes are thus needed to improve the catalytic efficiency of the treatment system. Furthermore, in spite of the abundance of *Dehalococcoides mccartyi* and of the related dechlorination functional genes (up to nearly 10^7 copies/L for *tceA* and *vcrA*), TCE degradation appeared to be relatively slow and incomplete, likely due to an ineffective utilization of the generated hydrogen. Thus, also in this case, further research efforts are certainly warranted to increase the rate and yield of TCE conversion, possibly into harmless non-chlorinated end products.

Chapter IV

Toluene-driven anaerobic biodegradation of chloroform in a continuous-flow bioelectrochemical reactor

Adapted from:

Tucci, M., Fernández-Verdejo, D., Resitano, M., Ciacia, P., Guisasola, A., Blánquez, P., Marco-Urrea, E., Viggi, C.C., Matturro, B., Crognale, S., Aulenta, F., 2023. Toluene-driven anaerobic biodegradation of chloroform in a continuous-flow bioelectrochemical reactor. Chemosphere 338, 139467. https://doi.org/10.1016/J.CHEMOSPHERE.2023.139467

IV.1 Introduction

Due to their widespread usage, chlorinated compounds and aromatic hydrocarbons are among the most frequent groundwater and soil contaminants (Rivett et al., 2011). Their occurrence in subsurface environments is mainly caused by industrial activities, surface runoff, accidental spills from tanks and pipes, improper handling or disposal practices (Blázquez-Pallí et al., 2019; Collins et al., 2002). Due to their toxicity and persistence in the environment, these contaminants pose high risks to human health and the ecosystem (Chary and Fernandez-Alba, 2012). Bioremediation is considered a very effective approach to treat these kinds of pollutants, having in general lower requirements in terms of costs, equipment, labour and energy, and a lower environmental impact compared with conventional physicochemical techniques, such as air sparging and activated carbon adsorption, which also typically result in a phase transfer of contaminants without an effective degradation (Lhotský et al., 2017). However, the presence of multiple types of contaminants in the same site may complicate operations and increase the costs of bioremediation, since different treatments need to be implemented in different times and space to meet the distinct metabolic needs of the different microbial degraders (Megharaj et al., 2011; Rabus et al., 2016). As aromatic hydrocarbons are preferentially degraded via oxidative pathways, the microbial community requires availability of high potential electron acceptors such as oxygen or nitrate (Allard and Neilson, 1997; Jabbar et al., 2022). On the contrary, the reductive dechlorination of chlorinated compounds, carried out by organohalide-respiring bacteria (OHRB), requires an electron donor (*i.e.* molecular hydrogen) while the contaminant serves as the respiratory electron acceptor (Farhadian et al., 2008).

Theoretically, it would be possible to exploit the oxidation of aromatic hydrocarbons as source of electrons for the reduction of chlorinated compounds. However, since most OHRB are restricted to using H_2 as electron donor, the possibility of carrying out the simultaneous removal of both types of pollutants in a single-step reaction is very limited (Soder-Walz et al., 2022). Microbial electrochemical systems (MESs) are being proposed as a promising alternative

to conventional bioremediation strategies. They are able to provide inexhaustible source and/or sink of electrons to sustain microbial metabolism in form of a solid electrode, thus avoiding the drawbacks connected to the injection of air, oxygen or other chemicals in the aquifer (He and Su, 2015). Many studies on bioremediation with MESs focused on Microbial Fuel Cells, which can spontaneously oxidize organic compounds at the anode by using oxygen as the terminal electron acceptor at the cathode (Kronenberg et al., 2017). However, in contaminated subsurface environments, the access to O_2 is strongly limited due to rapid depletion, thus hindering the biodegradation of pollutants (Wartell et al., 2021). In Microbial Electrolysis Cells (MECs), a potential difference is applied to the electrodes in order to catalyze sluggish or thermodynamically unfavourable oxidation reactions at the (bio)anode and/or reduction reactions at the (bio)cathode (Kadier et al., 2016). Several studies demonstrated the possibility to use MECs to treat aromatic hydrocarbons at the anode (Friman et al., 2013; Marzocchi et al., 2020; Enza Palma et al., 2018a, 2018b; Tucci et al., 2022) or chlorinated compounds at the cathode (Aulenta et al., 2011; Lai et al., 2017; Leitão et al., 2015; Verdini et al., 2015) in anaerobic conditions. Nevertheless, the research on coupling aromatic hydrocarbon oxidation at the anode and chlorinated compounds reduction at the cathode with MECs is still very limited (Tucci et al., 2022b). Recently, we proposed a prototype of MEC named “Bioelectric well” (Enza Palma et al., 2018b): its tubular design allows insertion in groundwater wells and piezometers for in-situ groundwater treatment. Moreover, the absence of membrane between anode and cathode minimizes the ohmic losses and facilitates its upscaling. Recent works proved that the bioelectric well is able to remove at the same time oxidable (toluene, TPH) and reducible (sulphate, TCE) contaminants from a synthetic groundwater (Cruz Viggi et al., 2022; Tucci et al., 2021). In this study we performed the simultaneous degradation of toluene, as a model aromatic hydrocarbon, and chloroform (CF), a highly toxic and possibly carcinogen chlorinated pollutant (Yamamoto et al., 2002), in a continuously fed bioelectric well operated for over 190 days. Importantly, CF biodegradation has never been previously studies in a

continuous-flow bioelectrochemical reactor. Here, toluene was oxidized by the electroactive microbial consortium at the anode, while CF was converted to harmless end products via a two-step process involving first a reductive hydrogenolysis step leading to dichloromethane (DCM) followed by the fermentation to acetate and formate.

IV.2 Experimental Section

IV.2.1 Chemicals and electrode potentials

All chemicals used for the experiments were of analytical grade. All of them were purchased from Merck KGaA (Germany). De-ionized water (Millipore, Germany) was used to prepare the mineral medium and all other solutions. All potentials reported in this work are referred to the standard hydrogen electrode (SHE).

IV.2.2 Reactor setup and operations

The bioelectric well was set up as previously reported in **III.2.1 Reactor setup and operations** (Tucci et al., 2021a): the anode consisted of a cylinder made of 8 contiguous graphite rods (purity: 99.995%, length: 30 cm, ø: 0.6 cm; Merck KGaA, Germany), whereas the cathode was a stainless steel mesh (dimensions: 3 x 30 cm; type 304, Alpha Aesar, USA) (**Fig. IV-1A**). Anode and cathode were contained in a 250 mL glass cylinder and were kept separated by a polyethylene mesh (ø: 1 cm, length 30 cm; **Fig. IV-1B**), which allowed free circulation of the electrolyte. The distance between the anodic and the cathodic surfaces was 2mm. The two electrodes were connected to an external circuit with titanium wires (ø: 0.81mm Alfa Aesar, USA). During the experiments, the anode was polarized at +0.4 V vs. SHE by means of an IVIUMnSTAT potentiostat (IVIUM Technologies, The Netherlands). This potential was chosen according to the findings of previous studies with the bioelectric well, where the bioelectrochemical oxidation peak of toluene on graphite ranged between 0.2 and 0.4V (Tucci et al., 2022c). The counter electrode potential was periodically measured throughout the experiment. A saturated Ag/AgCl electrode (+0.198 V vs. SHE; AMEL, Italy) was used as reference electrode.

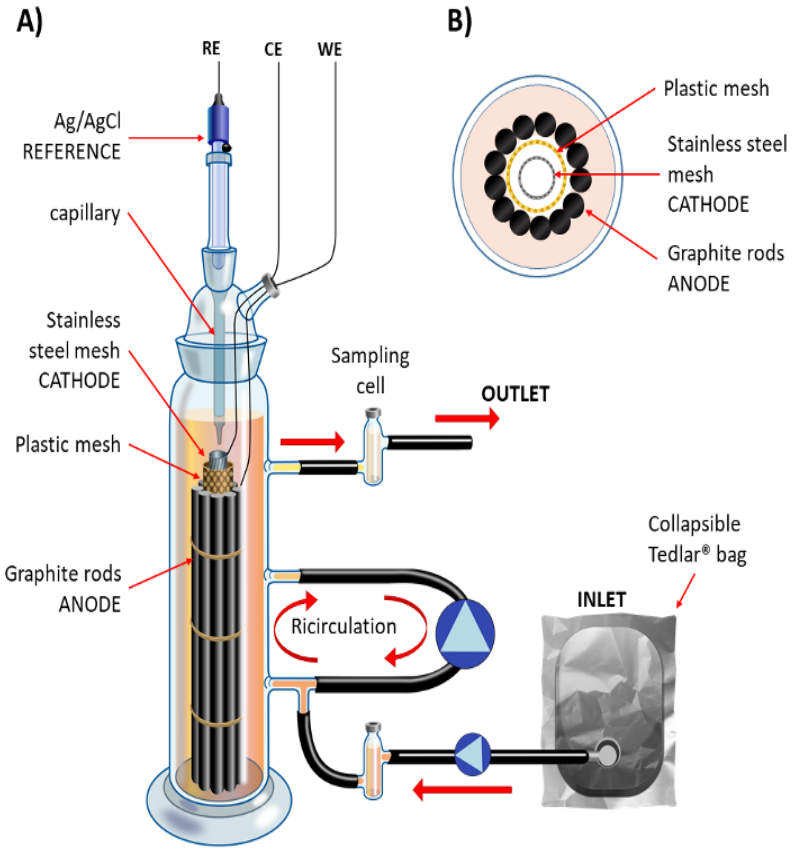

Figure IV-1 *– The bioelectric well: A) schematic representation of the setup used for the experiments, where WE is the working electrode, CE is the counter electrode and RE is the reference electrode; B) cross-sectional view showing the relative position of electrodes.*

To ensure the presence of microbes able to degrade toluene, the reactor was inoculated with 0.25 L of real groundwater contaminated with petroleum hydrocarbons collected from a petrochemical site in Italy. During the experiment, the reactor was fed in continuous mode with mineral medium (pH 7) in which O_2 was eliminated through N_2 sparging. The medium composition is reported in the **Table II-1**. The medium was spiked with the contaminants toluene and CF as summarized in **Table IV-1**. Acetate was also added to the medium to study the impact of a readily available substrate on the reactor performances. The inlet was stored in 5 L collapsible Tedlar® gas bags and pumped in the reactor through the bottom port (flow rate: 0.63 L d^{-1}, HRT 11 h) by means of a peristaltic pump (120S,

Watson Marlow, Falmouth, UK). The treated effluent was discharged from the upper port by passive overflow. Flow-through sampling cells (volume: 25 mL) were installed at the inlet and at the outlet of the reactor for liquid and gas monitoring. The liquid phase of the reactor was constantly recycled with another peristaltic pump (flow rate: 192 mL min^{-1}; model: 323, Watson Marlow, Falmouth, UK) to avoid gradients of substrates, products and/or biomass. The tubes were made of Viton® (Merk KGaA, Germany) to minimize volatilization losses and adsorption of organic contaminants. During the whole study the system was maintained at room temperature (*i.e.,* 24 ± 3°C).The experiment lasted 190 days, during which different conditions were tested (**Tab. IV-1**). The first run was an acclimation phase for the toluene degrading consortium in absence of CF. Then, CF was added to the mineral medium at a concentration of 14 mg L^{-1} and the reactor was inoculated (10% vol/vol) with two microbial cultures: one enriched with *Dehalobacter spp*. and the other with *Dehalobacterium formicoaceticum*, capable to perform the reductive hydrogenolysis of CF to DCM and the subsequent fermentation of DCM to acetate and formate, respectively (Fernández-Verdejo et al., 2022; Trueba-Santiso et al., 2020, 2017). At this point three different concentrations of toluene (in the range of 15-36 mg L^{-1}) were tested from runs 2 to 4. In runs 5 and 6 the electrodes were disconnected from the potentiostat to study the removal of contaminants at open circuit potential (OCP). Finally, in runs 6 and 7 acetate was omitted from the mineral medium and during run 7 the system was reconnected to the potentiostat and polarized.

Table IV-1 *- Operational conditions for all the different runs operated with the bioelectric well*

Run	Days	Toluene ($\mu mol\ L^{-1}$)	Chloroform ($\mu mol\ L^{-1}$)	Acetate ($\mu mol\ L^{-1}$)	Polarization (V vs. SHE)
1	0-13	260	/	920	+0.4
2	14-36	260	120	920	+0.4
3	37-46	390	120	920	+0.4
4	47-80	160	120	920	+0.4
5	81-114	130	120	920	OCP
6	115-127	100	120	/	OCP
7	128-190	100	120	/	+0.4

IV.2.3 Cyclic voltammetries

The bioanode and (bio)cathode developments were monitored with Cyclic voltammetries (CVs, scan rate: 1 mV s^{-1}) using an IVIUMnSTAT potentiostat (IVIUM Technologies, The Netherlands). The stainless-steel cathode and the graphite anode were used as counter electrode during the anodic and cathodic CVs, respectively. For all CVs, an Ag/AgCl electrode (+0.198 V vs. SHE; AMEL, Italy) was used as reference.

IV.2.4 Gas-chromatographic analyses

The quantification of O_2, H_2 and CH_4 was performed using a gas-chromatograph (Agilent 8860, GC system USA) equipped with a thermal conductivity detector (TCD); the quantification of toluene, CF and acetate was performed with a gas-chromatograph (Agilent 8860, GC system USA) equipped with a flame ionization detector (FID). The methods for the GC, the calibration ranges and detection limits (LOD) are reported in the **Table II-2**. Gas-phase concentrations were converted into liquid-phase concentrations using tabulated Henry's Law constants (Sander, 2015).

IV.2.5 High-Throughput rRNA Gene Sequencing and Bioinformatic Analysis

The liquid effluent (15 mL) and the biofilm grown on the graphite rods were collected at the end of the operation, filtered through polycarbonate membranes (pore size 0.2 mm, 25 mm diameter, Nuclepore) and immediately stored at -20°C. The DNA extraction was performed by using the DNeasy PowerSoil Pro Kit (QIAGEN - Germantown, MD) following manufacturer's instructions. The genomic DNA was utilized as template for the amplification of the V1-V3 region of 16S rRNA gene of *Bacteria* (27F 5'-AGAGTTTGATCCTGGCTCAG-3'; 534R 5'-ATTACCGCGGCTGCTGG-3') following the procedure for library preparation and sequencing described elsewhere (Simona Crognale et al., 2019). The samples were paired end sequenced (2x301bp) on a MiSeq platform (Illumina) using a MiSeq Reagent kit v3, 600 cycles (Illumina, USA) following the standard guidelines for preparing and loading samples. Phix control library was spiked at a concentration of 20%. Bioinformatics analysis were performed using QIIME2 v. 2018.2 (Bolyen et al., 2019) following the procedure reported elsewhere (Simona Crognale et al., 2021). High-throughput sequencing of the V1-V3 region of the bacterial 16S rRNA gene yielded a total of 16,934 sequence reads after quality control and bioinformatics processing that resolved into 150 amplicon sequence variants (ASVs).

IV.2.6 Quantification of key-functional genes

The genomic DNA was also used as template for the quantification of functional genes involved in the upper pathway of anaerobic toluene degradation (*bssA, bcrC, bzdN, bamB*), CF to DCM reduction (*cfrA*) and DCM fermentation (*mecE, mecF*). 16S rRNA of *Dehalobacter* spp. and *D. formicoaceticum* were also quantified. Absolute quantification assays were performed via Digital Droplet PCR (ddPCR) with the QX200™ Droplet Digital™ PCR System (Bio-rad, United States) as describe elsewhere (Di Franca et al., 2022).

The steps for the quantification assays included: i) preparation of the PCR reaction mixture for each targeted gene (22 µl total volume: ddPCR EvaGreen Supermix ® (Bio-Rad, United States), 3 µl of DNA as a template, and 900 nM of

each primer); ii) droplets generation (20 µl of PCR mixture and 70 µl of Droplet Generation Oil® (Bio-Rad, United States) with the QX200 Droplet Generator (Bio-Rad, United States); iii) PCR amplification on 40 µl of the droplets' mixture with a T100 thermal cycler (Bio-Rad, United States) (cycling conditions: 5 min at 95°C, 39 cycles for 30 s at 95°C and 1 min at 60°C (ramping rate set to 2°C/s), 5 min at 4°C, 5 min at 90°C, ending at 4°C); iv) quantitative data reading with QX200 Droplet Reader (Bio-Rad, United States) to determine the positive and negative fluorescent droplets and calculate the targeted gene concentrations. The data were analyzed using the QuantaSoft® software (Bio-Rad, United States) by calculating the ratio of the positive droplets over the total droplets in each sample. Quantitative data have been reported as gene copies L^{-1} of liquid effluent or gene copies cm^{-1} of graphite rod (95% confidence intervals).

IV.2.7 Calculations

The removal rate *r* (µmol L^{-1} d^{-1}) of toluene and CF were calculated using the following equation:

$$r = \frac{\Delta Conc.}{V_r} Q \qquad (1)$$

where *ΔConc.* (µmol L^{-1}) is the difference between the concentration of toluene or CF measured in the influent (C_{In}) and the concentration measured in the effluent (C_{out}), V_r (L) is the empty volume of the reactor and *Q* (L d^{-1}) is the flow rate of the influent.

The relative removal $q_{\%}$ of toluene and CF were calculated as follows:

$$q_{\%} = \frac{\Delta Conc}{C_{in}} \times 100 \qquad (2)$$

IV.3 Results and discussion

IV.3.1 Reactor performances

The bioelectric well was operated for 190 days in different conditions (**Tab. IV-1**). In **figure IV-2A** the current profile for all the different runs is reported. After a start-up phase with toluene as the only contaminant (run 1), the current started

to increase and CF was added (run 2). Then, the current reached a steady level with an average value of 3.4 mA (runs 3 and 4). During run 5 and 6 the system was kept in OCP, and thereafter re-connected in run 7. It can be noticed how, as soon as the electrodes were polarized again, the current increased until it reached values similar to those of the previous polarized runs. The recorded CVs clearly point to a gradual formation of an electroactive biofilm on the anode, starting from T0 to the end of run 3 (**Fig. IV-2B**). Indeed, it can be noticed the formation of peaks associated with a redox couple (red line) and a time-dependent increase of the oxidative current. The cathodic reductive current also increased overtime, probably due to the accumulation of hydrogenase-containing microorganisms at the electrode, which can facilitate H_2 formation at the cathode (**Fig. IV-2C**) (Aulenta et al., 2012). Furthermore, the measured cathodic potential maintained a value of 0.77± 0.07 V vs. SHE throughout the experiment, which is suitable for H_2 generation.

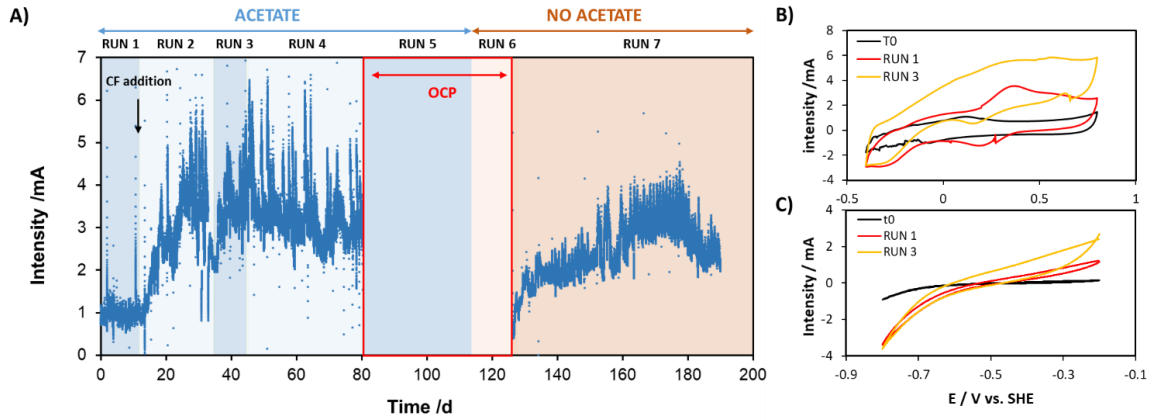

Figure IV-2 *– A) Current trend of the bioelectric well during the different runs. B) CVs of the (bio)anode at T0, in run 1 and 3. C) CVs of the (bio)cathode at T0, in run 1 and 3.*

The current generation is strictly linked to the degradation of toluene, as it can be observed in **figure IV-4A**. At the beginning of the experiment, electroactive bacteria started to degrade toluene at the anode in presence of acetate. However, even at the lowest influent toluene concentration (i.e. 160 µmol L^{-1}), only a fraction of the toluene load was removed. Conversely, during run 7, where acetate was not present in the inlet, almost 100% of toluene was degraded.

During OCP (runs 5 and 6), as expected, negligible toluene degradation was observed. The consumption of acetate was also monitored (**Fig. IV-3**): acetate was completely consumed during the polarized runs (1-4), while almost no removal was observed during OCP (run 5). When acetate was omitted from the inlet (runs 6 and 7), no residual amounts were detected in the reactor. Regarding CF, the degradation started quickly as soon as it was added to the reactor (**Fig. IV-4B**). As a result, the dechlorination product DCM (deriving from the reductive hydrogenolysis of CF) started to being produced. At the same time, DCM fermentation commenced, hence slowly decreasing its concentration in the reactor.

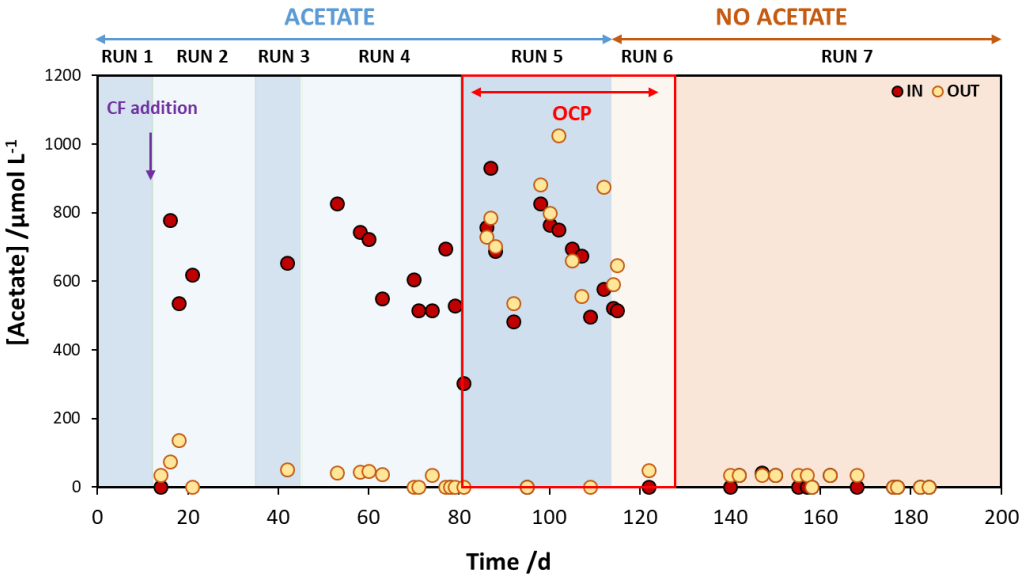

Figure IV-3 *– Trend of acetate concentration in the inlet and in the outlet of the reactor*

During OCP, the dechlorination of CF slowed down but it was still present, being probably sustained by DCM fermentation and the endogenous decay of biomass. Indeed, it is well documented that the slow release of electron donors generated by fermentation processes is effective in sustaining reductive dechlorination processes (Amanat et al., 2022; Yang and McCarty, 2000). When the system was polarized again (run 7), the previous level of CF removal was restored. It is worth noticing that, towards the end, almost all CF and its metabolite DCM were

removed. Furthermore, no adverse effects on toluene degradation were observed with the addition of CF. Methanogenesis started at the beginning of run 1, sustained by electrochemically produced H_2 (**Fig. IV-4C**). However, methane generation decreased over time after CF addition, probably due to the inhibitory effect caused by this contaminant on methanogens (Yu and Smith, 2000). During OCP runs (5 and 6) no hydrogen was generated, and thus no CH_4 was produced. Once almost all CF was removed by the dehalogenating bacteria (run 7), methanogenesis started again.

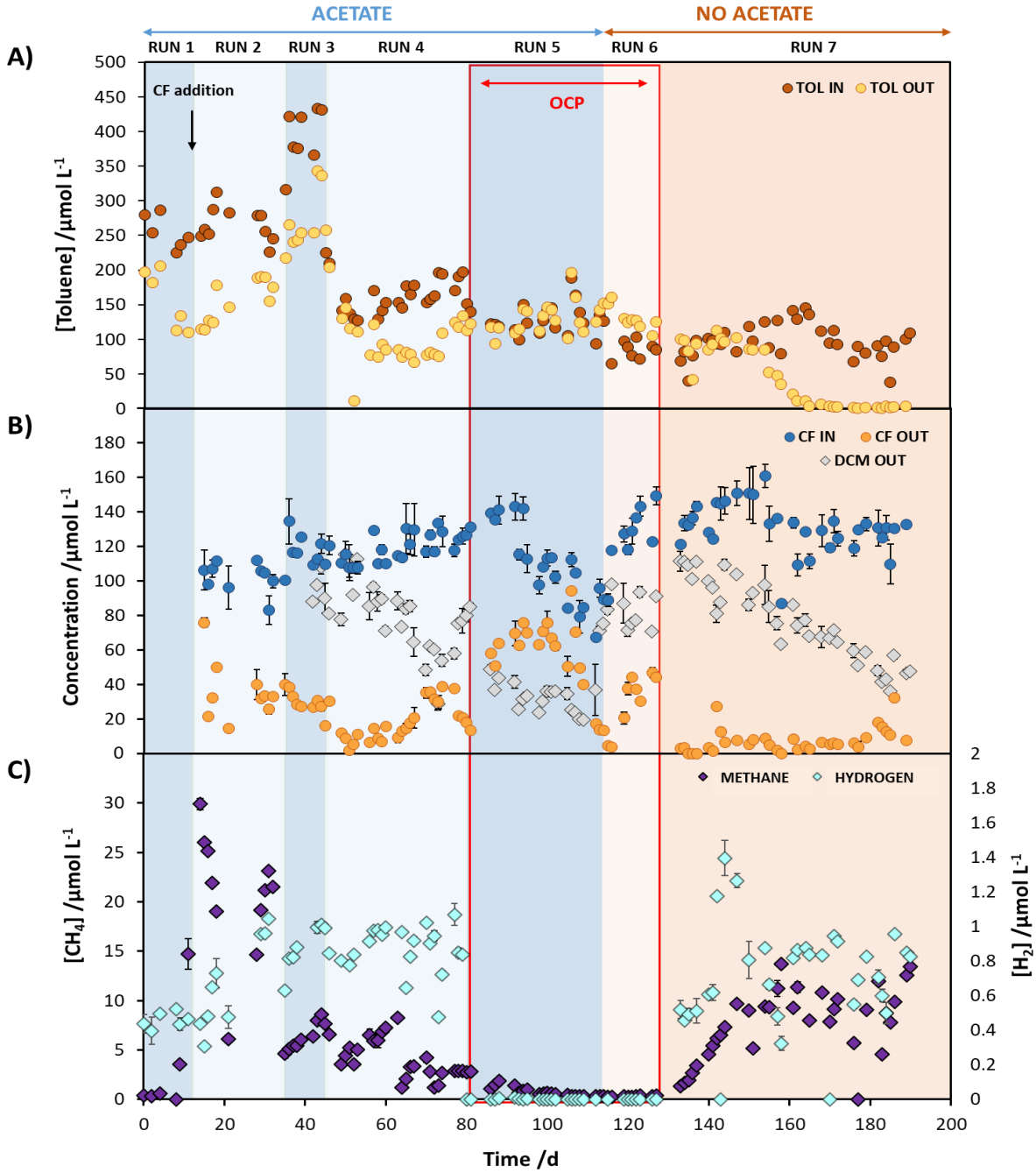

Figure IV-4 *– A) Trend of toluene concentration in the inlet and in the outlet of the reactor. B) Trend of CF concentration in the inlet and in the outlet of the reactor and DCM formation in the outlet. C) Trend of H_2 and CH_4 formation in in the outlet of the reactor.*

Table IV-2 *– Reactor performances in terms of toluene and CF removal during polarized mode vs. OCP mode in absence of acetate.*

	Polarized (Run 7)	**OCP** (Run 6)
Tol. rem. Rate (µmol L^{-1} d^{-1})	47 ± 3	0.1 ± 0.2
Tol. rem. %	96 ± 1	0.2 ± 0.2
CF rem. Rate (µmol L^{-1} d^{-1})	60 ± 1	47 ± 2
CF rem. %	94 ± 1	77 ± 1

During the polarized run, in absence of acetate (run 7), 47 µmol L^{-1} d^{-1} of toluene and 60 µmol^{-1} d^{-1} of CF were removed, corresponding to 96% and 94% of the contaminant load, respectively (**Tab. IV-2**). This proves the effectiveness of the bioelectrochemical system, since only 0.1 µmol L^{-1} d^{-1} of toluene (i.e. 0,2%) and 47 µmol L^{-1} d^{-1} of chloroform (i.e. 77%) were removed during OCP. Nevertheless, the degradation rate of toluene obtained in this work is considerably lower than the ones obtained in previous studies with the bioelectric well, which were as high as 336 and 150 µmol L^{-1} d^{-1} when sulphate and TCE were used as co-contaminants, respectively (Cruz Viggi et al., 2022; Tucci et al., 2021a). It is likely that the co-contamination with acetate and CF limited the presence of toluene-degrading microorganisms within the microbial community, the first one through competition and the second through inhibition. As a matter of fact, CF has well documented toxic effects on bacteria, including anaerobic consortia (Pollice et al., 2001). As a result, the microbial community showed a reduced toluene degradation potential and thus a lower removal rate. The maximum CF consumption rate obtained in this experiment (60 µmol L^{-1} d^{-1}) was lower as compared to the one obtained in previous experiments conducted with a two-vessel BES (132 µmol L^{-1} d^{-1}) (Fernández-Verdejo et al., 2022). The reason

behind this decrease in CF degradation rate could be the lower supplied concentration of CF in the system, leading to overall lower reaction kinetics. A similar phenomenon was observed with toluene in previous studies conducted with the bioelectric well where a clear dependency of bioreaction rates on substrate concentration, in the mg/L range, was observed (Tucci et al., 2022c).

IV.3.2 Effects of toluene concentration and acetate addition

The influent toluene concentration is a key-factor influencing the kinetics of the anodic bio-oxidation (**Fig. IV-5A**). In this study, toluene removal increased with the inlet concentration up to 280 µmol L^{-1}, where the system became apparently saturated. This is in contrast with previous studies, where a direct correlation between the amount of toluene and its removal rate was observed in a similar system up to 434 µmol L^{-1} (Tucci et al., 2022c). Once more, the effect of the co-contamination with CF may be the cause for the limitations in the toluene removal efficacy. Conversely, CF removal rate did not seem correlated to the concentration of toluene (**Fig. IV-5B**). This is likely due to the fact that, during cycles 2, 3 and 4, electrons were also generated by the oxidation of acetate, thus masking a possible correlation with the concentration of toluene.

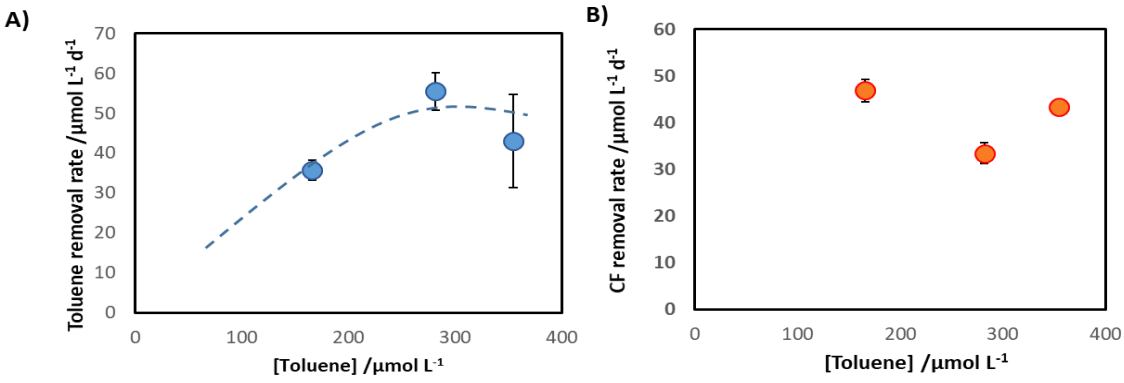

Figure IV-5 *– Effect of the toluene concentration on the toluene A) and CF B) removal rates calculated as averages of the cycles 2,3 and 4.*

In **figure IV-6** it is possible to see how the degradation of toluene was lower when acetate was added to the inlet, both in absolute terms and as percentage of the contaminant load in the inlet. This phenomenon is probably caused by the fact that both toluene and acetate competed for the active catalytic sites at the anodic biofilm, with acetate likely being preferentially metabolized compared to toluene (Edwards and Grbić-Galić, 1994; Zhang et al., 2010). It is worth noticing that higher toluene degradation in absence of acetate indirectly resulted in higher CF removal. However, the mechanism behind this phenomenon is unclear and warrants further investigation. It is worth noticing that only in the absence of acetate (run 7), it was possible to reach an almost complete degradation of both contaminants.

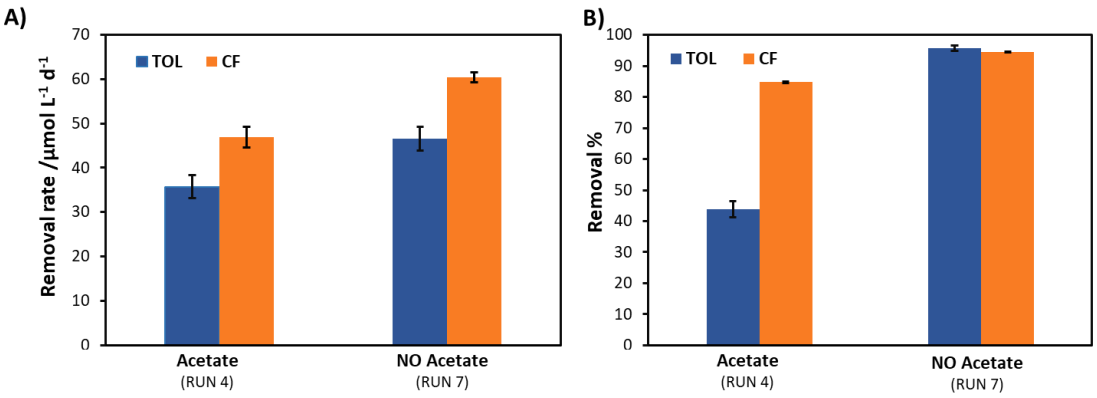

***Figure IV-6**- Effect of acetate on the removal of toluene and CF in terms of rate A) and percentage B) of the contaminant load in the influent. The error bar indicates the standard error of the mean.*

IV.3.3 Characterization of the mixed microbial communities

The amplicon sequencing of the 16S rRNA gene revealed a highly selected microbial community both in the liquid effluent and in the biofilm taken at the end of the operation of the reactor (**Fig. IV-7**). In particular, the liquid effluent was mostly constituted by members of the genus *Propionicicella* (~62% of total reads) capable to produce acetic and propionic acids. Some *Propionicicella* strains (i.e. *P. superfundia* (Bae et al., 2006), have been isolated from groundwater contaminated with chlorinated ethanes and vinyl chloride and are facultative anaerobe capable of utilizing fermentative metabolic strategies. *Candidatus*

Endomicrobium, unidentified members of family *Lentimicrobiaceae* and *Acetobacterium* were also found (≥ 8%, each), the latter known to produce acetate and formate when grown in mixed bacterial culture with DCM and H2 (Trueba-Santiso et al., 2017). Furthermore, reads affiliated with families *Anaerolineaceae, Burkholderiaceae, Geobacteraceae,* and *Rikenellaceae* counted together up to 6.5% of total reads suggesting the potentialities of the effluent's microbiome in hydrocarbon degradation (Weelink et al., 2010). *Burkholderiaceae* is considered a key family of toluene degradation with several members, as for example *Ralstonia pickettii*, involved in the complete toluene degradation pathway via two successive ring-hydroxylating reactions (Lünsmann et al., 2016). The dominant role of this family can be due to occurrence of toluene monooxygenase and dioxygenases-encoding genes, which would allow the microorganisms harbouring this type of enzymes to be adapted to grow on some aromatic compounds (Martínez-Lavanchy et al., 2015). Differently from the liquid effluent, the microbiome composition of the biofilm grown on graphite rods was mostly represented by unidentified members of *Actinobacteria* order OPB41 (41.0%). The direct involvement of members of this order in toluene degradation was not discussed so far even though they were reported as a component of microbial community in previous works concerning hydrocarbons degradation (Chen et al., 2016; Laso-Pérez et al., 2019). In line with previous evidence in similar bioelectrochemical studies (Tucci et al., 2022c, 2022a), the enrichment of the electroactive microbiome in the biofilm was suggested by the presence of members of family *Anaerolinaceae* (19.0%) and genus *Geobacter* (8.6%). Furthermore, 6.5% of total reads were affiliated with family *Lentimicrobiaceae*, comprising strictly anaerobic gram-negative bacteria able to form a consortium with other electroactive microorganisms to convert acetate into electric energy (Xiao et al., 2015; Zhu et al., 2022).

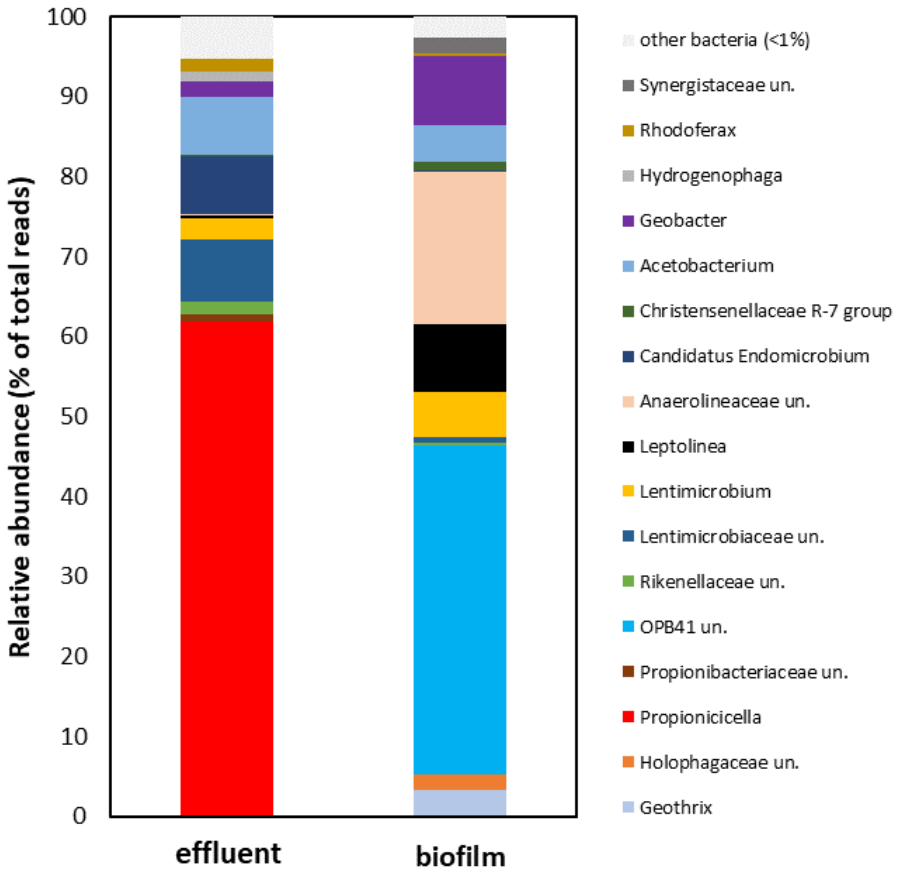

Figure IV-7 - Bacterial community composition revealed by the 16S rRNA gene amplicon sequencing. Data are expressed as relative abundance (% of total reads) of genera (≥ 1 % in at least one sample) in the liquid effluent of the reactor and biofilm grown on graphite rods.

The key functional enzymes involved in the initial two steps of the anaerobic toluene and CF degradation pathways (Lueders, 2017; Tang and Edwards, 2013; Von Netzer et al., 2016) have been quantified both in the liquid effluent and on the biofilm established on the graphite rods (**Fig. IV-8**).

The functional genes involved in the anaerobic toluene degradation are the benzylsuccinate synthase (*bssA*), encoding for the enzyme that catalyzes the anaerobic toluene activation by fumarate addition (Winderl et al., 2007); the *bcrC*, *bzdN* genes encoding for the ATP-dependent class I benzoyl-CoA reductases (Kuntze et al., 2011); the *bamB* gene encoding for the ATP-independent class II benzoyl CoA reductase (Löffler et al., 2011). According to kinetic data, these

genes were highly abundant both in the effluent and in the biofilm of the graphite rods (**Fig. IV-8A**). In the liquid effluent, genes involved in the toluene degradation accounted for 1,73E+09 (*bcrC*), 4,62E+08 (*bzdN*), 4,95E+08 (*bamB*) and 2,75E+08 (*bssA*) gene copies L^{-1} (**Fig. IV-8A**). Similarly, in the biofilm of the graphite rods, the same concentration trend was observed, with *bcrC* gene as the most abundant one (1,1E+07 gene copies cm^{-1} graphite rod). Regarding the CF degradation, the presence of the anaerobic bacteria *Dehalobacter spp.,* responsible for the reductive hydrogenolysis of CF to DCM, and of *D. formicoaceticum* involved in the fermentation of DCM to acetate and formate, were also ascertained both in the liquid effluent and on the graphite surface, although not spotted by the 16S rRNA gene amplicon sequencing (Grostern et al., 2010; Justicia-Leon et al., 2014). Moreover, process-specific biomarker genes were quantified to track CF to DCM (*cfrA* gene) transformation and DCM fermentation (*mecE* and *mecF* homologous genes belonging to the methylene chloride catabolism gene cassette, recently identified as prognostic and diagnostic tools supporting bioremediation of matrices impacted by DCM (Murdoch et al., 2022). 16S rRNA of *Dehalobacter* (*dre* gene in **Fig. IV-8B**) was found with 1,63E+09 16S rRNA gene copies L^{-1} effluent and 4,15E+06 gene copies cm^{-1} graphite. *cfrA* gene was also found at high concentration in the liquid effluent (1.74E+09 gene copies L^{-1}) and on the graphite surface (1,18E+06 gene copies cm^{-1}). These results are in line with the observed performances of the reactor and previous evidence (Tucci et al., 2022c, 2022a) suggesting that, though likely catalyzed by different microorganisms, toluene utilization in the liquid medium and on the graphite's biofilm shared the same initial degradation steps likely commencing with fumarate addition and involving benzoyl-CoA as a central intermediate. Moreover, *D. formicoaceticum* was highly abundant in the liquid effluent (3,54E+08 gene copies L^{-1}) and in the biofilm (4,15E+06 gene copies L^{-}cm). Similarly, *mecE* and *mecF* homologous genes were found both in the liquid effluent and on the graphite surface with high concentrations (**Fig. IV-8B**).

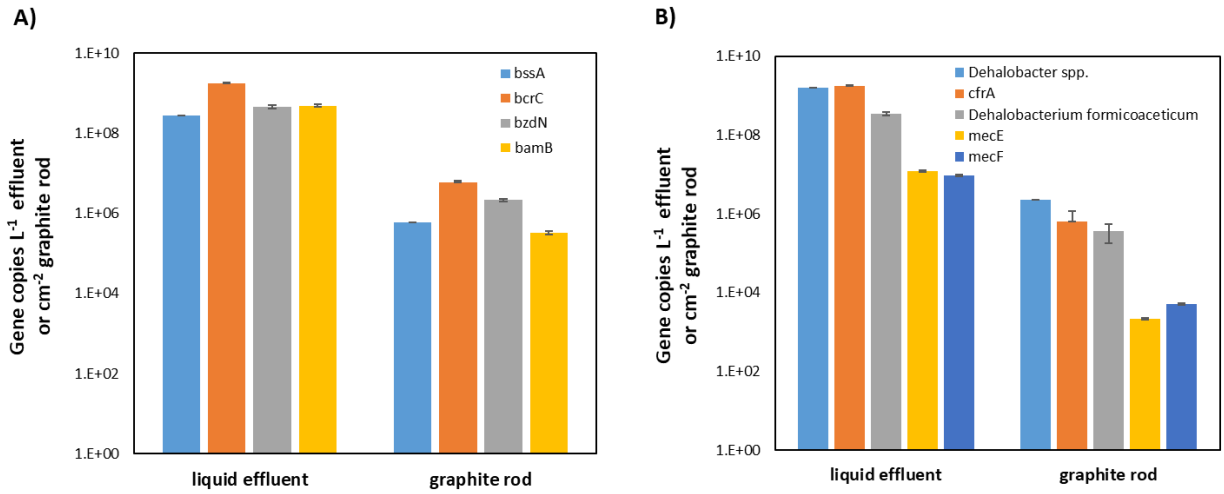

Figure IV-8 *– Quantification of functional genes involved in toluene degradation (bssA, bcrC, bzdN, bamB) (7A), in CF to DCM degradation (Dehalobacter spp., cfrA) and in DCM fermentation (D. formicoaceticum, mecE and mecF genes)*

IV.4 Conclusions

For the first time, the removal of toluene was coupled with the CF degradation in a single- stage bioelectrochemical reactor. The bioelectric well proved once again to be effective in treating complex mixtures of contaminants and exploiting both the oxidation and the reduction reaction simultaneously. Furthermore, the reactor was able to achieve almost complete removal of the target contaminants. However, the presence of CF reduced the reactor's capability of degrading toluene as compared to previous studies. Indeed, it is likely that CF partially inhibited the activity of the anodic toluene-degrading microbial community. Another important finding is that a readily biodegradable substrate such as acetate has an adverse effect on the degradation of toluene, probably due to its competitive inhibition effects for the catalytic sites of the electroactive biofilm.

Taken as a whole, these results highlight the importance of studying the effect of multiple contaminants on the performance of novel bioremediation technologies, in order to properly address real-world scenarios. Thus, our findings are an important stepping-stone towards the application of the bioelectric well for in-situ bioremediation of multi-contaminated subsurface environments.

Chapter V

Anaerobic treatment of groundwater co-contaminated by toluene and copper in a single chamber bioelectrochemical system

Adapted from:

Resitano, M., Tucci, M., Mezzi, A., Kaciulis, S., Matturro, B., D'Ugo, E., Bertuccini, L., Fazi, S., Rossetti, S., Aulenta, F., Viggi, C.C., 2024. Anaerobic treatment of groundwater co-contaminated by toluene and copper in a single chamber bioelectrochemical system. Bioelectrochemistry 158, 108711. https://doi.org/10.1016/J.BIOELECHEM.2024.108711

V.1 Introduction

Petroleum hydrocarbons (PHs) and heavy metals (HMs) are the most frequent pollutants among all contaminated sites across Europe, as reported by Pérez and Rodríguez in a recent survey (Payá Pérez and Rodríguez Eugenio, 2018). Both these classes of compounds have the potential to act as carcinogens, mutagens, or allergens in humans, and they can lead to a range of other toxic effects when they enter the aquatic food chain (Sonone et al., 2021; Tang et al., 2011). Most literature studies focused on the removal of a specific contaminant through a single mechanism, while achieving the simultaneous elimination of multiple pollutants continues to pose a challenge (Deng et al., 2013). In fact, the different contaminants present in subsurface environments may possess different physicochemical properties, and the method implemented to remove one pollutant can inhibit the removal of other pollutants (Markowicz et al., 2016). It is also important to underline that the co-occurrence of these compounds in contaminated sites is quite frequent, and their combined toxicity usually surpasses the sum of their individual toxic effect (Gauthier et al., 2014). Combining multiple contaminant removal techniques into a single process can be advantageous in terms of versatility and economic benefits (Bi et al., 2021). Numerous approaches have been investigated for the remediation of soil and water contaminated with a combination of PHs and HMs. Some approaches can be used to treat both soil and water contaminated by these pollutants, such as biological degradation (Polti et al., 2014; Zhou et al., 2014) and extraction processes with surfactants and chelating solutions (Cao et al., 2013). Other technologies are specific for water treatment, such as: adsorption on various carbon-based materials (e.g. activated carbon, magnetic ordered carbon, lignite, etc.) (Li and Helmreich, 2014; Yang et al., 2015), photocatalytic reduction (Deng et al., 2017; Hu et al., 2014), and electrochemical methods, like capacitive deionization combined with electro-oxidation hybrid systems (Chen et al., 2023) and electrocoagulation with Fenton processes utilizing sacrificial anodes (Ya et al., 2018). In recent years, bioelectrochemical systems (BESs) are attracting increasing attention as a promising alternative to conventional remediation

strategies. BESs can provide a virtually endless reservoir of electrons, to support microbial metabolism through solid electrodes, that can potentially serve as virtually inhexustible electron donors (i.e., as cathodes) or electron acceptors (i.e., as anodes) for prompting reduction or oxidation of contaminants, respectively. Electrodes can thus avoids the disadvantages associated with the introduction of air, oxygen, or other chemicals into the aquifer (Padhye et al., 2023), thereby making the treatment process greener and more sustainable. Microbial electrolysis cells (MECs) are a type of BESs in which an electric potential is applied to the electrodes to facilitate otherwise slow or energetically unfavourable oxidation reactions at the (bio)anode and/or reduction reactions at the (bio)cathode (Kadier et al., 2016). MECs have been applied for the treatment of PHs at the anode (Cruz Viggi et al., 2023; Friman et al., 2013; Marzocchi et al., 2020; Enza Palma et al., 2019; Tucci et al., 2022c, 2022b, 2021a; Zhang et al., 2010) or removal and recovery of HMs at the cathode (Hemdan et al., 2022; Mitov et al., 2018; Modin et al., 2012; Wang and Ren, 2014; Wang et al., 2022). However, there have been only limited attempts to address the simultaneous degradation in electrified systems of both PHs and HMs. Few notable examples include the work of Chen et al. (Chen et al., 2023), where the combination of capacitive deionization and electro-oxidation (CDI-EO) achieved the simultaneous removal of heavy metals and organic contaminants within a single apparatus. Notably, it achieved the removal of Cu^{2+} ions through cathodic electrosorption and electrodeposition. Another noteworthy study employed electrochemical Fenton treatment for the concurrent removal of heavy metals and organic pollutants from surface finishing wastewater (Ya et al., 2018). In another study, Zhang et al., developed a highly efficient treatment approach for real wastewater containing organic matter, heavy metals, and sulphate, employing a sulfur-cycle-mediated Microbial Fuel Cell (MFC) (Zhang et al., 2018). Lastly, Gambino et al. focused their work on the simultaneous removal of organic matter and heavy metals from marine sediment through the utilization of sediment-based microbial fuel cells (SMFCs) (Gambino et al., 2021). In the above cited papers, the investigated matrix typically consisted of wastewaters or sediments/soils, and

the oxidizable component was represented by undefined "organic substances" present in the wastewaters, and not specifically by petroleum hydrocarbons.

To the best of our knowledge, no prior studies have explored the application of bioelectrochemical processes for the concurrent treatment of groundwater contaminated with PHs and HMs. Our previous studies proved the efficacy of bioelectrochemical systems in simultaneously treating multiple groundwater contaminants, paving the way for the application in real-world scenario (Cruz Viggi et al.,2022; Tucci et al., 2021a). We demonstrated that oxidizable and reducible contaminants could be efficiently removed in a single stage bioelectrochemical treatment. The oxidizable compounds treated at the anode were represented by toluene as model substrate, while at the cathode sulphate (Tucci et al., 2021a), trichloroethene (Cruz Viggi et al., 2022) and chloroform (Tucci et al., 2023) have been degraded by reductive biological processes. In this work, we studied for the first time the application of a bioelectrochemical system to the simultaneous removal PHs and HMs from contaminated groundwater with a membrane-less single-chamber reactor. The configuration of the reactor was different from that used in the previous studies, as well as the feeding and operational conditions. The system was spiked with toluene as model PH and Cu^{2+} as model HM. Toluene was chosen as model contaminant because it's widely studied as model contaminant being one of the most pervasive soil and groundwater pollutant due to its high mobility and water solubility (Zanello et al., 2021). Copper was chosen being one of the most studied metals in BES studies for HM recovery from contaminated waters (Hemdan et al., 2022; Mitov et al., 2018; Modin et al., 2012; Wang and Ren, 2014; Wang et al., 2022). The removal of toluene at the anode, together with the reduction and precipitation of copper at the cathode were evaluated. Overall, this study provides evidence for a novel application of bioelectrochemical systems for the remediation of sites polluted with mixtures of toluene and copper, which can then be applied to sites contaminated by other combinations of PH and HM.

V.2 Experimental section

V.2.1 Experimental setup and operations

The experimental setup used in this study consisted in single-chamber bioelectrochemical cells, from now on referred to as *E-cell*, made of gastight borosilicate glass bottles sealed with Teflon-faced butyl rubber stoppers, having a total volume of 250 mL. Tested in batch mode (Fig. V-8). The cells had a two-electrode configuration and were equipped with two graphite rods (purity: 99.995%, length: 7.5 cm, ø: 0.6 cm; Sigma-Aldrich), one serving as anode and the other as cathode, with a potential difference of 1 V applied between them by an IVIUMnSTAT potentiostat (IVIUM Technologies). The chosen cell voltage was high enough to address potential losses and support electrode reactions at the highest possible rates, yet below the value that would favour water electrolysis. The anode and the cathode coexisted in the single-chamber cell without physical separation. The nominal surface area of the electrodes (calculated by taking into account only the part of the electrode that was immersed in the liquid phase) was 9.7 cm^2. The distance between the anode and the cathode was approximately 2 cm. Titanium wires (ø: 0.81 mm, Alfa Aesar) connected the anode and the cathode to the potentiostat. Each cell was filled with 180 mL of anaerobic mineral medium (Viggi et al., 2020), the composition of which is reported in the **Table II-1**. Upon setup, the cells were flushed with a N_2/CO_2 (70:30 v/v) gas mixture to establish anaerobic conditions, and the pH was maintained at a value of about 7 by adding an anaerobic solution of bicarbonate (10% w/v) as a buffer. At the start of the experimentation, two replicated cells were inoculated with 20 mL of groundwater from a PH-contaminated site in Italy. The groundwater contained electroactive bacteria capable of degrading hydrocarbons, as confirmed by previous experiments (Cruz Viggi et al., 2022; Tucci et al., 2023). In parallel, different control experiments (each in duplicate) were also set up. These included abiotic, non-polarized tests, carried out using an identical experimental setup as in the *E-cell*, with the aim of assessing the possible contribution of abiotic adsorption mechanisms on the observed toluene and copper removal. Similarly, abiotic and polarized tests were carried to evaluate the possible contribution of

electrochemical reactions on toluene and copper removal. The cells were kept out at room temperature (25±2 °C) and in the dark to avoid the growth of photosynthetic microorganisms. Throughout the study in batch mode, the cells were spiked with toluene (5 mg/L) and Cu^{2+} (10 mg/L) at the start of successive cycles, as reported in **Table V-1**. Copper was spiked in Run III-V, after evaluating that an electroactive biofilm had established on the anodes during Runs I and II. Regarding toluene and copper, added concentrations were those commonly found in contaminated groundwater. The cells were regularly sampled and analysed for toluene, gases and copper concentration. Electrochemical potentiostatic measurements were carried out with the potentiostat.

Table V-1: *Main operating conditions applied during the different experimental runs.*

Run	Operational period (days)	Polarization (V vs. SHE)	Toluene concentration (mg/L)	Cu^{2+} concentration (mg/L)
I	1-7	1.0	5	0
II	8-14	1.0	5	0
III	15-52	1.0	5	10
IV	53-101	1.0	5	10
V	102-122	(Open circuit potential)	5	10

V.2.2 Analytical Methods

Gaseous samples were taken from the cells using gastight syringes and analyzed for toluene and other gases using a gas-chromatograph (Agilent 8860, GC system) equipped with a flame ionization detector (FID) and a thermal conductivity detector (TCD). Gas-phase concentrations were converted into liquid-phase concentrations using tabulated Henry's Law constants (Sander, 2015). The GC method, calibration ranges and LOD of analytical methods are reported in the **Table II-2**. Liquid samples were filtered (nylon filters, pore size 0.2 mm, 47 mm diameter, Nuclepore), immediately acidified with 1% HNO_3 Suprapur

(Sigma-Aldrich) and analyzed by ICP-OES (Model 5800, Agilent) to determine the bulk liquid Cu concentration.

V.2.3 Microscopy analysis of the microbial communities

In order to visualise the 3D structure of the biofilms grown on the graphite electrodes, cells were stained with 4′,6-diamidino-2-phenylindole (DAPI) solution, at room temperature in the dark for 15 min, followed by a second staining of 0.15 mM calcofluor-white (Sigma-Aldrich Chemie GmbH), at room temperature in the dark for 4 min, for EPS visualization. The stained biofilms were then observed under a confocal laser scanning microscope (CSLM; Olympus FV1000). Both cells and EPS of each biofilm were excited by 405 nm light and emitted at 430 to 470 nm (blue color). Graphite surface was visualized by its reflection signal (635 nm line of a diodo laser). The three-dimensional reconstruction of CSLM images was elaborated by the software IMARIS 7.6 (Bitplane) with 3D volume rendering mode.

V.2.4 DNA extraction and high-throughput 16S rRNA gene sequencing

The bulk effluent (20 mL) and the graphite rods (both anode and cathode) were collected at the end of the experiment. Graphite rods were vortexed in 40 mL PBS 1X (8g/L of NaCl, 0.2g/L of KCl, 1.44g/L of Na_2HPO_4, 0.24g/L of KH_2PO_4) for 15 mins in order to disrupt the biofilm grown on the rods surface. The effluent and the PBS-suspended biofilm were filtered through hydrophilic polycarbonate membranes (0.2 µm pore size, 25 mm diameter, Millipore) and immediately used for DNA extraction. DNA was extracted by using the DNeasy PowerLyzer PowerSoil Kit (QIAGEN) according to the manufacturer's instructions. 4 ng of DNA were used a template for library construction via PCR amplification targeting the V1–V3 region of the 16S rRNA gene (primers 27F: 5'-AGAGTTTGATCCTGGCTCAG-3'; 534R: 5'-ATTACCGCGGCTGCTGG-3'). The V1–V3 region of the 16S rRNA gene was specifically targeted due to its well-established utility in identifying bacterial taxa within microbial communities. PCR reactions were conducted in a total volume of 25 µL, comprising Phusion Master

Mix High Fidelity (Thermo Fisher Scientific) and 0.5 μM of 27F and 534R primers with adaptors. All PCR reactions were performed in duplicate and subsequently pooled. The amplicon libraries were purified using Agencourt® AMpureXP-beads (Beckman Coulter), and their concentrations were measured using a Qubit 3.0 fluorometer (Thermo Fisher Scientific). The purified libraries were equimolarly pooled and then diluted to 4 nM. A Phix control was added at a 10% ratio to the pooled libraries. Subsequently, the samples were paired-end sequenced (2 × 301 bp) on a MiSeq instrument (Illumina) using a MiSeq Reagent kit v3, 600 cycles (Illumina), following standard guidelines. The procedure employed for library preparation has been also reported elsewhere (Di Franca et al., 2022; Tucci et al., 2023). Bioinformatic analysis was performed after checking read quality with FastQC software (v 0.11.7), as reported elsewhere (Callahan et al., 2016). The Silva 132–99 database was used to assign the taxonomy (release December 2017, https://www.arb-silva.de/documentation/release-132/). A dataset of amplicon sequence variants (ASVs) was generated including 3767 ASVs from the cathode, 17410 ASVs from the anode and 32231 ASVs from the bulk effluent. Sequencing data have been deposited in the DDBJ/ENA/GenBank under the BioProject PRJNA1039752.

V.2.5 X-ray photoelectron spectroscopy of graphite electrodes

The surface chemical composition of the graphite rods was assessed through X-ray photoelectron spectroscopy (XPS). This analysis was conducted using a VG Escalab MkII spectrometer (VG Scientific Ltd) equipped with a 5-channeltron detection system and an unmonochromatized radiation source of Al Kα (1486.6 eV). Spectra were registered in selected-area mode, operating with electrostatic lenses and fixing the entrance slit of analyser at A3x12, to collect photoelectrons from a sample area of about 3 mm diameter. The binding energy (BE) scale was calibrated positioning the C1s peak of graphite at BE = 284.6 eV. All the spectra were acquired at the pass energy of 50 eV. Spectroscopic data were acquired and processed using Avantage v.5 software, using a peak-fitting routine with Shirley background and Scofield sensitivity factors for elemental quantification.

V.2.6 Scanning Electron Microscopy (SEM) and Energy Dispersive Spectroscopy (EDS) of graphite electrodes

The graphite electrodes were broken into small pieces, fixed with glutaraldehyde 2.5% in Na-cacodylate buffer 0.1M for 1h at room temperature, washed in buffer and post-fixed with osmium tetroxide 1% in 0.1M Na-cacodylate for an additional 1h. After rinsing, samples were dehydrated through a graded series of ethanol solutions, from 30% to 100%. Then, ethanol was gradually substituted by hexamethyldisilane (HMDS) through an incubation of 30 min in 1:1 (ethanol: HMDS) solution, followed by pure HMDS for 1 h and then by a final drying process under chemical hood for 1h (totally removing HMDS and leaving to evaporate all the liquid phase). The dried graphite rods were mounted on aluminium stubs with silver paint, carbon coated and analyzed by FE-SEM Quanta Inspect F (FEI - Thermo Fisher Scientific) equipped with an EDAX detector used for the EDS analysis on the cathode surface.

V.2.7 Calculations

The coulombic efficiency (CE) for each cycle was calculated as the ratio between the transferred charge (that is the integral of the electric current over time) and the theoretical charge deriving from the oxidation of the toluene, according to the following equation:

$$CE\ (\%) = \frac{\int i(t) \times dt}{\Delta_{tol} \times 36 \times F} \quad (1)$$

where i is the measured electric current (mA), F is the Faraday's constant, Δ_{tol} is the amount of removed toluene (mmol) and 36 is the number of mmol of electrons released from the complete oxidation of 1 mmol of toluene.

The cathode capture efficiency (CCE) of each cycle was calculated as the ratio between the cumulative equivalents of produced methane ($mmoleq_{CH4}$) and the cumulative equivalents deriving from current ($mmoleq_i$), according to the following equation:

$$CCE\,(\%) = \frac{mmoleq_{CH4}}{mmoleq_i} \quad (2)$$

V.3 Results and discussion

V.3.1 Bioelectrochemical experiments

From the chemical analysis, it can be observed that toluene was removed almost completely (95% and 99% of removal in Run I and II, respectively), and the duration of the cycles was relatively short (around 6 days for each cycle), pointing to the presence at the anode of an electroactive biofilm capable of efficiently oxidizing toluene. As shown in Figure 1A, the rapid and quantitative toluene depletion during the first two cycles corresponded to two current peaks of 0.06 and 0.04 mA, respectively. When toluene was completely depleted, the current dropped to the initial values in both cycles. This fact indicates that current generation was dependent on the presence of toluene, which most likely served as the main carbon and energy source for the anodic biofilm. The resulting average CEs were 62.9±7.9% and 72.1±16.7% in the first and in the second run, respectively. It can be hypothesized that toluene was converted into electric current through the formation of intermediates, such as VFA (Volatile Fatty Acids), which accumulated in the cells medium and were not totally converted into current, as indicated by CEs substantially lower than 100%. In a previous work, it was found that the bioelectrochemical degradation of toluene proceeded via a syntrophic pathway involving cooperation between different microbial populations. Firstly, hydrocarbon degraders quickly converted toluene into metabolic intermediates probably by breaking the aromatic ring upon fumarate addition. Subsequently, fermentative bacteria converted these intermediates into volatile fatty acids (VFA) and likely H_2, which were then used as substrates by electroactive microorganisms forming the anodic biofilm (Tucci et al., 2022c). A similar removal mechanism can therefore be hypothesized. Methane production started immediately at the beginning of both cycles, reaching concentrations of 0.25 and 0.21 mg/L in Run I and II, respectively (**Fig. V-1C**). Average values of CCEs of 72.9±6.6% and 86.3±9.4% were calculated in Run I and II, respectively.

These fairly high CCE values are consistent with methane production being driven by the hydrogen produced at the cathode (**Fig. V-8**). Since after Runs I and II an electroactive biofilm was well established on the anodes, toluene was added along with copper (in the form of Cu^{2+}) to assess the possibility of simultaneously removing hydrocarbons and heavy metals through bioelectrochemical processes. In both cycle III and IV, the presence of Cu^{2+} significantly slowed down the removal of toluene, likely due to inhibition phenomena. Many bacterial species are efficiently killed on copper or copper alloy surfaces. It is thought that contact killing proceeds by a mechanism whereby the metal-bacterial contact damages the cell envelope, which, in turn, makes the cells susceptible to further damage by copper ions (Mathews et al., 2013). Nevertheless, toluene was completely removed in both cycles. Despite toluene removal was slower and substantially delayed (particularly during Run IV) compared to the cycles carried out in the absence of Cu^{2+}, current production reached remarkably higher current peaks accounting to 0.09-0.11 mA (**Fig. V-1A**), thus nearly doubling the values recorded in the previous cycles (Run I and II). The corresponding CE were higher than 200% in both cycles. This finding could be due to two different factors: the hydrogen formed at the cathode was partially re-oxidized at the anode via a so-call electron recycling process (Korth et al., 2020), and/or the intermediates of toluene (such as VFA, as above mentioned), that had been accumulated during the first two feeding cycles, were now fully and more rapidly oxidized at the anode, resulting in high current peaks. Further investigations would be warranted to shed light on this interesting behavior. Regarding copper, its concentration decreased significantly immediately after addition in both cycles, likely because of adsorption phenomena onto the graphite electrodes. After this initial rapid removal mechanism, copper concentration progressively decreased down to values below instrumental detection limits in both cycles (**Fig. V-1B**). While toluene is not adsorbed on the electrodes, as demonstrated in the control test (Fig.V-3), thus confirming the possibility of simultaneously removing toluene and copper through bioelectrochemical oxidation and cathodic reduction, respectively. Copper

addition also slowed down methane production during cycle III and IV, although ultimately methane reached even higher concentrations than in the previous cycles, also in line with the higher generated electric current (**Fig. V-1C**). On the contrary, the cathode capture efficiencies (towards methane production) decreased. In fact, CCEs of 38.7±0.5% and 35.3±10.3% were calculated in Run III and IV, respectively. The cathode capture efficiencies decreased since in these cycles the hydrogen was no longer only converted into methane, but it was also re-oxidized at the anode, as previously hypothesized. Copper electro-reduction may also have contributed (up to 20%, based on the removed copper) to reducing the yield of conversion of electric current into methane.

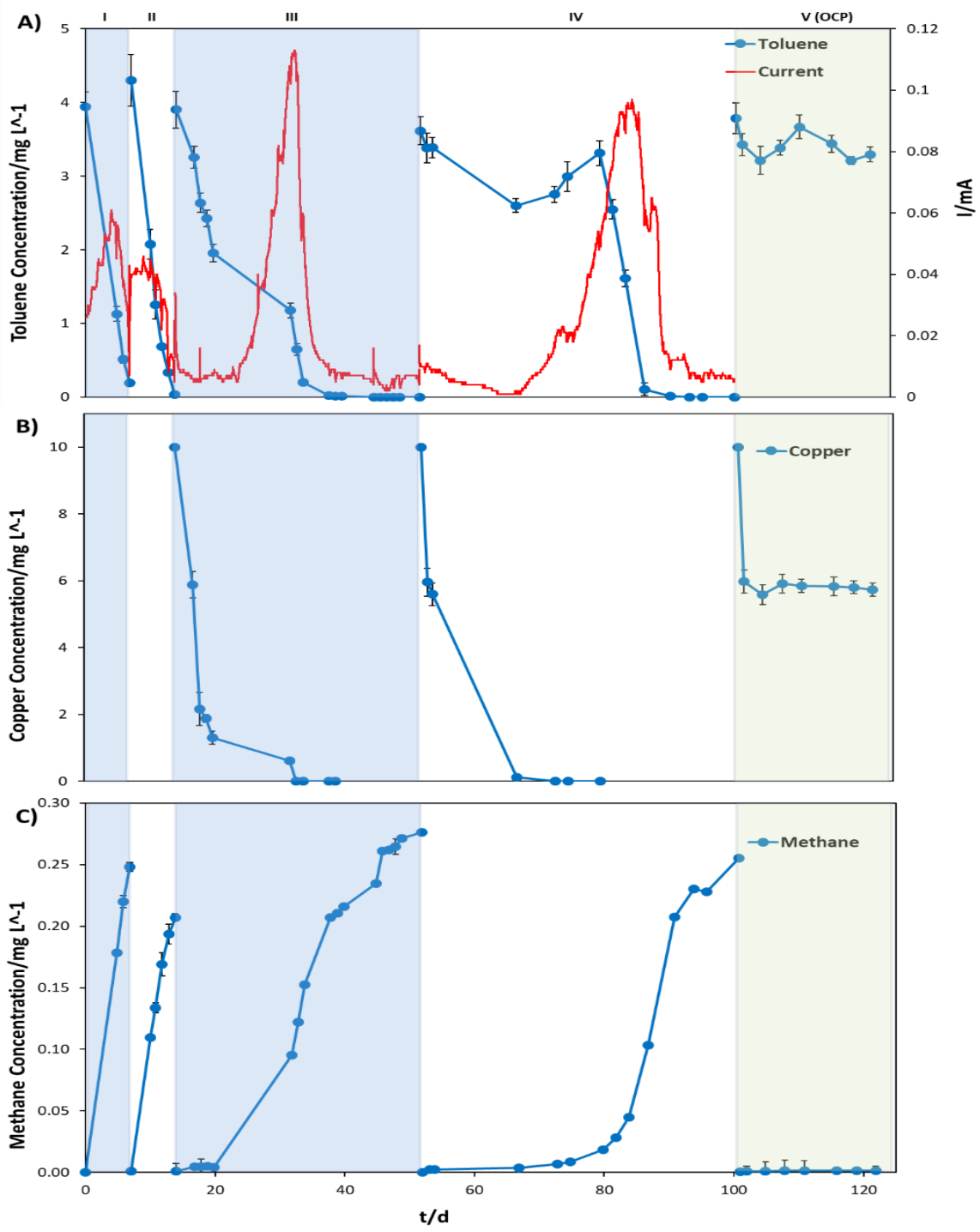

Figure V-1: *Performances of the bioelectric cell. Trends of: A) toluene removal and current generation; B) copper removal; C) methane production.*

During the last operational run (V), the circuits of the two bioelectrochemical cells were disconnected and maintained at open circuit potential (OCP) after toluene

and copper were added. Upon removal of polarization, toluene degradation ceased almost immediately, as well as the production of methane. Except for the sharp decrease observed right after its addition, which is likely due to adsorption phenomena, copper concentration remained constant throughout the OCP cycle. This evidence confirms that the removal in the previous cycles was primarily dependent by the polarization. An additional experiment was conducted using two identical cells without inoculum and not connected to the potentiostat, to assess the possible adsorption of copper onto graphite rods or other abiotic mechanisms involved in the copper removal. Control cells were operated in batch mode for about 120 days, showing an initial decrease after metal addition likely due to adsorption phenomena, and remaining approximately constant throughout the experiment (**Fig. V-2**). The trend of copper concentration observed in these abiotic and non-polarized experiments was similar to the one observed in the OCP run. Finally, an abiotic and polarized experiment was performed, to evaluate the possible contribution of electrochemical reactions on copper removal. This last experiment evidenced the absence of significant copper and toluene removal in not inoculated conditions, even when a potential difference of 1 V is applied between the anode and the cathode (**Fig. V-3**). To summarize, the following removal mechanism can be hypothesized: during polarization toluene was converted into metabolic intermediates (such as VFAs), which were in turn oxidized at the anode, generating an electric current that was used at the cathode for the reduction and precipitation of copper (**Fig. V-4**). Further insights into the mechanisms of contaminants removal are gathered through electrodes characterization.

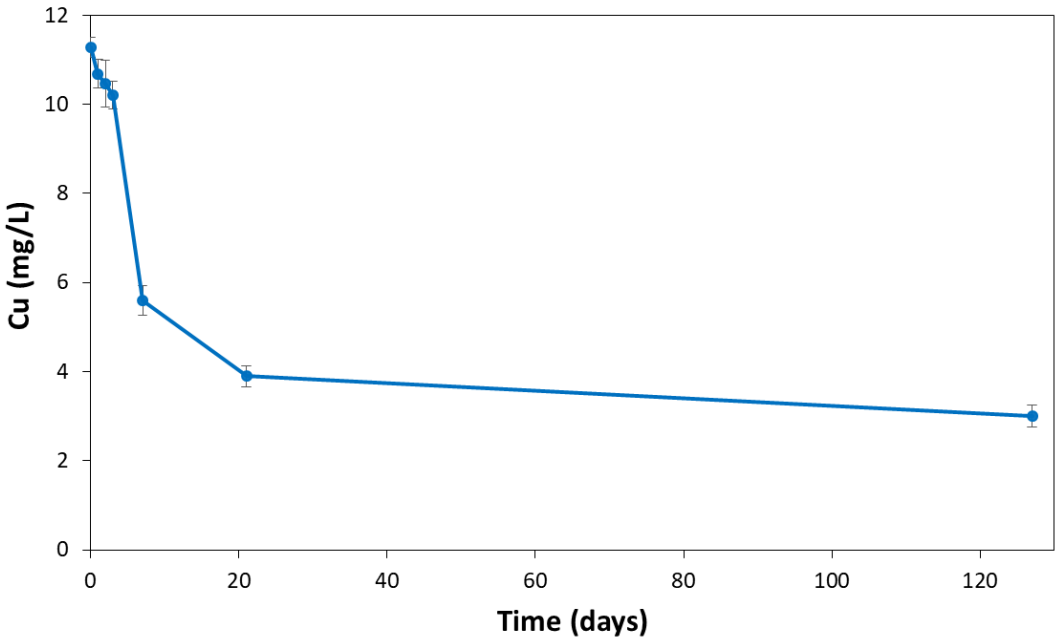

Figure V-2: *Copper concentration during time in abiotic and non-polarized experiments.*

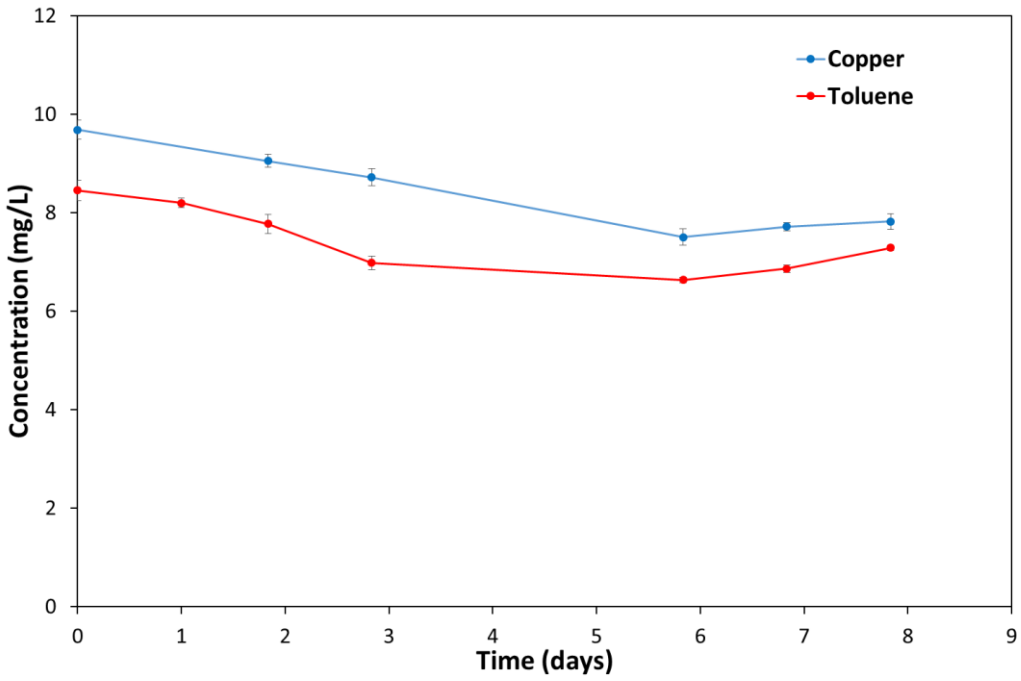

Figure V-3: *Copper and toluene concentration during time in abiotic and polarized experiments (1V).*

V.3.2 Electrodes characterization

At the end of the experiment, graphite rods were collected for the microbiological characterization of the biofilm and the analysis of the chemical composition of the surface. Electrodes characterization was aimed at clarifying the mechanisms of contaminants removal observed in the bioelectrochemical experiments.

V.3.3 Anode characterization

The anode collected from the cells at the end of the experimental period was divided in different parts for subsequent microbiological, microscopy and spectroscopy analyses.

Figure V-4A shows the CLSM combined images showing the spatial distribution (X−Y, X−Z, and Y−Z planes) of DAPI stained cells and EPS (stained by Calcofluor White) attached to the graphite electrode used as anode. The CLSM revealed the presence of a nearly 20 µm-thick biofilm on the surface of the electrode. Both cells and EPS are blue, while the surface of the electrode is visualized by its reflection signal in the same microscopic field, and appears grey. The presence of a biofilm was confirmed by SEM images of the anode (**Fig. V-4B**), which show an electrode uniformly covered by a biofilm, mostly composed by bacilli (morphology: ~1 µm long and 0.5 µm wide) and to a lesser extent by cocci.

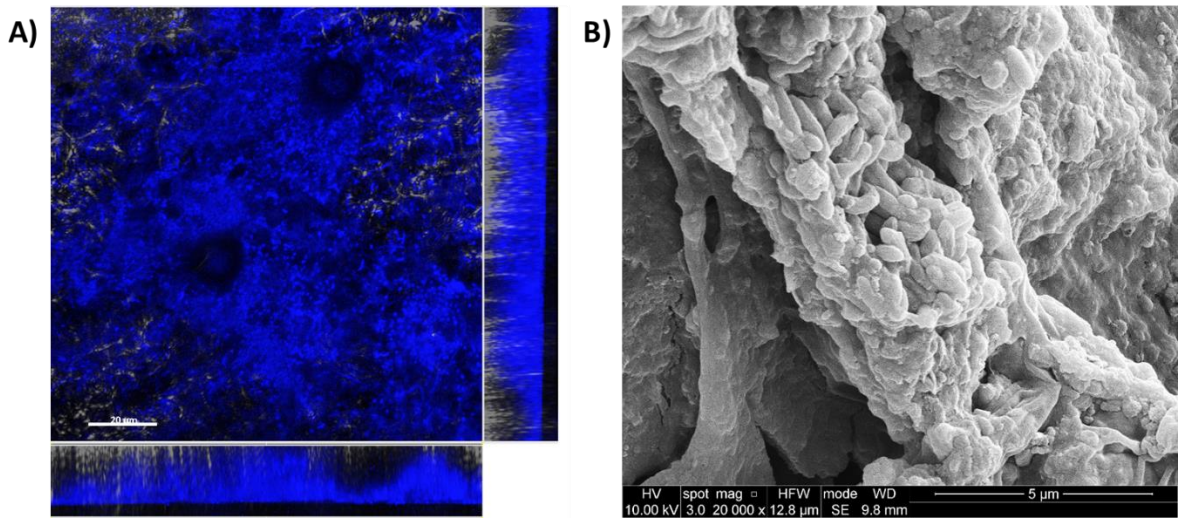

Figure V-4: *A) CLSM combined images showing the spatial distribution (X−Y, X−Z, and Y−Z planes) of DAPI stained cells and EPS attached to the graphite electrode used as anode. B) SEM*

micrograph of the anodic biofilm. Both CLSM and SEM images were taken at the end of the cells operation.

The 16S rRNA gene amplicon sequencing revealed a highly selected microbial community of the biofilm collected at the end of the experiment from the anode surface and the bulk effluent (**Fig. V-5**). The bacterial composition of the bulk effluent was also analyzed. In particular, the anodic biofilm was dominated by members of the class of *Alphaproteobacteria* (41%) and members of *Actinobacteria* (40%) and *Firmicutes* (11%) phyla. They were all previously identified in bioelectrochemical systems and reported to be involved in the syntrophic degradation of aromatic hydrocarbons, as detailed below.

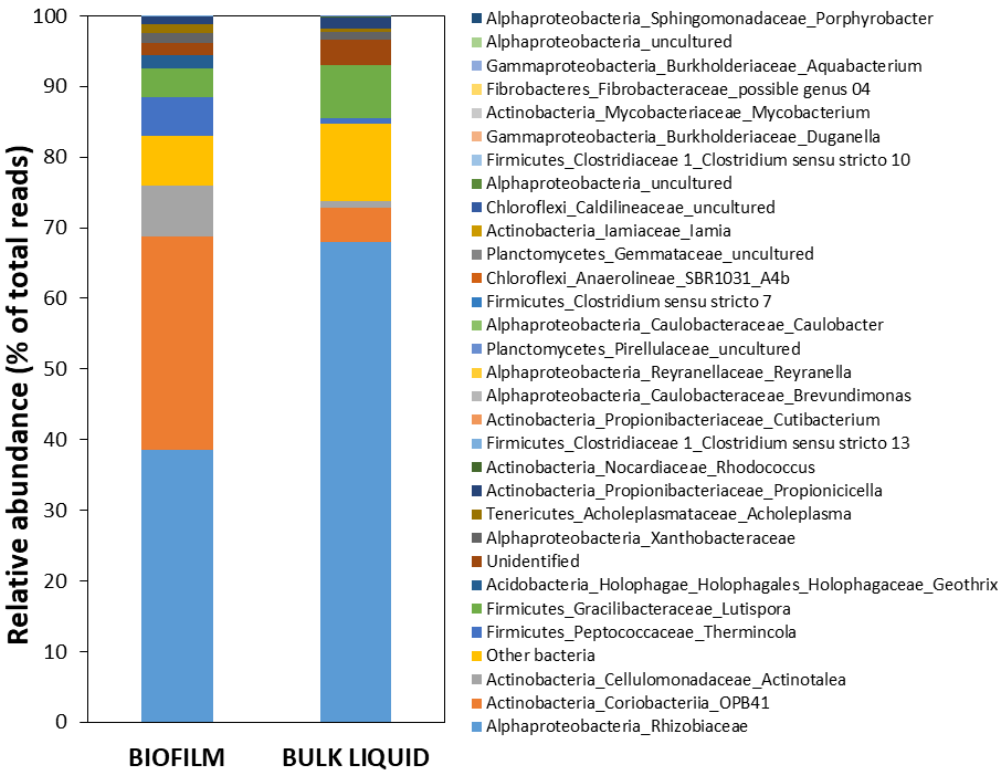

Figure V-5: *Bacterial community composition revealed by the 16S rRNA gene amplicon sequencing. Data are reported as the relative abundance of ASVs as a percentage of total reads in both the biofilm on the anode surface and the bulk liquid.*

The most abundant bacterial taxa found on the anode surface were *Rhizobiaceae* (39.5 % of total reads). Similarly, also within the bulk effluent, *Rhizobiaceae* were

dominant (68%). Members of this family have been reported to be involved in the degradation of aromatic hydrocarbons (Singha and Pandey, 2020; Teng et al., 2015; Zhang et al., 2012). In particular, the single sequence ASV1 was the most abundant found on the anode surface and in the bulk effluent of the bioelectrochemical reactor developed in the current study. The ASV1 sequence shows 100% similarity (BLAST analysis, RID: NENPHDUZ013) with *Aminobacter* species, the latter previously identified as genera capable of degrading toluene in polluted environments (Konya et al., 2023), and also found in anode microbial communities in MFCs (Phung et al., 2004). Interestingly, *Rhizobiaceae* were highly abundant also in the bioelectrochemical reactor of a previous study treating toluene, where the authors hypothesized that it could drive the degradation of toluene leading to the production of key intermediates useful for the subsequent fermentative processes for VFA and H_2 production (Tucci et al., 2022c). Other taxa present in the biofilm on the anode surface were affiliated with *Actinobateria*, including *Coriobacteriia_OPB41* (30%) and *Cellulomonadaceae_Actinotalea* (7%). A direct involvement of unidentified members of Actinobacteria order OPB41 in toluene or hydrocarbons degradation was not discussed so far even though they were reported as a component of microbial community in previous works concerning hydrocarbons degradation (Chen et al., 2016; Laso-Pérez et al., 2019; Tucci et al., 2023, 2022c). Anyway, Khomyakova and colleagues have recently isolated two pure cultures of anaerobic actinobacteria belonging to *OPB41* (Khomyakova et al., 2022). In particular, strain M08DHBT has the ability to grow on the aromatic compound 3,4-dihydroxybenzoic acid. This compound, with a trivial name protocatechuate, could be formed during aerobic or anaerobic degradation of lignin-associated phenolic compounds. Analysis of strain M08DHBT genome did not reveal any complete aerobic or anaerobic pathways of aromatic compounds degradation, but some crucial determinants of protocatechuate oxidation have been identified. *Actinotalea* was recently identified in the anodic community of a MFC (Szydlowski et al., 2022). Szydlowski and colleagues identified the presence of numerous sequences related to electron transfer in its genome, e.g., the type IV pilus biosynthesis gene pilB,

confirming that this organism can respire through anodes, just like the model electrogenic microorganism *Geobacter*. They also documented the presence of novel and unique enzymes, such as NADH translocases, that could provide resilience to high Cu content. *Actinotalea* is also reported to be involved in aromatic hydrocarbons degradation (Kang et al., 2023; Li et al., 2019) both in electrified (Li et al., 2019) and in not electrified (Kang et al., 2023) systems. Both kind of the cited systems were amended with electrically conductive particles of biochar. Member of *Firmicutes,* such as *Peptococcaceae_Thermincola* (5.5%) and *Gracilibacteraceae_Lutispora* (5%), were also found on the anode surface. *Firmicutes* were also found to be involved in the anaerobic biodegradation of polycyclic aromatic hydrocarbons (PAHs). Members of this family were the most abundant microorganisms in bioaugmented inocula for the remediation of PAH contaminated soils (Ferraro et al., 2021). *Firmicutes* were also identified in the bioanode biofilm of BES for accelerating the anaerobic biodegradation of Resorcinol, a typical aromatic contaminant as well as a key central intermediate (other than benzoyl-CoA) involved in anaerobic biodegradation of aromatics (Yang et al., 2021). In particular *Thermincola* members have been previously found in a toluene/TCE degrading bioelectrochemical reactor (Cruz Viggi et al., 2022), as well as in a tubular microbial fuel cell to remove benzene and toluene, together with the exoelectrogens *Geobacter* as the main species on the anodic surface (Lin et al., 2022).These previous evidences suggest a role of T*hermincola* member in toluene biodegradation. Regarding the *Lutispora* member found on the anode surface, it has been previously reported this microorganism as key degrader of VFA, which end products are acetate, isobutyrate, propionate and isovalerate (Hashemi et al., 2022), thus suggesting a role in the VFA metabolism within the system. As expected, the bulk effluent showed a similar composition to the anode biofilm, with *Alphaproteobacteria* (70%), *Actinobacteria* (11%) and *Firmicutes* (9.8%). Overall, the microbiological characterization of the electrogenic biofilm revealed a highly selected bacterial community competent in the biodegradation of toluene. It is likely that members of Rhizobiaceae, particularly Aminobacter, along with Coriobacteriia_OPB41, and to a lesser

extent Peptococcaceae_Thermincola, are the primary bacterial players responsible for toluene degradation within the system, while Lutispora likely contributes to toluene transformation into VFAs. X-ray photoelectron spectroscopy was finally employed to identify the chemical species present on the surface of the graphite rods retrieved at the end of the experiment. For comparative purposes, an identical, unused graphite rod was also analyzed. Besides trace amounts of impurities mainly consisting of silicon (as SiO_2), oxygen (as OH^-), and alumina (as Al_2O_3), photoemission spectra of the untreated graphite rod revealed only the presence of graphitic carbon (C 1s spectrum, C-C bond at 284.6 eV). In contrast, the C 1s spectrum of the anode clearly revealed, in addition to graphite, a second component at 288.2 eV due to the bonds of C = O and/or C-N, most likely attributable to the presence of adherent bacterial cells. Consistently, the nitrogen spectrum revealed the presence of N 1s peak located at BE = 400.4 eV, which is characteristic for C = NH, C-NH_2 bonds.

V.3.4 Cathode characterization

The cathode collected at the end of the experiment was partitioned into various segments for subsequent analysis. The surface of the cathodes coming from the electrified cells showed a reddish coloration to the naked eye, which is typical of copper deposition. The microbiological characterization of the cathode revealed a very low number of ASVs (3767) from the 16S rRNA gene sequencing with a heterogeneous bacterial composition, confirming that no significant biological process took place at the cathode. As proof of this, SEM images of the cathode (**Fig. V-6**) showed no significant presence of microorganisms and confirmed uniform Cu electrodeposition over the surface of the cathode. Specifically, it can be observed the presence of spherical copper nanoparticles, with size ranging between 200 and 300 nm. Copper nanostructures have recently garnered significant attention in the literature. This is primarily because the face-centered cubic structure of copper is considered an ideal alternative material, owing to its remarkable stability, excellent electrical conductivity, catalytic properties, and cost-effectiveness when compared to metals such as silver and gold (Sui et al.,

2010; Xu et al., 2010). Various shapes of copper nanostructures, including cubes, prisms, spheres and wires, have been obtained using a variety of techniques of deposition (Mandke and Pathan, 2012). Electrochemical deposition stands out as a promising method for making copper nanoparticles due to its user-friendliness and cost-effectiveness. Several research groups have reported the synthesis of spherical copper nanoparticles similar to those obtained in this study through electrodeposition techniques (Mandke and Pathan, 2012; Pagnanelli, 2019; Pedersen et al., 2008; Yeshchenko et al., 2007).

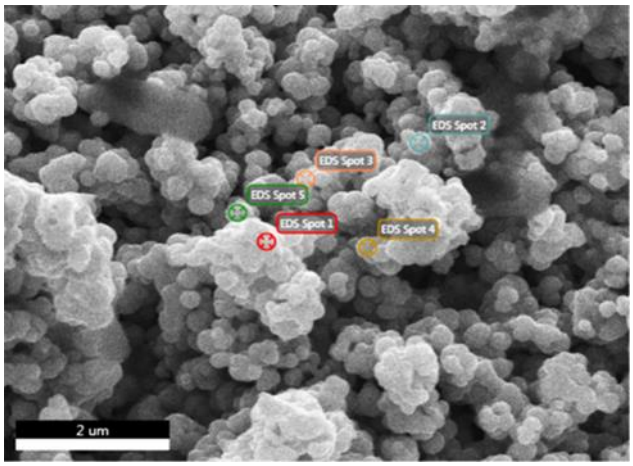

Figure V-6: *SEM micrograph of the spherical copper nanoparticles, showing the five different spots in which Energy Dispersive Spectroscopy (EDS) analysis was performed*

Energy Dispersive Spectroscopy (EDS) analysis was performed in five different spots, as showed in **Figure V-6**, to determine the elemental composition of the cathodic deposit. The EDS measures resulted in an average atomic ratio of Cu:O = 2.07 ± 0.14 % (**Fig. V-7**), confirming that copper was abiotically reduced and deposited at the cathode as Cu_2O. Copper electrodeposition as cuprous oxide was confirmed by XPS analysis, which revealed, in addition to what was found for the anode (peaks related to graphite, bonds of C = O and/or C-N and bonds of C = NH, $C\text{-}NH_2$, all attributable to bacterial cells, although the latter are present in smaller percentages), the presence of Cu peaks at 933.2 eV attributable to Cu_2O and Cu peaks at 935.5 eV most likely assigned to $Cu(OH)_2$.

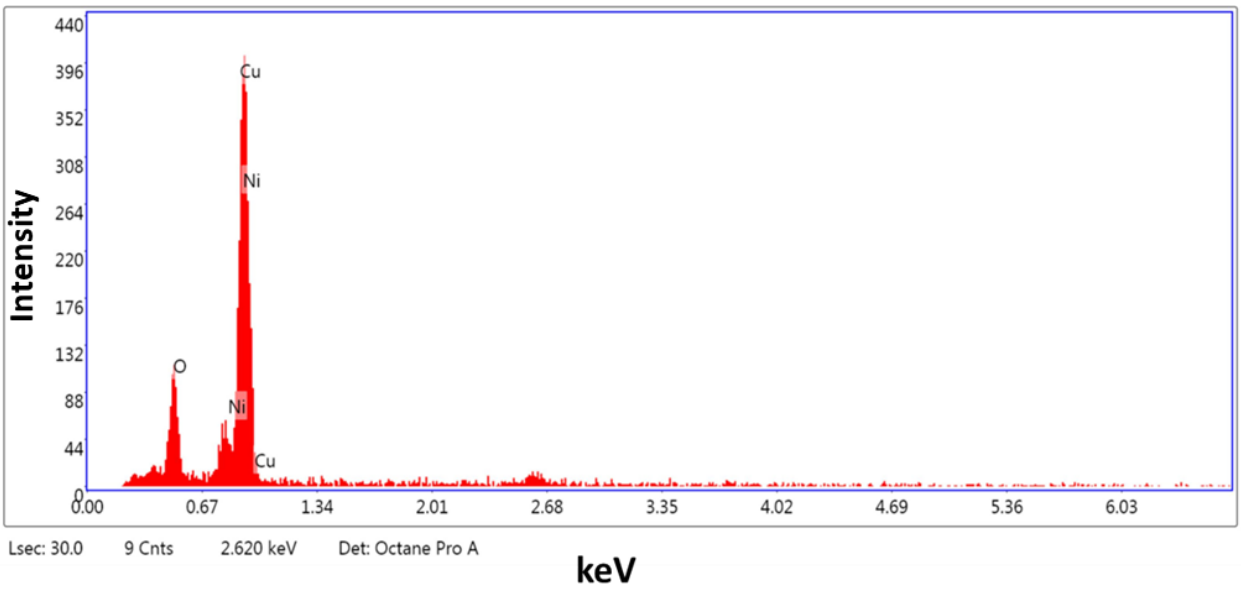

Figure V-7: *Energy Dispersive Spectroscopy (EDS) analysis of the cathodic deposit.*

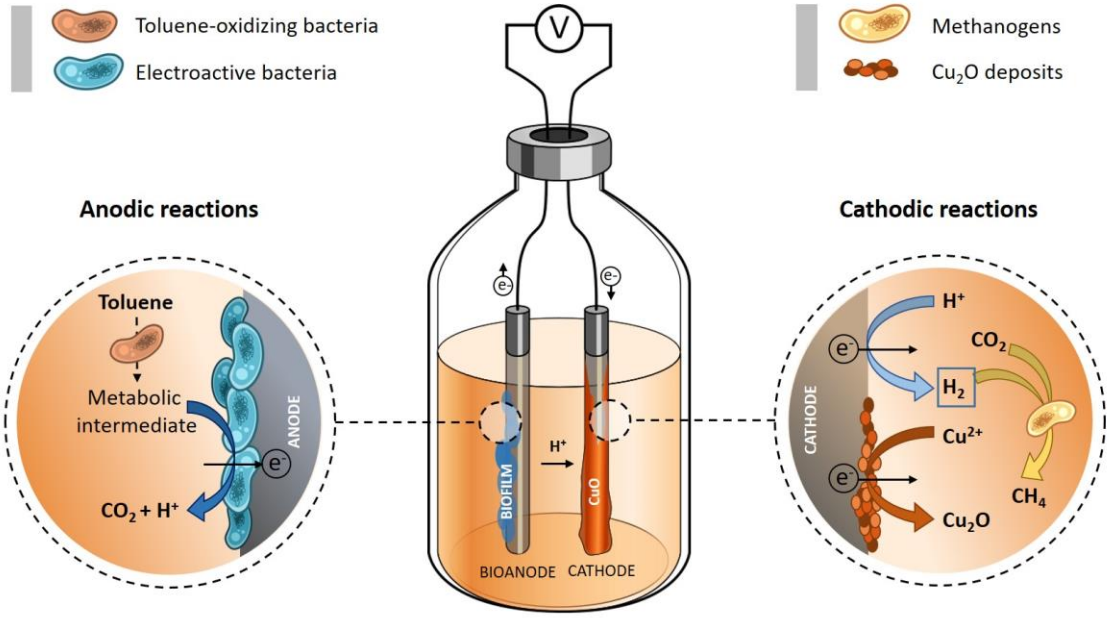

Figure V-8*: Schematic proposed mechanisms for the bioelectrochemical treatment of a groundwater co-contaminated by toluene and copper.*

V.4 Conclusions

For the first time, the degradation of toluene was coupled with copper removal in a single-chamber bioelectrochemical cell. The system was able to achieve almost complete removal of both toluene and copper, exploiting both the oxidation and the reduction reaction simultaneously. Through a comprehensive set of chemical and microbiological analyses, the mechanism of contaminants removal was elucidated: toluene was oxidized at the bioanode, generating an electric current that was used at the cathode for the abiotic reduction and precipitation of copper. Electrodes characterization evidenced a highly selected and competent microbial community in the anodic biofilm, directly engaged in the biodegradation of toluene, and a uniform electrodeposition of spherical copper nanoparticles across cathode surface. The herein studied bioelectrochemical process is at an initial stage of development and would warrant further investigations in order to single out the operating conditions for contaminants removal, primarily in terms of reactor design, electrode materials, and applied working conditions (e.g., cell voltage). It would also be interesting to assess process performance in the presence of even more complex mixtures of contaminants to verify the possible occurrence of competitive effects. The recovery of metal nanoparticles from the electrode can possibly open new opportunities in the broad area of the valorization of contaminated (waste)water from a circular economy perspective.

.

Chapter VI

Innovative approach for water remediation: bioelectroremediation combined with carbon nanotubes conductive membranes for ultrafiltration

VI.1 Introduction

VI.1.1 Environmental Problem

Groundwater is the largest source of drinking water, but its usability is compromised by various pollutants (European Environment Agency, 2022). The presence of multiple contaminants from both human and geological sources necessitates the development of sustainable technologies to deal with them. Among others, nitrate pollution, largely due to intensive agriculture, is a global concern.(Bijay-Singh and Craswell, 2021). The World Health Organization (WHO) identifies nitrate as a hazardous inorganic contaminant in groundwater (WHO and UNICEF, 2021) and the Nitrates Directive (91/767/EU) sets a nitrate concentration limit of 11.3 mg $N\text{-}NO_3^-$ L^{-1} (50 mg NO_3^- L^{-1}) in drinking water (Commission, 2000) .Conventional treatments for nitrate-polluted groundwater typically use separation technologies that, while effective, are often energy-intensive and produce waste brines requiring further treatment (e.g., Ion exchange, reverse osmosis, reverse electrodialysis) (Fernández-López et al., 2023). On the contrary, biological denitrification, which reduces nitrate all the way to atmospheric nitrogen gas (N_2) in four biochemical steps, offers environmental and economic benefits because nitrate is ultimately converted into a harmless product, thus eliminating the need of waste disposal and (at least potentially) allowing nearly complete water recovery (Thakur and Medhi, 2019).

However, contaminated groundwater typically lacks sufficient electron donors to allow such a reaction to occur, thus necessitating a continuous supply of chemicals like acetate or hydrogen gas.

VI.1.2 Electro-bioremediation

An alternative method to remove nitrates by biological means without the need for supplying chemicals is electro-bioremediation. This method is a primary microbial electrochemical technology (MET) and emerges as a sustainable alternative for groundwater treatment. MET is based on bioelectrochemical systems (BES) harnessing the capacity of electroactive microorganisms to

perform oxidation and reduction reactions with solid electron conductors (e.g., electrodes). Thereby, these electroactive microorganisms are able to use the anode and the cathode as an inexhaustible electron acceptor or donor, respectively, allowing the removal of pollutants by using electricity as the sole external input (Puig et al., 2012).

In this approach, autotrophic denitrification uses the cathode as an electron donor and inorganic carbon as the carbon source, addressing the issue of insufficient electron donors in groundwater and eliminating the need for chemical additives (Pous et al., 2015; Puggioni et al., 2022). When nitrate is the target pollutant, autotrophic denitrification can be performed using only the cathode as electron donor and inorganic carbon as carbon source, which is usually largely available in groundwater in form of bicarbonate. Interestingly, autotrophic denitrifications typically characterized by an extremely low biomass growth, which eliminates (or at least minimizes) the need for sludge removal and disposal (Ceballos-Escalera et al., 2024a, 2024b, 2021). This technique also offers significant advantages over conventional treatments, such as reducing environmental impacts such as brine production or chemicals dosing. The challenges to implement this technology are that using a biofilm, some bacteria may still be released into the effluent. The use of a membrane ensures that no microorganisms are released to the effluent, thereby reducing the need for water clarification and disinfection. Additionally, there is limited research on the effect of electrode materials on denitrification rates. Scaling up these technologies remains a challenge, but integrating electrochemistry with well-established methods like ultrafiltration (UF) could potentially improve the scalability of the system (Rashed et al., 2023a, 2023b).

VI.1.3 Ultrafiltration and conductive membranes

Recently, electrocatalytic membrane reactors (ECMRs) have been developed the simultaneous separation and electrocatalytic degradation of organic pollutants. In ECMRs, electrically conductive membranes function as both filters and active electrodes for water treatment (Huang et al., 2015). Consequently, designing

active electrodes membranes involves creating selective membrane layers that are highly porous and electrically conductive (Sun et al., 2021). Engineered carbonaceous nanomaterials such as CNTs have been increasingly reported as typical buildings units for the active electrodes in electrochemical cells and ECMRs due to their intrinsic physicochemical and electrical properties. When voltage is applied, these membranes interact with contaminants via electro-oxidation, electrostatic adsorption, and electrostatic repulsion, processes responsible for water decontamination (Liu et al., 2022).

VI.1.4 Aims of the study

The rationale of this study is to combine nitrate electro-bioremediation processes with ultrafiltration technology, utilizing conductive membranes that would serve as both electrodes and membranes. This approach could allow driving the filtration of water and the biodegradation of contaminants directly on the membrane, thereby reducing membrane's fouling issues and co-localize the contaminant and the microorganism by mechanically forcing their contact, to enhance the biodegradation process.

VI.2 Experimental Section

VI.2.1 Bioreactor Setup

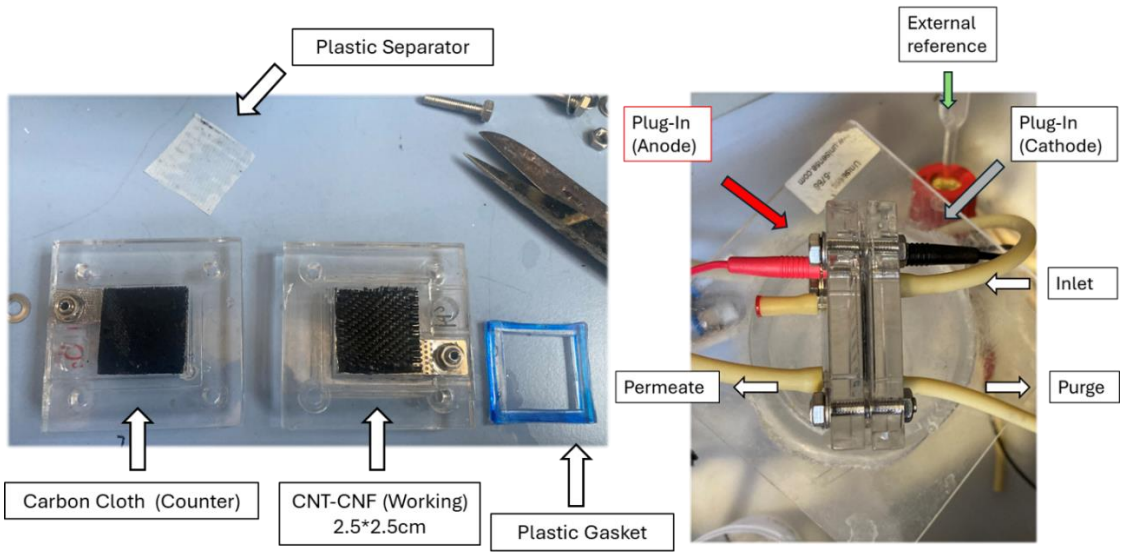

Figure VI-1 *Experimental setup of the Bioelectrochemical system, featuring a CNT-CNF membrane as the working electrode (left), a carbon cloth counter electrode, and a plastic separator. The right side includes plug-ins for the anode and cathode, an external reference*

The setup consisted of two replicates of a rectangular plastic cell with a net volume of 1.5 mL. Each cell included a carbon cloth layer in contact with an electrical collector as the anode (counter electrode), measuring 2.5 cm x 2.5 cm, and a CNT-CNT layer in contact with an electrical collector as the cathode (working electrode), also measuring 2.5 cm x 2.5 cm, with a working area of 6.25 cm^2. The two electrodes were physically separated by a plastic separator (PTFE) to prevent contact between them (**Fig.VI-1**). The electrodes were connected to the potentiostat (VSP, BioLogic, France) using banana plug-in connectors and worked in galvanostatic mode, current applied -2 mA, resulted in -0.2 V vs Ag/AgCl of cathodic potential. The cell was connected to an external buffer tank with a liquid volume of 100 mL and a headspace volume of 20 mL. An Ag/AgCl saturated KCl reference electrode (SE 11, Xylem Analytics Germany Sales GmbH & Co. KG Sensortechnik Meinsberg, Germany) was positioned externally to the cell along the recirculation line. The cell had an inlet line, a purge line, and an outlet line where the permeate flowed out (**Fig. VI-1**). At the beginning of the test, the system was set anoxic by flushing with N_2 gas. Temperature was maintained at a value of 25±1 °C and pH at 7.4±0.05**.**

VI.2.2 CNT-CNF membrane

CNT-based membranes were fabricated by dry spinning of carbon nano tubes (CNT) layers from the CNT forest using layer by a layer stacking method previously reported to produce resilient CNT assemblies for sensing and energy storage applications (Gbordzoe et al., 2017; Y. Wang et al., 2015; Zhang et al., 2018). The CNT layers were collected on a rotating drum collector supported by synthesized carbon nano fibers (CNF) support membranes at a fixed speed of 15 rpm. The membrane used is a 30 layers CNTs 1K twill carbon fiber. CNTs 263 µm, 51.6 mg cm^{-3}, 850 Ω/ω (Kumari et al., 2021; Rashed et al., 2023a, 2023b).

VI.2.3 Reactor start-up and operation

The system was inoculated with a pure culture of *Thiobacillus denitrificans* and operated with a medium prepared with distillate water and contained; 420.0 mg L^{-1} $NaHCO_3$ as inorganic carbon source, 7.5 mg L^{-1} KH_2PO_4 , 1.9 mg L^{-1} Na_2HPO_4 , 100.0 mg L^{-1} NaCl, 75.2 mg L^{-1} $MgSO_4 \times 7H_2O$, 10.0 mg L^{-1} NH_4Cl and 0.1 mL L^{-1} of a trace minerals solution (Balch et al., 1979; Ceballos-Escalera et al., 2021). The system was set anoxic by flushing with dinitrogen gas at the beginning of each cycle. In batch mode, the three lines are connected to a serum bottle functioning as a buffer tank, with a liquid volume of 100 mL and a headspace volume of 20 mL. When nitrate was exhausted, half of the liquid volume was removed and replaced with fresh mineral medium containing nitrate enough to set an initial concentration of 60 mgN L^{-1}. From day 0 to 76 (5 batch cycles), the system was operated under galvanostatic mode at -2mA, which allowed to obtain a cathode potential around -0.2V vs Ag/AgCl. While from day 48 to 76 (2 batch cycles), the system was operated under open circuit conditions.

VI.2.4 Biotic OCP Membrane-less Control

A 120 mL serum bottle was used, containing an inoculum and 100 mL of mineral medium, with an initial nitrate concentration of 80 mgN L^{-1}. The reactor was made anaerobic at the start of the experiment by flushing it with pure N_2. The test was conducted for 360 hours, during which liquid samples were collected, filtered

using a 0.22 µm filter, and analyzed by ionic chromatography (ICS 5000, Dionex, USA). The reactor was kept under agitation using a submerged magnetic stirrer and a magnetic plate.

VI.2.5 Control with Membrane Immersed in Inoculated Medium

In the same 120 mL serum bottle, with the same inoculum and mineral medium (pH ~7) and nitrate, a 2.5x2.5 cm section of CNT-CNF membrane was added after initial membrane-less operation. The system was re-flushed with N_2 to restore anaerobic conditions, and the test continued for an additional 300 hours.

VI.2.6 Abiotic Control with Polarized Membrane

A parallel abiotic control experiment was set up, following the same bioreactor configuration but without the addition of inoculum. The mineral medium was supplemented with 60 mgN L^{-1} of nitrate, and the CNT-CNF membrane was polarized as the cathode using a galvanostatic technique with a constant current of -2 mA, replicating the conditions of the main biotic reactor.

VI.2.7 Ecotoxicological testing of conductive membranes

Six 120 mL serum bottles (3 with membrane and 3 without) were prepared. Each bottle contained inoculum from the main reactor, mineral medium with 120 mg/L of nitrate, and 5 g/L of thiosulfate. The bottles were stirred using a multi-position magnetic stirrer. Daily sampling was performed, with liquid-phase samples filtered using a 0.22 µm filter for nitrate, nitrite, and sulfate analysis. Unfiltered samples were used to measure optical density (OD) and pH evolution.

VI.2.8 Electrochemical Characterization of the membranes

Electrochemical impedance spectroscopy. AC amplitude 10mV, Frequency Range: scan from 100 kHz to 100mHz**.** Two-electrode configuration, CNT-CNF membrane setted as working electrode and carbon cloth as counter electrode.

VI.2.9 Cyclic Voltammetries

Scan Rates: 10mV/s**,** Scanning potential window: from 0 to -1V**,** Number of Cycles: 3 For all CVs, an Ag/AgCl electrode (+0.198 V vs. SHE; AMEL, Italy) was used as reference.

VI.2.10 Permeability Test and Permeate Flow

For the Permeability test, the membrane placed into the reactor, where a pressure difference is applied across the membrane. The permeate is collected, and the flux is calculated. Permeate flow refers to the rate at which the permeate passes through the membrane. Permeate flow is measured by collecting the permeate over time and calculating the flow rate (Equation 2)

VI.2.11 Chemical analyses and calculations

All liquid samples were analysed in the laboratory by ionic chromatography (ICS 5000, Dionex, USA) according to APHA standard water measurements (APHA, 2005) with special attention to these ions: nitrate (NO_3^-), nitrite (NO_2^-). A N_2O liquid-phase microsensor (Unisense, Denmark) located in the recirculation loop of the reactor.

Nitrate Removal Rate was calculated as the milligram of Nitrate removed divided by the day and the surface area of the electrode-membrane.

$$\text{Nitrate Removal Rate} = \frac{NO3-(mg)}{Time\ (days)\ X\ Surface\ area\ (m^2)} \quad (1)$$

Permeability was calculated as the ratio between liters per square meter per hour (LMH) and the transmembrane pressure (TMP). LMH is a measure of specific permeate flux, defined as the volume of liquid (in liters) that passes through one square meter of membrane surface per hour it is used to express the efficiency of the membrane in terms of its capacity to filter liquid. A high LMH value indicates good permeability of the membrane. While TMP stands for transmembrane pressure, which is the difference in pressure between the feed side and the permeate side of the membrane. It indicates the driving force required to push the fluid through the membrane and depends on the resistance offered by the

membrane and any fouling that may occur. TMP is a critical parameter because it influences both the permeate flux and the lifespan of the membrane.

$$Permeability = \frac{LMH}{TMP} \quad (2)$$

$$LMH = \frac{Permeate\ volume\ (L)}{Membrane\ surface\ area\ (m^2)\ X\ Time\ (h)} \quad (3)$$

$$TMP = \frac{P\ feed\ (mBar) + P\ retentate(mBar)}{2} - P\ permeate(mBar) \quad (4)$$

Where:

P_{feed} is the pressure on the feed side,

$P_{retentate}$ is the pressure on the retentate side

$P_{permeate}$ is the pressure on the permeate side

The faradaic efficiency of the denitrifying biocathode was calculated as the ratio between the cumulative equivalents of nitrate removed ($mmoleq_{NO3^-}$) and the cumulative equivalents deriving from current applied ($mmoleq_i$), according to the following equation:

$$Faradaic\ Efficiency = \frac{mmoleqNO3^-}{mmoleqi} \quad (5)$$

VI.3 Results and Discussion

VI.3.1 Batch Mode with synthetic groundwater

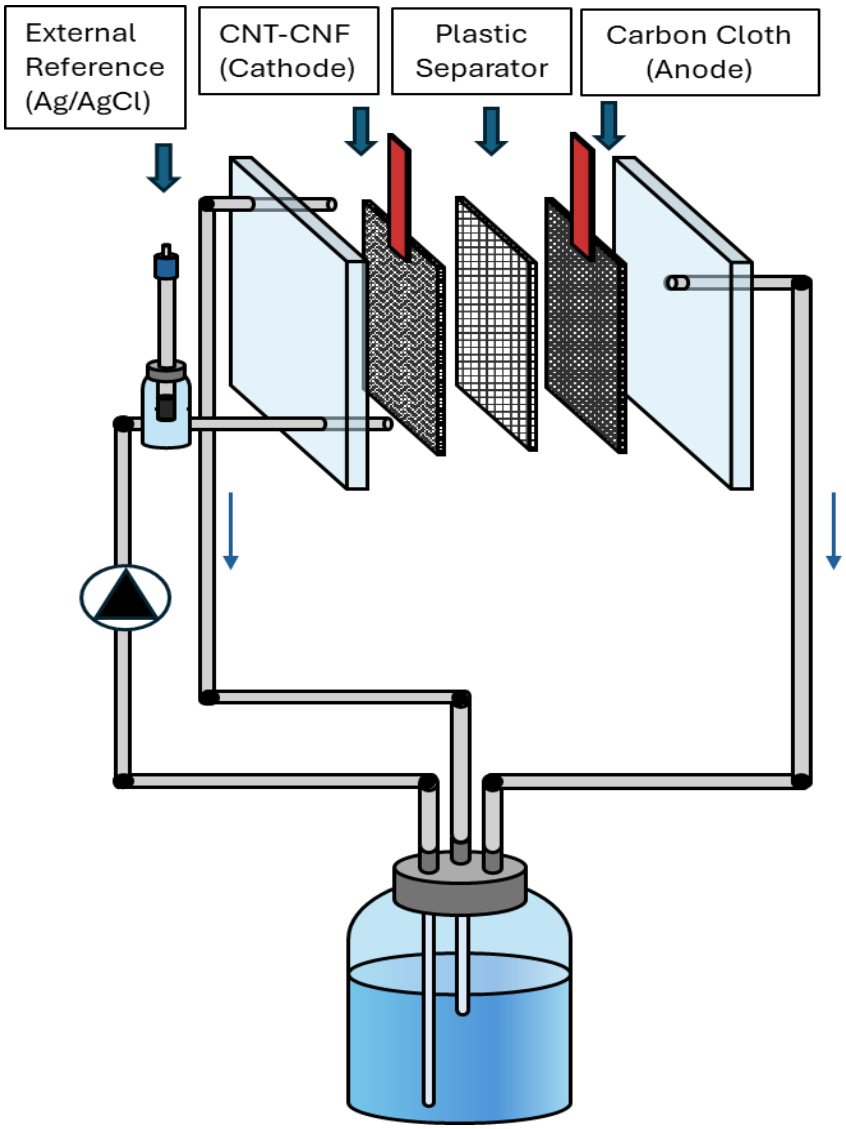

Figure VI-2 *Schematic representation of the electrochemical reactor system. The diagram illustrates the flow of influent through the reactor*

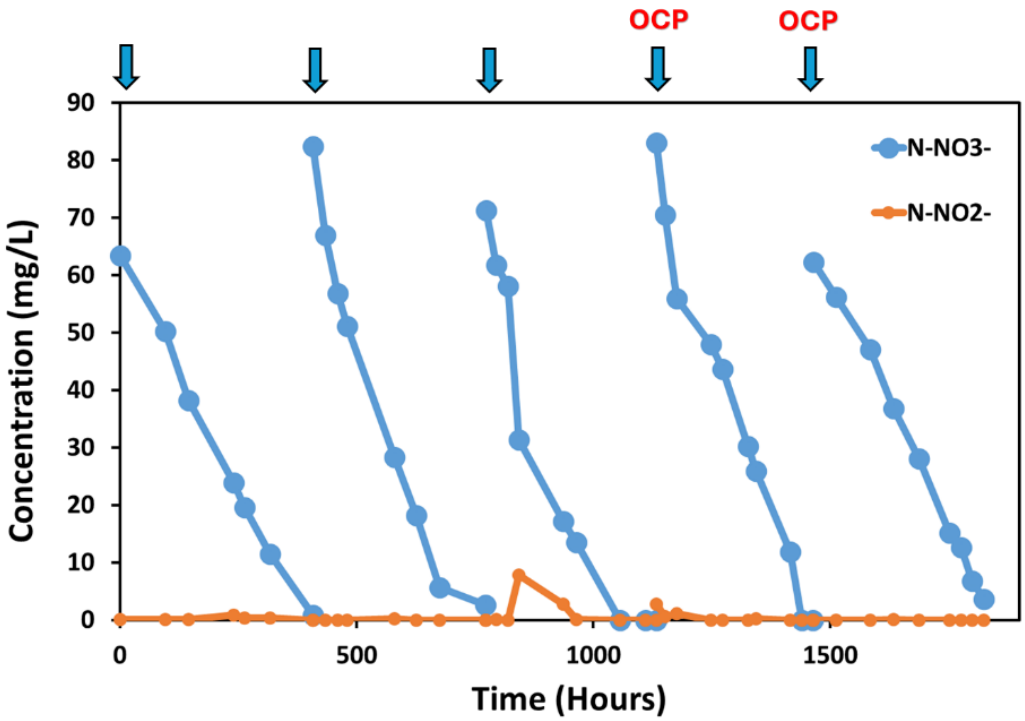

Figure VI-3 *Evolution of nitrate ($N\text{-}NO_3^-$) and nitrite ($N\text{-}NO_2^-$) concentrations. The blue line represents nitrate concentration. The orange line shows nitrite concentration, remaining low throughout the experiment. The arrows indicate the distinct nitrate spikes associated with each treatment cycle, with the last two cycles conducted under open circuit conditions (OCP).*

The concentrations of nitrate and nitrite anions were systematically monitored over time during a total of 5 feeding cycles in batch mode operation (**Fig. VI-3**). In each cycle, nitrate was completely removed, and no accumulation of nitrite was observed. During the first cycle, the rate of nitrate removal was notably the slowest (609 mgN m^{-2} d^{-1}) attributed primarily to the initial metabolic adaptation phase of the microorganisms, during which they acclimated to the substrate and initiated the formation of a biofilm on the electrode-membrane. *Thiobacillus denitrificans* was initially grown using thiosulfate as an electron donor before being used as a reactor inoculum. Once inoculated, it adapted to using the electrode-membrane as an electron donor. As the process advanced into the second and third cycles, a marked increase in the removal rate was observed, respectively 1017 mgN m^{-2} d^{-1} and 972 mgN m^{-2} d^{-1}, which stabilized at a higher level, indicating that the microbial community had effectively adapted to the

environmental conditions and substrate availability. Throughout the entire experimental duration, no detectable accumulation of nitrite or nitrous oxide (N_2O) was observed, confirming the occurrence of complete denitrification. This fact is commonly observed in MET-based denitrification studies, confirming the good electrode-like behaviour of conductive membranes.

From the second cycle the optical density (OD at 600 nm) remained constant at 0.022 ± 0.0023, and the pH values measured along the whole experiment remained constant at 7.40 ± 0.05, which was expected as both anode and cathode were present in the same media.

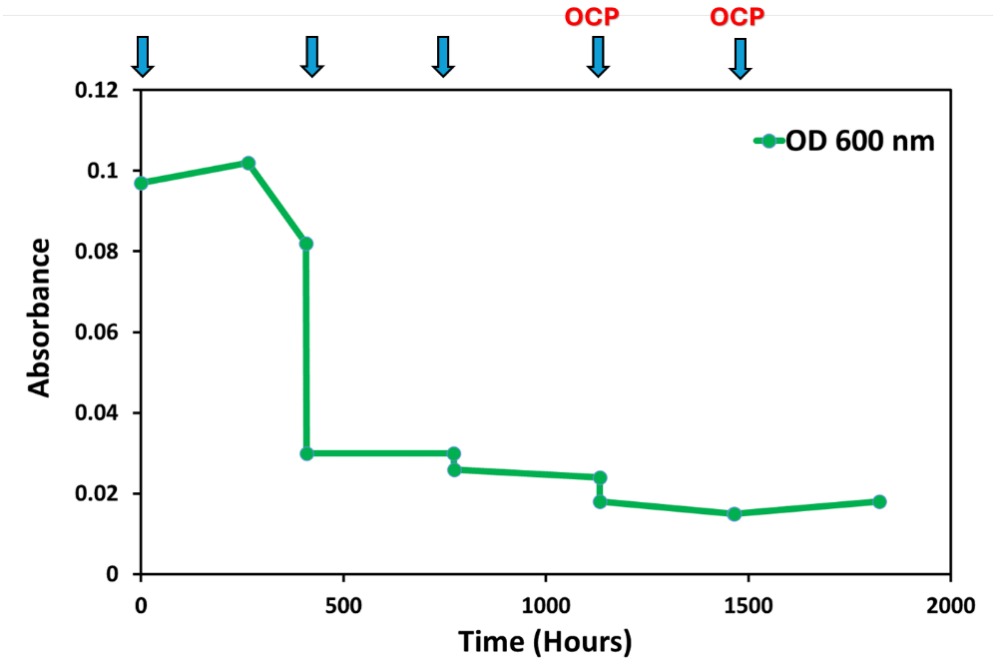

Figure VI-4 *Evolution of Optical Density at 600nm. The arrows indicate the distinct nitrate spikes associated with each treatment cycle, with the last two cycles conducted under open circuit conditions (OCP).*

In the fourth and fifth cycles, the system was operated under open circuit potential conditions as a control to observe the influence of polarization on the nitrate removal process. The nitrate removal rate observed during the fourth cycle was 848 mgN m^{-2} d^{-1}, which was comparable to the rates observed in the second and third cycles, 1017 mgN m^{-2} $d^{-1}$and 972 mgN m^{-2} d^{-1}, respectively. However, in the

fifth cycle, the removal rate 630 mgN m^{-2} d^{-1}, suggesting that polarization was necessary to maintain a higher nitrate removal rate.

We propose the following hypotheses to explain the observed nitrate removal in the absence of an external current supply:

i) Presence of an Electron Donor: One possibility is that an electron donor was naturally present in the system. To test this, we conducted an experiment where we monitored nitrate concentrations in a Biotic OCP membrane-less reactor. This allowed us to determine whether nitrate reduction can occur independently of any electrochemical processes. (**Figure VI-3, first cycle**)

ii) The Electrode alone facilitates Nitrate Removal: Another hypothesis is that the electrode-membrane CNT-CNF itself may support the removal of nitrates, possibly due to its surface characteristics or interactions with microbial communities. To evaluate this, we immersed the CNT-CNF in a solution containing both bacteria and nitrate, without applying any current, and tracked the changes in nitrate concentration. (**Figure VI-3 second cycle**)

iii) Electrode Capacitance: The third hypothesis involves the capacitance of the electrode. It is possible that the electrode and the conductive biofilm stores charge during the periods when current is applied and releases this stored energy to drive the reduction of nitrates even when no external current is supplied. Investigating the electrode's capacitance behavior could reveal whether this stored charge is sufficient to support ongoing nitrate removal in the absence of continuous power input.

VI.3.2 Biotic OCP membrane-less

Biotic Open Circuit Potential (OCP) Membrane-less Control: This control setup involves the operation of the system without the CNT-CNF membrane under biotic conditions, where microbial activity is present. In this scenario, both nitrate and sulfate concentrations remain stable over a duration of 350 hours, indicating

no significant removal or transformation of these anions in the absence of the membrane and the polarization (**Fig. VI-5**).

VI.3.3 Biotic OCP with membrane immersed

Membrane Immersed in Mineral Medium with Inoculum: This control setup examines the potential of the CNT-CNF membrane to donate electrons, an essential factor in its role in redox reactions. The membrane is submerged in a mineral medium inoculated with microorganisms. Over a period of 350 hours, the concentrations of nitrate remain stable as shown in **figure VI-5**, indicating that under these conditions, there is no significant electron donation by the CNT-CNF membrane, nor is there any notable reduction or transformation of nitrate or sulfate.

VI.3.4 Abiotic Polarized with flow through membrane

The same configuration of the main test, but abiotic and polarized in galvanostatic mode, applying the same current of -2mA and obtaining a voltage of -0.2 vs Ag/AgCl. Observed a removal rate of nitrate of 58 mgN m^{-2} d^{-1} (**Fig. VI-5**)

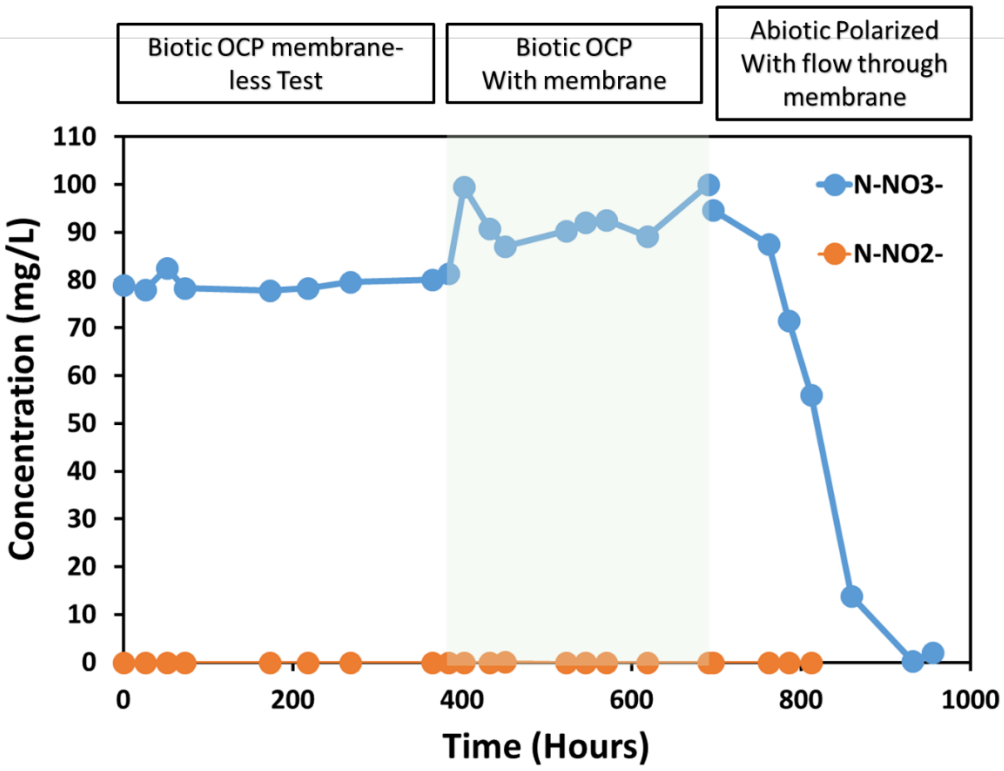

Figure VI-5 *Control Test - Evolution of nitrate ($N\text{-}NO_3^-$) and nitrite ($N\text{-}NO_2^-$) concentrations during the three different configuration of the control test. Biotic OCP membrane-less (from 0 to 350 hours). Biotic OCP with membrane dived (from 351 to 700 hours). Abiotic polarized flow through membrane (from 701 to 1000 hours)*

VI.3.5 Membranes Characterization: Permeability Test

Permeability testing and permeate flow analysis are critical for evaluating the performance of membranes. Shown in **figure *VI*-6**, the permeability test measured the ability of the membrane to allow substances to pass through it. The permeability is expressed in terms of flux, which is the amount of permeate passing through a unit area of the membrane per unit time (Liters per square meter per hour LMH) under a certain pressure difference (Trans-Membrane Pressure TMP).

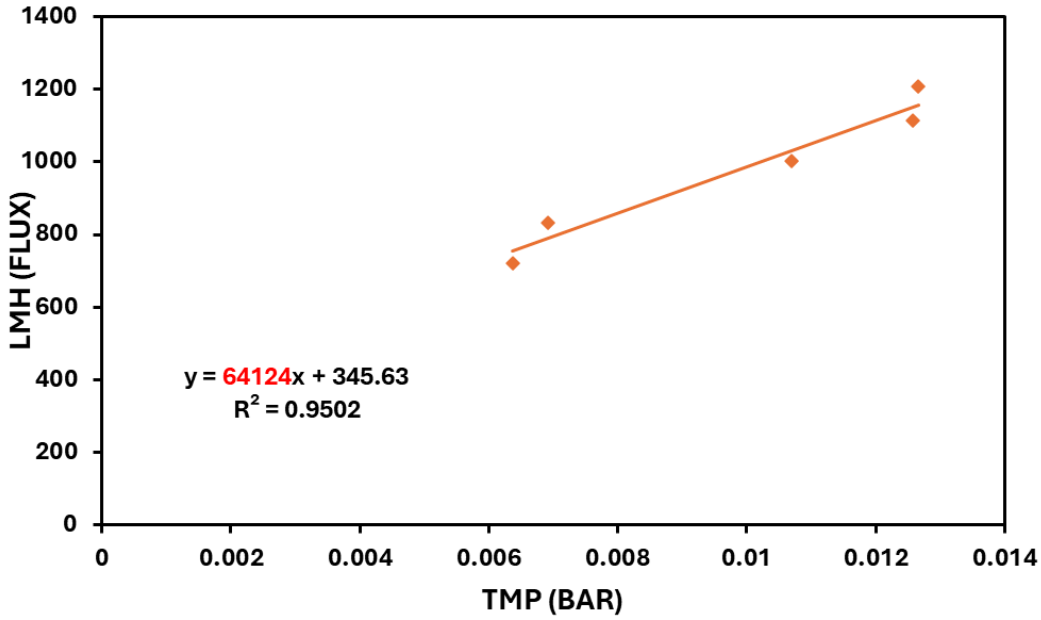

Figure VI-6 *Results from the permeability test , reported as LMH/TMP*

VI.3.6 Electrochemical Impedance Spectroscopy between Cathode and Anode

Electrochemical characterization of membranes using Electrochemical Impedance Spectroscopy (EIS) and Cyclic Voltammetry (CV) is crucial for understanding the membrane's properties. EIS is a powerful technique used to investigate the electrical properties of membranes over a wide range of frequencies. It provides information about the resistance, capacitance, and diffusion processes within the membrane. EIS is conducted using a two-electrode setup, where the membrane serves as the working electrode. A small AC perturbation 10 mV is applied over a range of frequencies from 100 kHz to 100mHz.

The data is presented in a Nyquist plot, where the imaginary part of the impedance (Z'') is plotted against the real part (Z'). The shape of the Nyquist plot can reveal important information. High-Frequency Region: a semicircle is observed, which corresponds to the charge transfer resistance. This change over time suggests an increase in surface heterogeneity and an additional impedance

contribution from the biofilm layer, which affects the overall electrochemical behaviour.

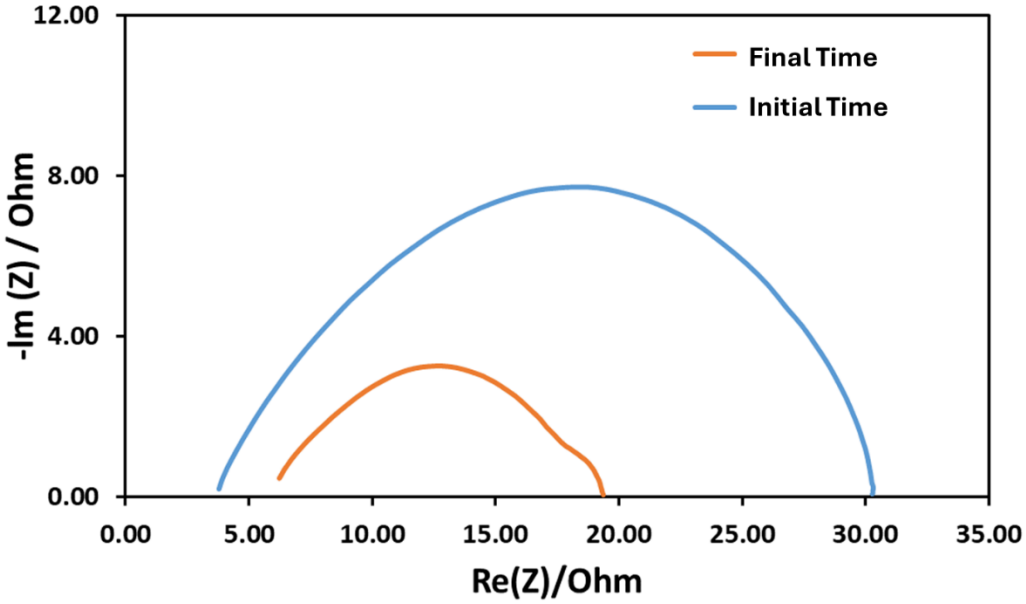

Figure VI-7 *The graph shows a Nyquist plot, where the imaginary part of the impedance (Z") is plotted against the real part (Z'). In orange the initial time of the membrane and in blue the final time after 2000 hours of operation.*

VI.3.7 Cyclic Voltammetry (H-type cell characterization)

Cyclic Voltammetry (CV) is used to investigate the electrochemical stability, redox behaviour, and ion transport properties of the membrane. It involves sweeping the potential of the working electrode-membrane linearly with time and recording the resulting current. CV is conducted in a three-electrode cell. Peaks in the voltammogram indicate redox processes occurring at the membrane surface. The position, shape, and height of these peaks can provide insights into the redox-active species within or interacting with the membrane.

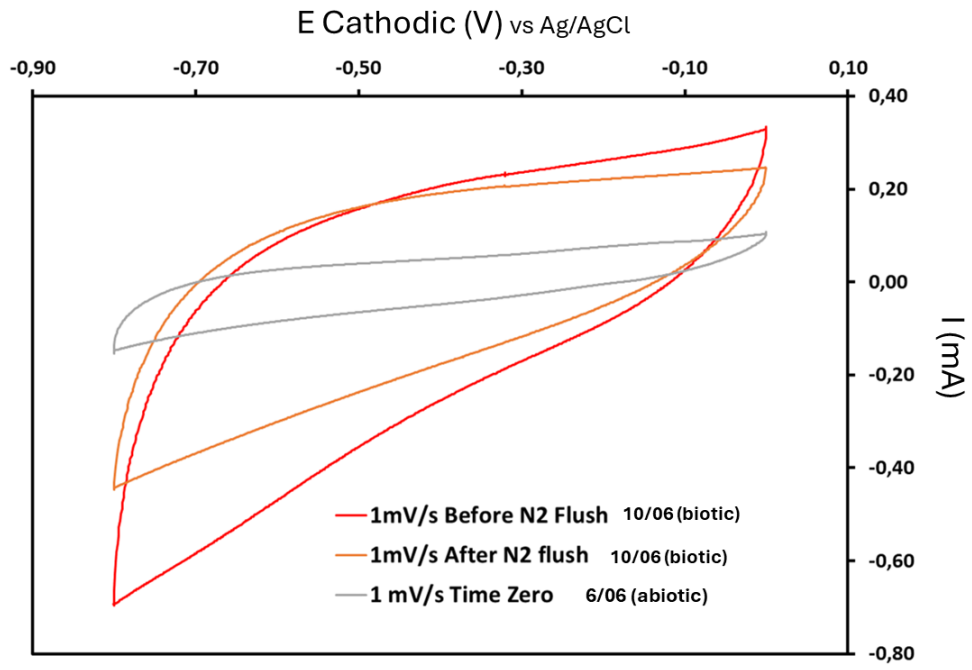

Figure VI-8 *Cyclic Voltammetries performed in a H-Type cell to characterize the CNT-CNF membrane at different times*

VI.3.8 Ecotoxicological Test for Assessing the Ecotoxicity of the CNT-CNF Membrane

This test involves an ecotoxicological assessment aimed at investigating the potential ecotoxicity of a novel carbon nanotube - carbon nanofiber (CNT-CNF) membrane. The experimental setup includes a Thiosulfate and Nitrate removal test, conducted with and without the inclusion of CNT-CNF membranes. The results provide insights into the comparative removal efficiencies of thiosulfate and nitrate in the presence and absence of the membranes, as well as any associated ecotoxicological impacts. No significant differences were observed in terms of nitrate removal rates, nitrite formation and elimination, or sulphate production from thiosulfate removal, demonstrating that the membrane did not exhibit measurable toxic effects on the bacteria involved in the removal of thiosulfate and nitrate, confirming its biocompatibility for use in similar environments.

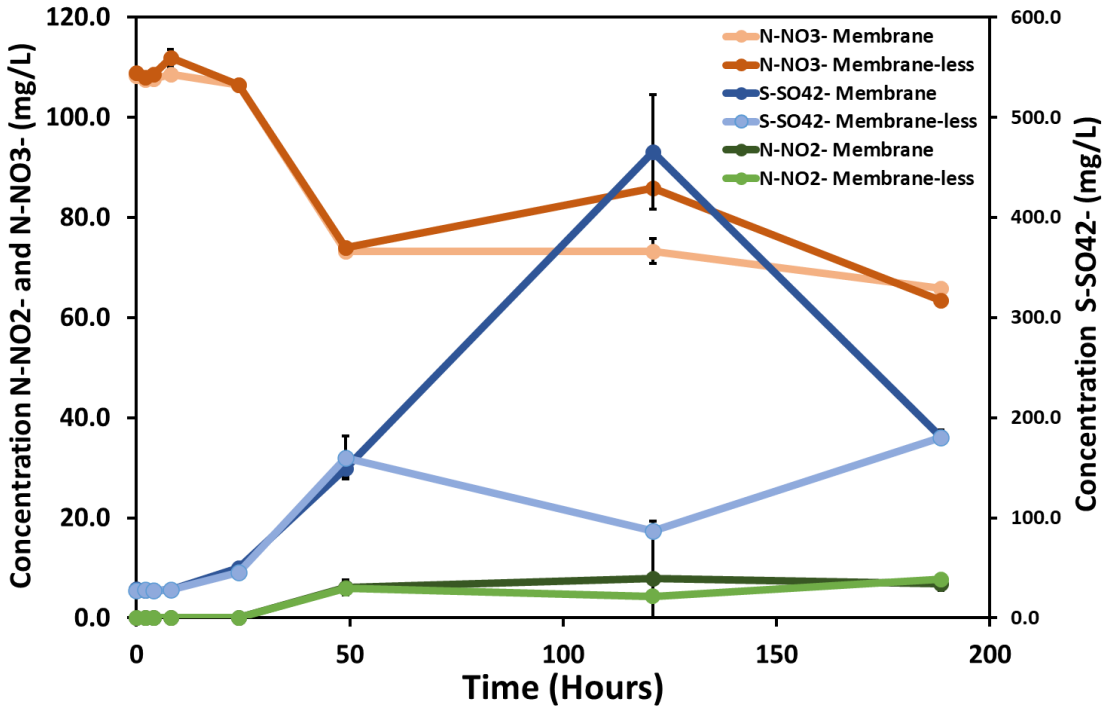

Figure VI-9 *The graph shows the results of the Ecotoxicological test done with and without membrane over 180 hours,*

VI.4 Conclusions

This study demonstrates the potential of integrating bioelectrochemical systems (BES) with conductive carbon nanotube (CNT) membranes for the effective remediation of nitrate-contaminated water. By leveraging electroactive microorganisms capable of autotrophic denitrification, the proposed system eliminates the need for external chemical electron donors. The membranes serve a dual role: not only do they act as ultrafiltration barriers, preventing microbial contamination of the effluent, but they also function as electrodes that facilitate the biodegradation of nitrates through bioelectrochemical processes. The experimental results indicate that the system efficiently removes nitrates, achieving complete denitrification without nitrite accumulation. The use of CNT-CNF membranes as cathodes enables the development of a biofilm that accelerates nitrate reduction over time, with removal rates stabilizing at values above 900 mgN m^{-2} d^{-1} after the adaptation phase. The transition to open circuit

potential (OCP) conditions provided insights into the reliance of the system on polarization to maintain high removal efficiency, suggesting that ongoing electron transfer from the cathode is essential. The combination of bioelectroremediation with CNT-CNF membrane filtration addresses several challenges faced by conventional treatment methods, such as high sludge production, the need for chemical dosing, and energy-intensive separation technologies. Additionally, this system significantly reduces fouling potential, as contaminants are biodegraded directly on the membrane surface, enhancing long-term operational stability. Furthermore, the CNT-CNF membrane's electrochemical characteristics, as evidenced by cyclic voltammetry (CV) and electrochemical impedance spectroscopy (EIS) analyses, indicate that it maintains good conductivity and stability, which are critical for the scalability of the technology. However, several challenges remain. The release of some bacteria from the biofilm still poses a potential issue, though ultrafiltration offers a promising solution for preventing microbial contamination. Potential scaling-up of the system would require further investigation, particularly in optimizing electrode materials and ensuring cost-effective membrane production. Overall, this innovative approach to water remediation, combining electro-bioremediation and conductive CNT membranes, offers a promising alternative for nitrate removal with minimal environmental impact, making it a potential candidate for future applications in groundwater treatment. Further studies are needed to optimize system performance, scale-up the technology, and evaluate long-term economic and ecological sustainability.

Chapter VII - Conclusions

VII.1 Conclusions

The main objective of this Ph.D research was to promote the development and optimization of microbial electrochemical technologies (METs) for the bioremediation of groundwater contaminated by complex mixtures of pollutants, including petroleum hydrocarbons (PH), chlorinated solvents, nitrate, and metals. Through experimental works conducted at the laboratory scale, both in batch and continuous flow modes, under a broad range of operating conditions, valuable insights were gained into the possibility to steer the electrode-driven biodegradation of different contaminants and mixtures thereof. The results obtained from these studies can support the future development of microbial electrochemical technologies (METs) as a promising technology for *in-situ* groundwater pollution treatment. The first set of experiments (**Chapter II**) explored the degradation of toluene, a model petroleum hydrocarbon, in a bioelectrochemical system referred to as a "bioelectric well." The study demonstrated that toluene degradation occurred through a syntrophic interaction between hydrocarbon degraders and electroactive microorganisms. Toluene was initially converted into metabolic intermediates such as volatile fatty acids (VFA), formate, and hydrogen, which were subsequently used by electroactive bacteria in the anodic biofilm. The toluene degradation rate was faster than the fermentation of intermediates, explaining the observed plateau in current generation despite a higher contaminant load. These results are significant for understanding syntrophic degradation of aromatic hydrocarbons and underscore the importance of promoting diverse microbial populations for efficient bioelectrochemical degradation processes. The study also identified limitations, such as the plateau in coulombic efficiency at higher concentrations due to the accumulation of intermediates, suggesting potential areas for process optimization in real-world applications. The second study (**Chapter III**) expanded on the first by investigating the simultaneous bioremediation of a mixture of toluene (a model hydrocarbon contaminant) and trichloroethylene (TCE, a model chlorinated solvent contaminant), demonstrating the feasibility of using a single-stage bioelectrochemical system for the degradation of mixed contaminants

requiring two opposing redox environments, namely oxidative and reductive. In this system, the oxidation of toluene at the graphite anode generated an electric current that fueled the abiotic production of hydrogen at the stainless-steel cathode, supporting the reductive dechlorination of TCE. Phylogenetic analysis confirmed the presence of microbial communities capable of both oxidizing toluene under anaerobic conditions and dechlorinating TCE, with degradation processes occurring in parallel. The study provided proof of concept for integrating oxidative and reductive bioremediation pathways within a single reactor. However, mass transport limitations hindered toluene oxidation and current generation, indicating that further process refinements, such as hydrodynamic optimization, are essential to improve overall efficiency. Additionally, while TCE degradation was achieved, the process was slower than expected, requiring further investigations to enhance hydrogen utilization and accelerate dechlorination. In a further exploration of mixed contaminant treatment, the third study (**Chapter IV**) examined the simultaneous removal of toluene and chloroform (CF), another chlorinated hydrocarbon commonly detected in contaminated groundwater. Again, the bioelectrochemical system achieved simultaneous degradation of both compounds, but the presence of CF negatively impacted toluene degradation rates, likely due to inhibitory effects on the anodic microbial community. This finding highlights the complexity of interactions between co-contaminants in bioelectrochemical systems and the importance of understanding microbial competition dynamics in multiple contamination scenarios. The study also demonstrated that acetate, a readily biodegradable substrate, was preferentially consumed over toluene, hindering its removal and complicating the design of systems capable of handling diverse contaminant profiles. The fourth study **(Chapter V**) introduced the bioelectrochemical removal of toluene and copper in a single-chamber reactor. Toluene oxidation at the anode generated an electric current that supported the abiotic reduction and precipitation of copper as Cu_2O nanoparticles at the cathode. This system demonstrated a dual-function approach, where microbial activity drove the oxidation of organic pollutants while simultaneously facilitating

the recovery of metals at the cathode. The study also highlighted the potential for coupling bioelectrochemical degradation with the recovery of valuable resources, thus potentially contributing to the circular economy. However, challenges remain, such as optimizing electrode materials, reactor design, and process scalability for real-world applications. The final phase of the research **(Chapter VI**) focused on integrating bioelectrochemical systems with membrane technology, specifically ultrafiltration, for the treatment of nitrate-contaminated water. This work was conducted at the Laboratory of Chemical and Environmental Engineering (LEQUIA) of the University of Girona (UdG), under the scientific supervision of Prof. Sebastià Puig. An innovative system combining bioelectroremediation and ultrafiltration was tested using carbon nanotube (CNT) conductive membranes. This dual-function system enabled the simultaneous biodegradation of nitrates by electroactive microorganisms and the filtration of contaminants directly at the membrane surface, achieving high nitrate removal efficiency. The use of conductive membranes as electrodes provided the added benefit of reducing membrane fouling by directly removing filtered contaminants, improving long-term operational stability. This research presents a promising alternative to conventional nitrate removal techniques, offering lower energy consumption, reduced chemical usage, and minimized sludge production. However, challenges such as bacterial release from biofilms and CNT membrane scalability require further investigation. Conducted research opens multiple possibilities for future investigations. First, the scalability of bioelectrochemical systems remains a critical challenge. Real-world applications will require optimizing reactor design, electrode materials, and operational parameters to ensure cost-effective and efficient contaminant removal. In particular, the influence of hydrodynamics and mass transport phenomena on process efficiency must be further explored. In fact, a challenging aspect of bioelectrochemical systems is that being surface-based technologies, they require high surface area electrodes to attain sufficiently high contaminants biodegradation rates as well as for treating large, contaminated areas. In the case of large contamination plumes, this would ultimately result in unacceptably high

costs of electrodes and consequent prohibitive capital expenditures (CAPEX) (Puig et al., 2021; Saxena et al., 2020) New strategy are thus warranted to overcome the unsustainable use of multitude of high-surface area electrodes, as the bioelectric well, posted at short distance one from the other. In principle, this could be achieved through the injection in the aquifer of environmentally safe (iron- or carbon-based) conductive (nano)particles. Upon transport and subsequent deposition over soil grains, these particles create an electrically conductive zone which could be exploited to control and fine-tune the delivery of electron donors or acceptors over a large distance, and accordingly drive the electro-bioremediation process in a more efficient manner. Further to extending the radius-of-influence of electrodes, such diffuse electro-conductive zones (DECZ) could also be exploited to promote the development of syntrophic anaerobic communities degrading contaminants via direct interspecies electron transfer (DIET) process. Clearly, this intriguing hypothesis would require future ad hoc investigations. Second, the interactions between different types of contaminants, as observed with the inhibitory effects of CF and acetate, highlight the need for more detailed studies on microbial community dynamics in environments with multiple contaminants. Understanding these interactions will be essential for adapting microbial electrochemical systems to specific contamination profiles. Third, combining pollutant degradation with resource recovery, as demonstrated by the bioelectrochemical copper recovery system, represents a promising direction for valorizing contaminated water and environmental remediation processes within the circular economy framework. Future research should focus on developing similar systems for other metals and contaminants, as well as optimizing the recovery process to enhance both economic and environmental sustainability, also in the broad context of municipal and industrial wastewater treatment. Finally, integrating bioelectrochemical processes with membrane filtration presents a unique opportunity to advance water treatment technologies. Further studies are needed to optimize conductive membrane materials, improve long-term stability, and address operational challenges, such as microbial release and fouling. Scaling this system for

practical applications will be crucial for advancing the field of bioelectroremediation. In conclusion, the work carried out in this thesis has made significant progress in understanding and applying microbial electrochemical technologies for groundwater remediation. The results provide a solid foundation for future research aimed at overcoming the technical and operational challenges of these innovative bioremediation systems. Clearly, in order to accelerate the transition of these novel technologies from the laboratory to the market, pilot studies conducted at field scale and highly representative conditions are urgently needed. Hopefully, results of these studies will catalyze the interest of stakeholder, authorities and also common people for bioelectrochemical technologies and their sustainable, tunable, and multifaceted features. By harnessing the potential of electroactive microbial communities, bioelectrochemical systems offer a promising solution to the pressing environmental issue of groundwater contamination, while also opening up possibilities for resource recovery and sustainable water treatment in the future.

Acknowledgements

The author's contribution to the articles “Syntrophy drives the microbial electrochemical oxidation of toluene in a continuous-flow ‘bioelectric well’,” “Coupling of bioelectrochemical toluene oxidation and trichloroethene reductive dechlorination for single-stage treatment of groundwater containing multiple contaminants,” and “Toluene-driven anaerobic biodegradation of chloroform in a continuous-flow bioelectrochemical reactor” was as follows: Investigation, Formal analysis, and Data curation. The author's contribution to the article “Anaerobic treatment of groundwater co-contaminated by toluene and copper in a single-chamber bioelectrochemical system” was as follows: Writing – original draft, Visualization, Investigation, Formal analysis, and Conceptualization."

References

Aelterman, P., Freguia, S., Keller, J., Verstraete, W., Rabaey, K., 2008. The anode potential regulates bacterial activity in microbial fuel cells. Appl. Microbiol. Biotechnol. 78, 409–418. https://doi.org/10.1007/s00253-007-1327-8

Akmirza, I., Pascual, C., Carvajal, A., Pérez, R., Muñoz, R., Lebrero, R., 2017. Anoxic biodegradation of BTEX in a biotrickling filter. Sci. Total Environ. 587–588, 457–465. https://doi.org/10.1016/j.scitotenv.2017.02.130

Allard, A.S., Neilson, A.H., 1997. Bioremediation of organic waste sites: A critical review of microbiological aspects. Int. Biodeterior. Biodegrad. 39, 253–285. https://doi.org/10.1016/S0964-8305(97)00021-8

Alvarez, P.J.J., Illman, W.A., 2005. Bioremediation and Natural Attenuation, Bioremediation and Natural Attenuation. John Wiley & Sons, Inc., Hoboken, NJ, USA. https://doi.org/10.1002/047173862X

Amanat, N., Matturro, B., Villano, M., Lorini, L., Rossi, M.M., Zeppilli, M., Rossetti, S., Petrangeli Papini, M., 2022. Enhancing the biological reductive dechlorination of trichloroethylene with PHA from mixed microbial cultures (MMC). J. Environ. Chem. Eng. 10, 107047. https://doi.org/10.1016/j.jece.2021.107047

Andersen, S.J., Pikaar, I., Freguia, S., Lovell, B.C., Rabaey, K., Rozendal, R.A., 2013. Dynamically adaptive control system for bioanodes in serially stacked bioelectrochemical systems. Environ. Sci. Technol. 47, 5488–5494. https://doi.org/10.1021/es400239k

Anglada, Á., Urtiaga, A., Ortiz, I., 2009. Contributions of electrochemical oxidation to waste-water treatment: Fundamentals and review of applications. J. Chem. Technol. Biotechnol. 84, 1747–1755. https://doi.org/10.1002/jctb.2214

Atashgahi, S., Lu, Y., Smidt, H., 2016. Overview of Known Organohalide-Respiring Bacteria—Phylogenetic Diversity and Environmental Distribution, in: Organohalide-Respiring Bacteria. Springer Berlin Heidelberg, Berlin, Heidelberg, pp. 63–105. https://doi.org/10.1007/978-3-662-49875-0_5

Aulenta, F., Bianchi, A., Majone, M., Petrangeli Papini, M., Potalivo, M., Tandoi, V., 2005. Assessment of natural or enhanced in situ bioremediation at a chlorinated solvent-contaminated aquifer in Italy: a microcosm study. Environ. Int. 31, 185–190. https://doi.org/10.1016/j.envint.2004.09.014

Aulenta, F., Canosa, A., Majone, M., Panero, S., Reale, P., Rossetti, S., 2008a. Trichloroethene Dechlorination and H 2 Evolution Are Alternative Biological Pathways of Electric Charge Utilization by a Dechlorinating Culture in a Bioelectrochemical System. Environ. Sci. Technol. 42, 6185–6190. https://doi.org/10.1021/es800265b

Aulenta, F., Catapano, L., Snip, L., Villano, M., Majone, M., 2012. Linking Bacterial Metabolism to Graphite Cathodes: Electrochemical Insights into the H2-Producing Capability of Desulfovibrio sp. ChemSusChem 5, 1080–1085. https://doi.org/10.1002/cssc.201100720

Aulenta, F., Majone, M., Tandoi, V., 2006. Enhanced anaerobic bioremediation of chlorinated solvents: Environmental factors influencing microbial activity and their relevance under field conditions. J. Chem. Technol. Biotechnol. 81. https://doi.org/10.1002/jctb.1567

Aulenta, F., Reale, P., Canosa, A., Rossetti, S., Panero, S., Majone, M., 2010. Characterization of an electro-active biocathode capable of dechlorinating trichloroethene and cis-dichloroethene to ethene. Biosens. Bioelectron. 25, 1796–1802. https://doi.org/10.1016/J.BIOS.2009.12.033

Aulenta, F., Reale, P., Catervi, A., Panero, S., Majone, M., 2008b. Kinetics of trichloroethene dechlorination and methane formation by a mixed anaerobic culture in a bio-electrochemical system. Electrochim. Acta 53, 5300–5305. https://doi.org/10.1016/j.electacta.2008.02.084

Aulenta, F., Rossetti, S., Matturro, B., Tandoi, V., Verdini, R., Majone, M., 2016. Redox Interactions of Organohalide-Respiring Bacteria (OHRB) with Solid-State Electrodes: Principles and Perspectives of Microbial Electrochemical Remediation, in: Organohalide-Respiring Bacteria. Springer Berlin Heidelberg, Berlin, Heidelberg, pp. 499–516. https://doi.org/10.1007/978-3-662-49875-0_21

Aulenta, F., Tocca, L., Verdini, R., Reale, P., Majone, M., 2011. Dechlorination of Trichloroethene in a Continuous-Flow Bioelectrochemical Reactor: Effect of Cathode Potential on Rate, Selectivity, and Electron Transfer Mechanisms. Environ. Sci. Technol. 45, 8444–8451. https://doi.org/10.1021/es202262y

Bacosa, H.P., Steichen, J., Kamalanathan, M., Windham, R., Lubguban, A., Labonté, J.M., Kaiser, K., Hala, D., Santschi, P.H., Quigg, A., 2020. Polycyclic aromatic hydrocarbons (PAHs) and putative PAH-degrading bacteria in Galveston Bay, TX (USA), following Hurricane Harvey (2017). Environ. Sci. Pollut. Res. 27, 34987–34999. https://doi.org/10.1007/s11356-020-09754-5

Bae, H.S., Moe, W.M., Yan, J., Tiago, I., da Costa, M.S., Rainey, F.A., 2006. Propionicicella superfundia gen. nov., sp. nov., a chlorosolvent-tolerant propionate-forming, facultative anaerobic bacterium isolated from contaminated

groundwater. Syst. Appl. Microbiol. 29, 404–413. https://doi.org/10.1016/j.syapm.2005.11.004

Bailey, J.E., 1980. Biochemical reaction engineering and biochemical reactors. Chem. Eng. Sci. 35, 1854–1886. https://doi.org/10.1016/0009-2509(80)80134-5

Balch, W.E., Fox, G.E., Magrum, L.J., Woese, C.R., Wolfe, R.S., 1979. Methanogens: reevaluation of a unique biological group. Microbiol. Rev. 43, 260–296. https://doi.org/10.1128/MMBR.43.2.260-296.1979

Baldwin, B.R., Nakatsu, C.H., Nebe, J., Wickham, G.S., Parks, C., Nies, L., 2009. Enumeration of aromatic oxygenase genes to evaluate biodegradation during multi-phase extraction at a gasoline-contaminated site. J. Hazard. Mater. 163, 524–530. https://doi.org/10.1016/j.jhazmat.2008.07.002

Beretta, G., Daghio, M., Tofalos, A.E., Franzetti, A., Mastorgio, A.F., Saponaro, S., Sezenna, E., 2020. Microbial Assisted Hexavalent Chromium Removal in Bioelectrochemical Systems. Water 2020, Vol. 12, Page 466 12, 466. https://doi.org/10.3390/W12020466

Bi, J., Tao, Q., Huang, X., Wang, J., Wang, T., Hao, H., 2021. Simultaneous decontamination of multi-pollutants: A promising approach for water remediation. Chemosphere 284, 131270. https://doi.org/10.1016/j.chemosphere.2021.131270

Bijay-Singh, Craswell, E., 2021. Fertilizers and nitrate pollution of surface and ground water: an increasingly pervasive global problem. SN Appl. Sci. 3, 1–24. https://doi.org/10.1007/s42452-021-04521-8

Blázquez-Pallí, N., Rosell, M., Varias, J., Bosch, M., Soler, A., Vicent, T.,

Marco-Urrea, E., 2019. Multi-method assessment of the intrinsic biodegradation potential of an aquifer contaminated with chlorinated ethenes at an industrial area in Barcelona (Spain). Environ. Pollut. 244, 165–173. https://doi.org/10.1016/j.envpol.2018.10.013

Bolden, A.L., Kwiatkowski, C.F., Colborn, T., 2015. New look at BTEX: Are ambient levels a problem. Environ. Sci. Technol. 49, 5261–5276. https://doi.org/10.1021/es505316f

Boll, M., Löffler, C., Morris, B.E.L., Kung, J.W., 2014. Anaerobic degradation of homocyclic aromatic compounds via arylcarboxyl-coenzyme A esters: Organisms, strategies and key enzymes. Environ. Microbiol. 16, 612–627. https://doi.org/10.1111/1462-2920.12328

Bolyen, E., Rideout, J.R., Dillon, M.R., Bokulich, N.A., Abnet, C.C., Al-Ghalith, G.A., Alexander, H., Alm, E.J., Arumugam, M., Asnicar, F., Bai, Y., Bisanz, J.E., Bittinger, K., Brejnrod, A., Brislawn, C.J., Brown, C.T., Callahan, B.J., Caraballo-Rodríguez, A.M., Chase, J., Cope, E.K., Da Silva, R., Diener, C., Dorrestein, P.C., Douglas, G.M., Durall, D.M., Duvallet, C., Edwardson, C.F., Ernst, M., Estaki, M., Fouquier, J., Gauglitz, J.M., Gibbons, S.M., Gibson, D.L., Gonzalez, A., Gorlick, K., Guo, J., Hillmann, B., Holmes, S., Holste, H., Huttenhower, C., Huttley, G.A., Janssen, S., Jarmusch, A.K., Jiang, L., Kaehler, B.D., Kang, K. Bin, Keefe, C.R., Keim, P., Kelley, S.T., Knights, D., Koester, I., Kosciolek, T., Kreps, J., Langille, M.G.I., Lee, J., Ley, R., Liu, Y.X., Loftfield, E., Lozupone, C., Maher, M., Marotz, C., Martin, B.D., McDonald, D., McIver, L.J., Melnik, A. V., Metcalf, J.L., Morgan, S.C., Morton, J.T., Naimey, A.T., Navas-Molina, J.A., Nothias, L.F., Orchanian, S.B., Pearson, T., Peoples, S.L., Petras, D., Preuss, M.L., Pruesse, E., Rasmussen, L.B., Rivers, A., Robeson, M.S., Rosenthal, P., Segata, N., Shaffer, M., Shiffer, A., Sinha, R., Song, S.J., Spear, J.R., Swafford, A.D., Thompson, L.R., Torres, P.J., Trinh, P., Tripathi, A., Turnbaugh, P.J., Ul-Hasan, S., van der Hooft, J.J.J., Vargas, F., Vázquez-

Baeza, Y., Vogtmann, E., von Hippel, M., Walters, W., Wan, Y., Wang, M., Warren, J., Weber, K.C., Williamson, C.H.D., Willis, A.D., Xu, Z.Z., Zaneveld, J.R., Zhang, Y., Zhu, Q., Knight, R., Caporaso, J.G., 2019. Reproducible, interactive, scalable and extensible microbiome data science using QIIME 2. Nat. Biotechnol. 37, 852–857. https://doi.org/10.1038/s41587-019-0209-9

Bond, D.R., Lovley, D.R., 2003. Electricity production by Geobacter sulfurreducens attached to electrodes. Appl. Environ. Microbiol. 69, 1548–1555. https://doi.org/10.1128/AEM.69.3.1548-1555.2003/ASSET/F4A7F315-959D-4605-A43B-3B7D1386F8C7/ASSETS/GRAPHIC/AM0331568007.JPEG

Bruce E. Logan, Bert Hamelers, René Rozendal, Uwe Shroder, Jurg Keller, Stefano Freguia, Peter Aelterman, W.V. and K.R., 2006. Critical Review Microbial Fuel Cells : Methodology and Technology. Environ. Sci. Technol. 40, 5181–5192.

Callahan, B.J., McMurdie, P.J., Rosen, M.J., Han, A.W., Johnson, A.J.A., Holmes, S.P., 2016. DADA2: High-resolution sample inference from Illumina amplicon data. Nat. Methods 13. https://doi.org/10.1038/nmeth.3869

Cao, M., Hu, Y., Sun, Q., Wang, L., Chen, J., Lu, X., 2013. Enhanced desorption of PCB and trace metal elements (Pb and Cu) from contaminated soils by saponin and EDDS mixed solution. Environ. Pollut. 174, 93–99. https://doi.org/10.1016/j.envpol.2012.11.015

Ceballos-Escalera, A., Pous, N., Balaguer, M.D., Puig, S., 2024a. Nitrate electro-bioremediation and water disinfection for rural areas. Chemosphere 352. https://doi.org/10.1016/j.chemosphere.2024.141370

Ceballos-Escalera, A., Pous, N., Bañeras, L., Balaguer, M.D., Puig, S., 2024b.

Advancing towards electro-bioremediation scaling-up: On-site pilot plant for successful nitrate-contaminated groundwater treatment. Water Res. 256. https://doi.org/10.1016/j.watres.2024.121618

Ceballos-Escalera, A., Pous, N., Chiluiza-Ramos, P., Korth, B., Harnisch, F., Bañeras, L., Balaguer, M.D., Puig, S., 2021. Electro-bioremediation of nitrate and arsenite polluted groundwater. Water Res. 190, 116748. https://doi.org/10.1016/j.watres.2020.116748

Cecconet, D., Callegari, A., Capodaglio, A.G., 2018. Bioelectrochemical systems for removal of selected metals and perchlorate from groundwater: A review. Energies 11. https://doi.org/10.3390/en11102643

Cecconet, D., Sabba, F., Devecseri, M., Callegari, A., Capodaglio, A.G., 2020. In situ groundwater remediation with bioelectrochemical systems: A critical review and future perspectives. Environ. Int. 137, 105550. https://doi.org/10.1016/j.envint.2020.105550

Chakraborty, R., O'Connor, S.M., Chan, E., Coates, J.D., 2005. Anaerobic degradation of benzene, toluene, ethylbenzene, and xylene compounds by Dechloromonas strain RCB. Appl. Environ. Microbiol. 71, 8649–8655. https://doi.org/10.1128/AEM.71.12.8649-8655.2005

Chary, N.S., Fernandez-Alba, A.R., 2012. Determination of volatile organic compounds in drinking and environmental waters. TrAC - Trends Anal. Chem. 32, 60–75. https://doi.org/10.1016/j.trac.2011.08.011

Chen, P., Zhang, L., Guo, X., Dai, X., Liu, L., Xi, L., Wang, J., Song, L., Wang, Y., Zhu, Y., Huang, L., Huang, Y., 2016. Diversity, biogeography, and biodegradation potential of actinobacteria in the deep-sea sediments along the

southwest Indian ridge. Front. Microbiol. 7, 1–17. https://doi.org/10.3389/fmicb.2016.01340

Chen, W., He, X., Jiang, Z., Li, B., Li, X. yan, Lin, L., 2023. A capacitive deionization and electro-oxidation hybrid system for simultaneous removal of heavy metals and organics from wastewater. Chem. Eng. J. 451, 139071. https://doi.org/10.1016/j.cej.2022.139071

Cheng, Q., Call, D.F., 2016. Hardwiring microbes via direct interspecies electron transfer: mechanisms and applications. Environ. Sci. Process. Impacts 18, 968–980. https://doi.org/10.1039/C6EM00219F

Cheng, S., Xing, D., Call, D., Logan, B., 2009. Direct biological conversion of electrical current into methane by electromethanogenesis. Environ. Sci. Technol. 43, 3953–3958.

Clark, I.C., Carlson, H.K., Iavarone, A.T., Coates, J.D., 2012. Bioelectrical redox cycling of anthraquinone-2,6-disulfonate coupled to perchlorate reduction. Energy Environ. Sci. 5, 7970. https://doi.org/10.1039/c2ee21594b

Coates, J.D., Anderson, R.T., Woodward, J.C., Phillips, E.J.P., Lovley, D.R., 1996. Anaerobic hydrocarbon degradation in petroleum-contaminated harbor sediments under sulfate-reducing and artificially imposed iron-reducing conditions. Environ. Sci. Technol. 30, 2784–2789. https://doi.org/10.1021/es9600441

Coates, J.D., Michaelidou, U., Bruce, R.A., O'Connor, S.M., Crespi, J.N., Achenbach, L.A., 1999. The ubiquity and diversity of dissimilatory (per-)chlorate-reducing bacteria. Appl. Environ. Microbiol. 65, 5234–5241.

Collins, C., Laturnus, F., Nepovim, A., 2002. Phytoremediation: BTEX and Trichloroethene. Environ. Sci. Pollut. Res. 9, 86–94.

Commission, E., 2000. ‘ Nitrates ’ Directive. Reproduction 1–8.

Crampon, Marc, Bodilis, J., Portet-Koltalo, Florence, Crampon, M, Portet-Koltalo, F, 2018. Linking initial soil bacterial diversity and polycyclic aromatic hydrocarbons (PAHs) degradation potential. J. Hazard. Mater. https://doi.org/10.1016/j.jhazmat.2018.07.088ï

Crognale, S., Braguglia, C.M., Gallipoli, A., Gianico, A., Rossetti, S., Montecchio, D., 2021. Direct conversion of food waste extract into caproate: Metagenomics assessment of chain elongation process. Microorganisms 9. https://doi.org/10.3390/microorganisms9020327

Cruz Viggi, C., Tucci, M., Resitano, M., Crognale, S., Di Franca, M.L., Rossetti, S., Aulenta, F., 2022. Coupling of bioelectrochemical toluene oxidation and trichloroethene reductive dechlorination for single-stage treatment of groundwater containing multiple contaminants. Environ. Sci. Ecotechnology 11, 100171. https://doi.org/10.1016/j.ese.2022.100171

Daghio, M., Aulenta, F., Vaiopoulou, E., Franzetti, A., Arends, J.B.A., Sherry, A., Suárez-Suárez, A., Head, I.M., Bestetti, G., Rabaey, K., 2017. Electrobioremediation of oil spills. Water Res. 114, 351–370. https://doi.org/10.1016/j.watres.2017.02.030

Daghio, M., Espinoza Tofalos, A., Leoni, B., Cristiani, P., Papacchini, M., Jalilnejad, E., Bestetti, G., Franzetti, A., 2018. Bioelectrochemical BTEX removal at different voltages: assessment of the degradation and characterization of the microbial communities. J. Hazard. Mater. 341, 120–127.

https://doi.org/10.1016/J.JHAZMAT.2017.07.054

Davoodi, S.M., Miri, S., Taheran, M., Brar, S.K., Galvez-Cloutier, R., Martel, R., 2020. Bioremediation of Unconventional Oil Contaminated Ecosystems under Natural and Assisted Conditions: A Review. Environ. Sci. Technol. 54, 2054–2067. https://doi.org/10.1021/acs.est.9b00906

Deng, J.H., Zhang, X.R., Zeng, G.M., Gong, J.L., Niu, Q.Y., Liang, J., 2013. Simultaneous removal of Cd(II) and ionic dyes from aqueous solution using magnetic graphene oxide nanocomposite as an adsorbent. Chem. Eng. J. 226, 189–200. https://doi.org/10.1016/j.cej.2013.04.045

Deng, Y., Tang, L., Zeng, G., Zhu, Z., Yan, M., Zhou, Y., Wang, Jiajia, Liu, Y., Wang, Jingjing, 2017. Insight into highly efficient simultaneous photocatalytic removal of Cr(VI) and 2,4-diclorophenol under visible light irradiation by phosphorus doped porous ultrathin g-C3N4 nanosheets from aqueous media: Performance and reaction mechanism. Appl. Catal. B Environ. 203, 343–354. https://doi.org/10.1016/j.apcatb.2016.10.046

Di Franca, M.L., Matturro, B., Crognale, S., Zeppilli, M., Dell'Armi, E., Majone, M., Petrangeli Papini, M., Rossetti, S., 2022. Microbiome Composition and Dynamics of a Reductive/Oxidative Bioelectrochemical System for Perchloroethylene Removal: Effect of the Feeding Composition. Front. Microbiol. 13, 1–12. https://doi.org/10.3389/fmicb.2022.951911

Edwards, E.A., Grbić-Galić, D., 1994. Anaerobic degradation of toluene and o-xylene by a methanogenic consortium. Appl. Environ. Microbiol. 60, 313–322. https://doi.org/10.1128/AEM.60.1.313-322.1994

El Fantroussi, S., Agathos, S.N., 2005. Is bioaugmentation a feasible strategy

for pollutant removal and site remediation? Curr. Opin. Microbiol. 8, 268–275. https://doi.org/https://doi.org/10.1016/j.mib.2005.04.011

Embree, M., Nagarajan, H., Movahedi, N., Chitsaz, H., Zengler, K., 2014. Single-cell genome and metatranscriptome sequencing reveal metabolic interactions of an alkane-degrading methanogenic community. ISME J. 8, 757–767. https://doi.org/10.1038/ismej.2013.187

Espinoza-Tofalos, A., Daghio, M., Palma, E., Aulenta, F., Franzetti, A., 2020. Structure and Functions of Hydrocarbon-Degrading Microbial Communities in Bioelectrochemical Systems. Water 12, 343. https://doi.org/10.3390/w12020343

European Environment Agency, 2022. Europes groundwater - a key resource under pressure 1–11.

Farhadian, M., Vachelard, C., Duchez, D., Larroche, C., 2008. In situ bioremediation of monoaromatic pollutants in groundwater: A review. Bioresour. Technol. 99, 5296–5308. https://doi.org/10.1016/j.biortech.2007.10.025

Feng, H., Yang, W., Zhang, Y., Ding, Y., Chen, L., Kang, Y., Huang, H., Chen, R., 2023. Electroactive microorganism-assisted remediation of groundwater contamination: Advances and challenges. Bioresour. Technol. 377, 128916. https://doi.org/10.1016/J.BIORTECH.2023.128916

Feng, Q., Song, Y.C., Li, J., Wang, Z., Wu, Q., 2020. Influence of electrostatic field and conductive material on the direct interspecies electron transfer for methane production. Environ. Res. 188, 109867. https://doi.org/10.1016/j.envres.2020.109867

Fernández-López, J.A., Alacid, M., Obón, J.M., Martínez-Vives, R., Angosto,

J.M., 2023. Nitrate-Polluted Waterbodies Remediation: Global Insights into Treatments for Compliance. Appl. Sci. 13. https://doi.org/10.3390/app13074154

Fernández-Verdejo, D., Cortés, P., Guisasola, A., Blánquez, P., Marco-Urrea, E., 2022. Bioelectrochemically-assisted degradation of chloroform by a co-culture of Dehalobacter and Dehalobacterium. Environ. Sci. Ecotechnology 12, 0–5. https://doi.org/10.1016/j.ese.2022.100199

Ferraro, A., Massini, G., Miritana, V.M., Panico, A., Pontoni, L., Race, M., Rosa, S., Signorini, A., Fabbricino, M., Pirozzi, F., 2021. Bioaugmentation strategy to enhance polycyclic aromatic hydrocarbons anaerobic biodegradation in contaminated soils. Chemosphere 275. https://doi.org/10.1016/j.chemosphere.2021.130091

Friman, H., Schechter, A., Nitzan, Y., Cahan, R., 2013. Phenol degradation in bio-electrochemical cells. Int. Biodeterior. Biodegrad. 84, 155–160. https://doi.org/10.1016/j.ibiod.2012.04.019

Fuchs, G., Boll, M., Heider, J., 2011. Microbial degradation of aromatic compounds- From one strategy to four. Nat. Rev. Microbiol. 9, 803–816. https://doi.org/10.1038/nrmicro2652

Gambino, E., Chandrasekhar, K., Nastro, R.A., 2021. SMFC as a tool for the removal of hydrocarbons and metals in the marine environment: a concise research update. Environ. Sci. Pollut. Res. 28, 30436–30451. https://doi.org/10.1007/s11356-021-13593-3

Gauthier, P.T., Norwood, W.P., Prepas, E.E., Pyle, G.G., 2014. Metal-PAH mixtures in the aquatic environment: A review of co-toxic mechanisms leading to more-than-additive outcomes. Aquat. Toxicol. 154, 253–269.

https://doi.org/10.1016/j.aquatox.2014.05.026

Gbordzoe, S., Yarmolenko, S., Hsieh, Y.Y., Adusei, P.K., Alvarez, N.T., Fialkova, S., Shanov, V., 2017. Three-dimensional texture analysis of aligned carbon nanotube structures. Carbon N. Y. 121, 591–601. https://doi.org/10.1016/j.carbon.2017.06.028

Gieg, L.M., Fowler, S.J., Berdugo-Clavijo, C., 2014. Syntrophic biodegradation of hydrocarbon contaminants. Curr. Opin. Biotechnol. 27, 21–29. https://doi.org/10.1016/j.copbio.2013.09.002

Goodfellow, M., Kampfer, P., Busse, H.-J., Trujillo, M.E., Suzuki, K., Ludwig, W., Whitman, W.B., 2012. The Actinobacteria, in: Bergey's Manual Of Systematic Bacteriology.

Hashemi, B., Horn, S.J., Lamb, J.J., Lien, K.M., 2022. Potential role of sulfide precipitates in direct interspecies electron transfer facilitation during anaerobic digestion of fish silage. Bioresour. Technol. Reports 20. https://doi.org/10.1016/j.biteb.2022.101264

He, Y.T., Su, C., 2015. Use of Additives in Bioremediation of Contaminated Groundwater and Soil, in: Advances in Bioremediation of Wastewater and Polluted Soil. pp. 145–164. https://doi.org/10.1016/j.colsurfa.2011.12.014

Hemdan, B., Garlapati, V.K., Sharma, S., Bhadra, S., Maddirala, S., Varsha, K.M., Motru, V., Goswami, P., Sevda, S., Aminabhavi, T.M., 2022. Bioelectrochemical systems-based metal recovery: Resource, conservation and recycling of metallic industrial effluents. Environ. Res. 204, 112346. https://doi.org/10.1016/j.envres.2021.112346

Holliger, C., Gaspard, S., Glod, G., Heijman, C., Schumacher, W., Schwarzenbach, R.P., Vazquez, F., 1997. Contaminated environments in the subsurface and bioremediation: Organic contaminants. FEMS Microbiol. Rev. 20, 517–523. https://doi.org/10.1016/S0168-6445(97)00030-2

Hou, R., Gan, L., Guan, F., Wang, Y., Li, J., Zhou, S., Yuan, Y., 2021. Bioelectrochemically enhanced degradation of bisphenol S: mechanistic insights from stable isotope-assisted investigations. iScience 24, 102014. https://doi.org/10.1016/j.isci.2020.102014

Hu, X., Ji, H., Chang, F., Luo, Y., 2014. Simultaneous photocatalytic Cr(VI) reduction and 2,4,6-TCP oxidation over g-C3N4 under visible light irradiation. Catal. Today 224, 34–40. https://doi.org/10.1016/j.cattod.2013.11.038

Huang, J., Wang, Z., Zhang, J., Zhang, X., Ma, J., Wu, Z., 2015. A novel composite conductive microfiltration membrane and its anti-fouling performance with an external electric field in membrane bioreactors. Sci. Rep. 5, 1–8. https://doi.org/10.1038/srep09268

Jabbar, N.M., Alardhi, S.M., Mohammed, A.K., Salih, I.K., Albayati, T.M., 2022. Challenges in the implementation of bioremediation processes in petroleum-contaminated soils: A review. Environ. Nanotechnology, Monit. Manag. 18, 100694. https://doi.org/10.1016/j.enmm.2022.100694

Jin, X., Angelidaki, I., Zhang, Y., 2016. Microbial Electrochemical Monitoring of Volatile Fatty Acids during Anaerobic Digestion. Environ. Sci. Technol. 50, 4422–4429. https://doi.org/10.1021/acs.est.5b05267

Kadier, A., Simayi, Y., Abdeshahian, P., Azman, N.F., Chandrasekhar, K., Kalil, M.S., 2016. A comprehensive review of microbial electrolysis cells (MEC)

reactor designs and configurations for sustainable hydrogen gas production. Alexandria Eng. J. 55, 427–443. https://doi.org/10.1016/j.aej.2015.10.008

Kang, Y., Ma, H., Jing, Z., Zhu, C., Li, Y., Wu, H., Dai, P., Guo, Z., Zhang, J., 2023. Enhanced benzofluoranthrene removal in constructed wetlands with iron-modified biochar: Mediated by dissolved organic matter and microbial response. J. Hazard. Mater. 443. https://doi.org/10.1016/j.jhazmat.2022.130322

Kato, S., Hashimoto, K., Watanabe, K., 2012. Microbial interspecies electron transfer via electric currents through conductive minerals. Proc. Natl. Acad. Sci. U. S. A. 109, 10042–10046. https://doi.org/10.1073/PNAS.1117592109/SUPPL_FILE/PNAS.201117592SI.PDF

Kiely, P.D., Regan, J.M., Logan, B.E., 2011. The electric picnic: Synergistic requirements for exoelectrogenic microbial communities. Curr. Opin. Biotechnol. 22, 378–385. https://doi.org/10.1016/j.copbio.2011.03.003

Konya, A., Fiddler, B.A., Bunch, O., Hess, K.Z., Ferguson, C., Krzmarzick, M.J., 2023. Lead or cadmium co-contamination alters benzene and toluene degrading bacterial communities. Biodegradation 34, 357–369. https://doi.org/10.1007/s10532-023-10021-w

Korth, B., Kuchenbuch, A., Harnisch, F., 2020. Availability of Hydrogen Shapes the Microbial Abundance in Biofilm Anodes based on Geobacter Enrichment . ChemElectroChem 7. https://doi.org/10.1002/celc.202000731

Kronenberg, M., Trably, E., Bernet, N., Patureau, D., 2017. Biodegradation of polycyclic aromatic hydrocarbons: Using microbial bioelectrochemical systems to overcome an impasse. Environ. Pollut. 231, 509–523.

https://doi.org/10.1016/j.envpol.2017.08.048

Kumari, P., Bahadur, N., Cretin, M., Kong, L., O'Dell, L.A., Merenda, A., Dumée, L.F., 2021. Electro-catalytic membrane reactors for the degradation of organic pollutants-A review. React. Chem. Eng. 6, 1508–1526. https://doi.org/10.1039/d1re00091h

Kuntze, K., Vogt.C., C., Richnow, H.H., Boll, M., 2011. Combined application of PCR-based functional assays for the detection of aromatic-compound-degrading anaerobes. Appl. Environ. Microbiol. 77, 5056–5061. https://doi.org/10.1128/AEM.00335-11

Laczi, K., Erdeiné Kis, Á., Szilágyi, Á., Bounedjoum, N., Bodor, A., Vincze, G.E., Kovács, T., Rákhely, G., Perei, K., 2020. New Frontiers of Anaerobic Hydrocarbon Biodegradation in the Multi-Omics Era. Front. Microbiol. 11, 1–20. https://doi.org/10.3389/fmicb.2020.590049

Lai, A., Aulenta, F., Mingazzini, M., Palumbo, M.T., Papini, M.P., Verdini, R., Majone, M., 2017. Bioelectrochemical approach for reductive and oxidative dechlorination of chlorinated aliphatic hydrocarbons (CAHs). Chemosphere 169. https://doi.org/10.1016/j.chemosphere.2016.11.072

Laso-Pérez, R., Hahn, C., Van Vliet, D.M., Tegetmeyer, H.E., Schubotz, F., Smit, N.T., Pape, T., Sahling, H., Bohrmann, G., Boetius, A., Knittel, K., Wegenera, G., 2019. Anaerobic degradation of non-methane alkanes by "candidatus methanoliparia" in hydrocarbon seeps of the gulf of Mexico. MBio 10. https://doi.org/10.1128/mBio.01814-19

Leahy, J.G., Colwell, R.R., 1990. Microbial degradation of hydrocarbons in the environment. Microbiol. Rev. 54, 305–315. https://doi.org/10.1128/mr.54.3.305-

315.1990

Leitão, P., Rossetti, S., Nouws, H.P.A., Danko, A.S., Majone, M., Aulenta, F., 2015. Bioelectrochemically-assisted reductive dechlorination of 1,2-dichloroethane by a Dehalococcoides- enriched microbial culture. Bioresour. Technol. 195, 78–82. https://doi.org/10.1016/j.biortech.2015.06.027

Lhotský, O., Krákorová, E., Linhartová, L., Křesinová, Z., Steinová, J., Dvořák, L., Rodsand, T., Filipová, A., Kroupová, K., Wimmerová, L., Kukačka, J., Cajthaml, T., 2017. Assessment of biodegradation potential at a site contaminated by a mixture of BTEX, chlorinated pollutants and pharmaceuticals using passive sampling methods – Case study. Sci. Total Environ. 607–608, 1451–1465. https://doi.org/10.1016/j.scitotenv.2017.06.193

Li, W.W., Yu, H.Q., 2015. Electro-assisted groundwater bioremediation: Fundamentals, challenges and future perspectives. Bioresour. Technol. 196, 677–684. https://doi.org/10.1016/J.BIORTECH.2015.07.074

Li, X., Li, Yue, Zhang, X., Zhao, X., Sun, Y., Weng, L., Li, Yongtao, 2019. Long-term effect of biochar amendment on the biodegradation of petroleum hydrocarbons in soil microbial fuel cells. Sci. Total Environ. 651, 796–806. https://doi.org/10.1016/j.scitotenv.2018.09.098

Li, Y., Helmreich, B., 2014. Simultaneous removal of organic and inorganic pollutants from synthetic road runoff using a combination of activated carbon and activated lignite. Sep. Purif. Technol. 122, 6–11. https://doi.org/10.1016/j.seppur.2013.10.025

Liang, B., Wang, L.Y., Mbadinga, S.M., Liu, J.F., Yang, S.Z., Gu, J.D., Mu, B.Z., 2015. Anaerolineaceae and Methanosaeta turned to be the dominant

microorganisms in alkanes-dependent methanogenic culture after long-term of incubation. AMB Express 5. https://doi.org/10.1186/s13568-015-0117-4

Liang, B., Wang, L.Y., Zhou, Z., Mbadinga, S.M., Zhou, L., Liu, J.F., Yang, S.Z., Gu, J.D., Mu, B.Z., 2016. High frequency of thermodesulfovibrio spp. and Anaerolineaceae in association with methanoculleus spp. in a long-term incubation of n-alkanes-degrading methanogenic enrichment culture. Front. Microbiol. 7, 1–13. https://doi.org/10.3389/fmicb.2016.01431

Lin, C.W., Zhu, T.J., Lin, L.C., Liu, S.H., 2022. Promoting biodegradation of toluene and benzene in groundwater using microbial fuel cells with cathodic modification. J. Water Process Eng. 47. https://doi.org/10.1016/j.jwpe.2022.102839

Liu, F., Rotaru, A.E., Shrestha, P.M., Malvankar, N.S., Nevin, K.P., Lovley, D.R., 2015. Magnetite compensates for the lack of a pilin-associated c-type cytochrome in extracellular electron exchange. Environ. Microbiol. 17, 648–655. https://doi.org/10.1111/1462-2920.12485

Liu, Y., Climent, V., Berná, A., Feliu, J.M., 2011. Effect of Temperature on the Catalytic Ability of Electrochemically Active Biofilm as Anode Catalyst in Microbial Fuel Cells. Electroanalysis 23, 387–394. https://doi.org/10.1002/elan.201000499

Liu, Y., Ren, Y., You, S., 2022. Electrified carbon nanotube membrane technology for water treatment, Electrochemical Membrane Technology for Water and Wastewater Treatment. INC. https://doi.org/10.1016/B978-0-12-824470-8.00013-9

Locatelli, L., Binning, P.J., Sanchez-Vila, X., Søndergaard, G.L., Rosenberg, L.,

Bjerg, P.L., 2019. A simple contaminant fate and transport modelling tool for management and risk assessment of groundwater pollution from contaminated sites. J. Contam. Hydrol. 221, 35–49. https://doi.org/10.1016/j.jconhyd.2018.11.002

Löffler, C., Kuntze, K., Vazquez, J.R., Rugor, A., Kung, J.W., Böttcher, A., Boll, M., 2011. Occurrence, genes and expression of the W/Se-containing class II benzoyl-coenzyme A reductases in anaerobic bacteria. Environ. Microbiol. 13, 696–709. https://doi.org/10.1111/j.1462-2920.2010.02374.x

Löffler, F.E., Yan, J., Ritalahti, K.M., Adrian, L., Edwards, E.A., Konstantinidis, K.T., Müller, J.A., Fullerton, H., Zinder, S.H., Spormann, A.M., 2013. Dehalococcoides mccartyi gen. nov., sp. nov., obligately organohalide-respiring anaerobic bacteria relevant to halogen cycling and bioremediation, belong to a novel bacterial class, Dehalococcoidia classis nov., order Dehalococcoidales ord. nov. and famil. Int. J. Syst. Evol. Microbiol. 63. https://doi.org/10.1099/ijs.0.034926-0

Logan, B.E., 2009. Exoelectrogenic bacteria that power microbial fuel cells. Nat. Rev. Microbiol. 2009 75 7, 375–381. https://doi.org/10.1038/nrmicro2113

Logan, B.E., Hamelers, B., Rozendal, R., Schröder, U., Keller, J., Freguia, S., Aelterman, P., Verstraete, W., Rabaey, K., 2006. Microbial Fuel Cells: Methodology and Technology†. Environ. Sci. Technol. 40, 5181–5192. https://doi.org/10.1021/ES0605016

Logan, B.E., Rabaey, K., 2012. Conversion of Wastes into Bioelectricity and Chemicals by Using Microbial Electrochemical Technologies. Science (80-.). 337, 686–690.

Lovley, D.R., 2011. Live wires: Direct extracellular electron exchange for bioenergy and the bioremediation of energy-related contamination. Energy Environ. Sci. 4, 4896–4906. https://doi.org/10.1039/c1ee02229f

Lovley, D.R., 2008. Extracellular electron transfer: wires, capacitors, iron lungs, and more. Geobiology 6, 225–231. https://doi.org/10.1111/j.1472-4669.2008.00148.x

Lovley, D.R., Woodward, J.C., 1996. Lovley 1996-!!!-benzene degradation coupled to Fe(III).pdf 62, 288–291.

Lueders, T., 2017. The ecology of anaerobic degraders of BTEX hydrocarbons in aquifers. FEMS Microbiol. Ecol. 93, 1–13. https://doi.org/10.1093/femsec/fiw220

Lünsmann, V., Kappelmeyer, U., Benndorf, R., Martinez-Lavanchy, P.M., Taubert, A., Adrian, L., Duarte, M., Pieper, D.H., von Bergen, M., Müller, J.A., Heipieper, H.J., Jehmlich, N., 2016. In situprotein-SIP highlights Burkholderiaceae as key players degrading toluene by para ring hydroxylation in a constructed wetland model. Environ. Microbiol. 18, 1176–1186. https://doi.org/10.1111/1462-2920.13133

Majone, M., Verdini, R., Aulenta, F., Rossetti, S., Tandoi, V., Kalogerakis, N., Agathos, S., Puig, S., Zanaroli, G., Fava, F., 2015. In situ groundwater and sediment bioremediation: barriers and perspectives at European contaminated sites. N. Biotechnol. 32, 133–146. https://doi.org/10.1016/j.nbt.2014.02.011

Majumdar, D., 2003. The Blue Baby Syndrome 20–30.

Malik, A., Katyal, D., Narwal, N., Kataria, N., Ayyamperumal, R., Khoo, K.S.,

2023. Sources, distribution, associated health risks and remedial technologies for inorganic contamination in groundwater: A review in specific context of the state of Haryana, India. Environ. Res. 236, 116696. https://doi.org/10.1016/J.ENVRES.2023.116696

Mandke, M. V., Pathan, H.M., 2012. Electrochemical growth of copper nanoparticles: Structural and optical properties. J. Electroanal. Chem. 686. https://doi.org/10.1016/j.jelechem.2012.09.004

Markowicz, A., Płaza, G., Piotrowska-Seget, Z., 2016. Activity and functional diversity of microbial communities in long-term hydrocarbon and heavy metal contaminated soils. Arch. Environ. Prot. 42, 3–11. https://doi.org/10.1515/aep-2016-0041

Martínez-Lavanchy, P.M., Chen, Z., Lünsmann, V., Marin-Cevada, V., Vilchez-Vargas, R., Pieper, D.H., Reiche, N., Kappelmeyer, U., Imparato, V., Junca, H., Nijenhuis, I., Müller, J.A., Kuschk, P., Heipieper, H.J., 2015. Microbial toluene removal in hypoxic model constructed wetlands occurs predominantly via the ring monooxygenation pathway. Appl. Environ. Microbiol. 81, 6241–6252. https://doi.org/10.1128/AEM.01822-15

Marzocchi, U., Palma, E., Rossetti, S., Aulenta, F., Scoma, A., 2020. Parallel artificial and biological electric circuits power petroleum decontamination: The case of snorkel and cable bacteria. Water Res. 173, 115520. https://doi.org/10.1016/j.watres.2020.115520

Masut, E., Battaglia, A., Ferioli, L., Legnani, A., Viggi, C.C., Tucci, M., Resitano, M., Milani, A., de Laurentiis, C., Matturro, B., Di Franca, M.L., Rossetti, S., Aulenta, F., 2021. A microcosm treatability study for evaluating wood mulch-based amendments as electron donors for trichloroethene (Tce) reductive

dechlorination. Water (Switzerland) 13. https://doi.org/10.3390/w13141949

Mathews, S., Hans, M., Mücklich, F., Solioz, M., 2013. Contact killing of bacteria on copper is suppressed if bacterial-metal contact is prevented and is induced on iron by copper ions. Appl. Environ. Microbiol. 79. https://doi.org/10.1128/AEM.03608-12

Megharaj, M., Ramakrishnan, B., Venkateswarlu, K., Sethunathan, N., Naidu, R., 2011. Bioremediation approaches for organic pollutants: A critical perspective. Environ. Int. 37, 1362–1375. https://doi.org/10.1016/j.envint.2011.06.003

Meng, L., Yoshida, N., Li, Z., 2022. Soil microorganisms facilitated the electrode-driven trichloroethene dechlorination to ethene by Dehalococcoides species in a bioelectrochemical system. Environ. Res. 209, 112801. https://doi.org/10.1016/j.envres.2022.112801

Mineo, S., 2023. Groundwater and soil contamination by LNAPL: State of the art and future challenges. Sci. Total Environ. 874, 162394. https://doi.org/10.1016/J.SCITOTENV.2023.162394

Mitov, M.Y., Bardarov, I.O., Chorbadzhiyska, E.Y., Hubenova, Y. V., 2018. Copper recovery combined with wastewater treatment in a microbial fuel cell. Bulg. Chem. Commun. 50, 136–140.

Modin, O., Aulenta, F., 2017. Three promising applications of microbial electrochemistry for the water sector. Environ. Sci. Water Res. Technol. 3, 391–402. https://doi.org/10.1039/c6ew00325g

Modin, O., Wang, X., Wu, X., Rauch, S., Fedje, K.K., 2012. Bioelectrochemical

recovery of Cu, Pb, Cd, and Zn from dilute solutions. J. Hazard. Mater. 235–236, 291–297. https://doi.org/10.1016/j.jhazmat.2012.07.058

Morris, J.M., Jin, S., 2007. Feasibility of using microbial fuel cell technology for bioremediation of hydrocarbons in groundwater. J. Environ. Sci. Heal. Part A 43, 18–23. https://doi.org/10.1080/10934520701750389

Morris, J.M., Jin, S., Crimi, B., Pruden, A., 2009. Microbial fuel cell in enhancing anaerobic biodegradation of diesel. Chem. Eng. J. 146, 161–167. https://doi.org/10.1016/J.CEJ.2008.05.028

Motlagh, A.M., Yang, Z., Saba, H., 2020. Groundwater quality. Water Environ. Res. 92, 1649–1658. https://doi.org/10.1002/WER.1412

Naudet, V., Revil, A., Rizzo, E., Bottero, J.-Y., Bégassat, P., 2004. Groundwater redox conditions and conductivity in a contaminant plume from geoelectrical investigations. Hydrol. Earth Syst. Sci. 8, 8–22. https://doi.org/10.5194/hess-8-8-2004

Okoh, E., Yelebe, Z.R., Oruabena, B., Nelson, E.S., Indiamaowei, O.P., 2020. Clean-up of crude oil-contaminated soils: bioremediation option. Int. J. Environ. Sci. Technol. 17, 1185–1198. https://doi.org/10.1007/s13762-019-02605-y

Padhye, L.P., Srivastava, P., Jasemizad, T., Bolan, S., Hou, D., Shaheen, S.M., Rinklebe, J., O'Connor, D., Lamb, D., Wang, H., Siddique, K.H.M., Bolan, N., 2023. Contaminant containment for sustainable remediation of persistent contaminants in soil and groundwater. J. Hazard. Mater. 455. https://doi.org/10.1016/j.jhazmat.2023.131575

Pagnanelli, F., 2019. Shape evolution and effect of organic additives in the

electrosynthesis of Cu nanostructures. J. Solid State Electrochem. 23. https://doi.org/10.1007/s10008-019-04360-z

Palma, E., Daghio, M., Espinoza Tofalos, A., Franzetti, A., Cruz Viggi, C., Fazi, S., Petrangeli Papini, M., Aulenta, F., 2018. Anaerobic electrogenic oxidation of toluene in a continuous-flow bioelectrochemical reactor: Process performance, microbial community analysis, and biodegradation pathways. Environ. Sci. Water Res. Technol. 4, 2136–2145. https://doi.org/10.1039/c8ew00666k

Palma, Enza, Daghio, M., Espinoza Tofalos, A., Franzetti, A., Cruz Viggi, C., Fazi, S., Petrangeli Papini, M., Aulenta, F., 2018a. Anaerobic electrogenic oxidation of toluene in a continuous-flow bioelectrochemical reactor: Process performance, microbial community analysis, and biodegradation pathways. Environ. Sci. Water Res. Technol. 4, 2136–2145. https://doi.org/10.1039/c8ew00666k

Palma, Enza, Daghio, M., Franzetti, A., Petrangeli Papini, M., Aulenta, F., 2018b. The bioelectric well: a novel approach for in situ treatment of hydrocarbon-contaminated groundwater. Microb. Biotechnol. 11, 112–118. https://doi.org/10.1111/1751-7915.12760

Palma, Enza, Espinoza Tofalos, A., Daghio, M., Franzetti, A., Tsiota, P., Cruz Viggi, C., Papini, M.P., Aulenta, F., 2019. Bioelectrochemical treatment of groundwater containing BTEX in a continuous-flow system: Substrate interactions, microbial community analysis, and impact of sulfate as a co-contaminant. N. Biotechnol. 53, 41–48. https://doi.org/10.1016/j.nbt.2019.06.004

Palma, E., Espinoza Tofalos, A., Daghio, M., Franzetti, A., Tsiota, P., Cruz Viggi, C., Papini, M.P., Aulenta, F., 2019. Bioelectrochemical treatment of

groundwater containing BTEX in a continuous-flow system: Substrate interactions, microbial community analysis, and impact of sulfate as a co-contaminant. N. Biotechnol. 53, 41–48. https://doi.org/10.1016/j.nbt.2019.06.004

Panagos, P., Van Liedekerke, M., Yigini, Y., Montanarella, L., 2013. Contaminated sites in Europe: Review of the current situation based on data collected through a European network. J. Environ. Public Health 2013. https://doi.org/10.1155/2013/158764

Patel, A.B., Shaikh, S., Jain, K.R., Desai, C., Madamwar, D., 2020. Polycyclic Aromatic Hydrocarbons: Sources, Toxicity, and Remediation Approaches. Front. Microbiol. 11, 562813. https://doi.org/10.3389/FMICB.2020.562813/BIBTEX

Patil, S.A., Hägerhäll, C., Gorton, L., 2012. Electron transfer mechanisms between microorganisms and electrodes in bioelectrochemical systems. Bioanal. Rev. 4, 159–192. https://doi.org/10.1007/s12566-012-0033-x

Payá Pérez, A., Rodríguez Eugenio, N., 2018. Status of local soil contamination in Europe – Revision of the indicator 'Progress in the management contaminated sites in Europe'. Publications Office. https://doi.org/doi/10.2760/093804

Pedersen, D.B., Wang, S., Liang, S.H., 2008. Charge-transfer-driven diffusion processes in Cu@Cu-oxide core-shell nanoparticles: Oxidation of 3.0 ± 0.3 nm diameter copper nanoparticles. J. Phys. Chem. C 112. https://doi.org/10.1021/jp710619r

Phung, N.T., Lee, J., Kang, K.H., Chang, I.S., Gadd, G.M., Kim, B.H., 2004.

Analysis of microbial diversity in oligotrophic microbial fuel cells using 16S rDNA sequences. FEMS Microbiol. Lett. 233, 77–82. https://doi.org/10.1016/j.femsle.2004.01.041

Pollice, A., Rozzi, A., Tomei, M.C., Di Pinto, A.C., Laera, G., 2001. Inhibiting effects of chloroform on anaerobic microbial consortia as monitored by the Rantox biosensor. Water Res. 35, 1179–1190. https://doi.org/10.1016/S0043-1354(00)00359-6

Polti, M.A., Aparicio, J.D., Benimeli, C.S., Amoroso, M.J., 2014. Simultaneous bioremediation of Cr(VI) and lindane in soil by actinobacteria. Int. Biodeterior. Biodegrad. 88, 48–55. https://doi.org/10.1016/j.ibiod.2013.12.004

Pous, N., Puig, S., Dolors Balaguer, M., Colprim, J., 2015. Cathode potential and anode electron donor evaluation for a suitable treatment of nitrate-contaminated groundwater in bioelectrochemical systems. Chem. Eng. J. 263, 151–159. https://doi.org/10.1016/j.cej.2014.11.002

Pradhan, B., Chand, Sujata, Chand, Sasmita, Rout, P.R., Naik, S.K., 2023. Emerging groundwater contaminants: A comprehensive review on their health hazards and remediation technologies. Groundw. Sustain. Dev. 20, 100868. https://doi.org/10.1016/J.GSD.2022.100868

Puggioni, G., Milia, S., Unali, V., Ardu, R., Tamburini, E., Balaguer, M.D., Pous, N., Carucci, A., Puig, S., 2022. Effect of hydraulic retention time on the electro-bioremediation of nitrate in saline groundwater. Sci. Total Environ. 845, 157236. https://doi.org/10.1016/J.SCITOTENV.2022.157236

Puig, S., Coma, M., Desloover, J., Boon, N., Colprim, J., Balaguer, M.D., 2012. Autotrophic denitrification in microbial fuel cells treating low ionic strength

waters. Environ. Sci. Technol. 46, 2309–2315. https://doi.org/10.1021/es2030609

Puig, S., Jourdin, L., Kalathil, S., 2021. Editorial: Microbial Electrogenesis, Microbial Electrosynthesis, and Electro-bioremediation. Front. Microbiol. 12, 1–2. https://doi.org/10.3389/fmicb.2021.742479

Rabaey, K., Angenent, L., Schröder, U., Keller, J., 2009. Bioelectrochemical Systems: From Extracellular Electron Transfer to Biotechnological Application. Water Intell. Online 8. https://doi.org/10.2166/9781780401621

Rabaey, K., Boon, N., Höfte, M., Verstraete, W., 2005. Microbial phenazine production enhances electron transfer in biofuel cells. Environ. Sci. Technol. 39, 3401–3408. https://doi.org/10.1021/es048563o

Rabaey, K., Boon, N., Siciliano, S.D., Verhaege, M., Verstraete, W., 2004. Biofuel cells select for microbial consortia that self-mediate electron transfer. Appl. Environ. Microbiol. 70, 5373–5382. https://doi.org/10.1128/AEM.70.9.5373-5382.2004

Rabus, R., Boll, M., Heider, J., Meckenstock, R.U., Buckel, W., Einsle, O., Ermler, U., Golding, B.T., Gunsalus, R.P., Kroneck, P.M.H., Krüger, M., Lueders, T., Martins, B.M., Musat, F., Richnow, H.H., Schink, B., Seifert, J., Szaleniec, M., Treude, T., Ullmann, G.M., Vogt, C., von Bergen, M., Wilkes, H., 2016. Anaerobic Microbial Degradation of Hydrocarbons: From Enzymatic Reactions to the Environment. J. Mol. Microbiol. Biotechnol. 26, 5–28. https://doi.org/10.1159/000443997

Rakoczy, J., Feisthauer, S., Wasmund, K., Bombach, P., Neu, T.R., Vogt, C., Richnow, H.H., 2013. Benzene and sulfide removal from groundwater treated in

a microbial fuel cell. Biotechnol. Bioeng. 110, 3104–3113. https://doi.org/10.1002/BIT.24979

Rashed, A.O., Huynh, C., Merenda, A., Qin, S., Maghe, M., Kong, L., Kondo, T., Dumée, L.F., Razal, J.M., 2023a. Carbon nanofibre microfiltration membranes tailored by oxygen plasma for electrocatalytic wastewater treatment in cross-flow reactors. J. Memb. Sci. 673. https://doi.org/10.1016/j.memsci.2023.121475

Rashed, A.O., Huynh, C., Merenda, A., Qin, S., Maghe, M., Kong, L., Kondo, T., Razal, J.M., Dumée, L.F., 2023b. Electrocatalytic ultrafiltration membrane reactors designed from dry-spun self-standing carbon nanotube sheets. Chem. Eng. J. 458. https://doi.org/10.1016/j.cej.2023.141517

Ravindiran, G., Rajamanickam, S., Sivarethinamohan, S., Sathaiah, B.K., Ravindran, G., Muniasamy, S.K., Hayder, G., 2023. A Review of the Status, Effects, Prevention, and Remediation of Groundwater Contamination for Sustainable Environment. Water 2023, Vol. 15, Page 3662 15, 3662. https://doi.org/10.3390/W15203662

Reddy, V.R., Behera, B., 2006. Impact of water pollution on rural communities: An economic analysis. Ecol. Econ. 58, 520–537. https://doi.org/10.1016/j.ecolecon.2005.07.025

Resitano, M., Tucci, M., Mezzi, A., Kaciulis, S., Matturro, B., D'Ugo, E., Bertuccini, L., Fazi, S., Rossetti, S., Aulenta, F., Viggi, C.C., 2024. Anaerobic treatment of groundwater co-contaminated by toluene and copper in a single chamber bioelectrochemical system. Bioelectrochemistry 158, 108711. https://doi.org/10.1016/J.BIOELECHEM.2024.108711

Riedl, S., Brown, R.., Alvarez Esquivel, D.., Wichmann, H., Huber, K.., Bunk, B.,

Overmann, J., Schröder, U., 2019. Cultivating Electrochemically Active Biofilms at Continuously Changing Electrode Potentials. ChemElectroChem 6, 2238–2247. https://doi.org/10.1002/celc.201900036

Ritalahti, K.M., Amos, B.K., Sung, Y., Wu, Q., Koenigsberg, S.S., Löffler, F.E., 2006. Quantitative PCR Targeting 16S rRNA and Reductive Dehalogenase Genes Simultaneously Monitors Multiple Dehalococcoides Strains. Appl. Environ. Microbiol. 72, 2765–2774. https://doi.org/10.1128/AEM.72.4.2765-2774.2006

Rivett, M.O., Wealthall, G.P., Dearden, R.A., McAlary, T.A., 2011. Review of unsaturated-zone transport and attenuation of volatile organic compound (VOC) plumes leached from shallow source zones. J. Contam. Hydrol. 123, 130–156. https://doi.org/10.1016/j.jconhyd.2010.12.013

Rosales-Sierra, A., Rosales-Mendoza, S., Monreal-Escalante, E., Celis, L.B., Razo-Flores, E., Cercado, B., 2017. Acclimation Strategy Using Complex Volatile Fatty Acid Mixtures Increases the Microbial Fuel Cell (MFC) Potential. ChemistrySelect 2, 6277–6285. https://doi.org/10.1002/slct.201701267

Rossmassler, K., Snow, C.D., Taggart, D., Brown, C., De Long, S.K., 2019. Advancing biomarkers for anaerobic o-xylene biodegradation via metagenomic analysis of a methanogenic consortium. Appl. Microbiol. Biotechnol. 103, 4177–4192. https://doi.org/10.1007/s00253-019-09762-7

Roustazadeh Sheikhyousefi, P., Nasr Esfahany, M., Colombo, A., Franzetti, A., Trasatti, S.P., Cristiani, P., 2017. Investigation of different configurations of microbial fuel cells for the treatment of oilfield produced water. Appl. Energy 192, 457–465. https://doi.org/10.1016/j.apenergy.2016.10.057

Rozendal, R.A., Hamelers, H.V.M., Euverink, G.J.W., Metz, S.J., Buisman, C.J.N., 2006. Principle and perspectives of hydrogen production through biocatalyzed electrolysis. Int. J. Hydrogen Energy 31, 1632–1640. https://doi.org/10.1016/j.ijhydene.2005.12.006

Sadañoski, M.A., Tatarin, A.S., Barchuk, M.L., Gonzalez, M., Pegoraro, C.N., Fonseca, M.I., Levin, L.N., Villalba, L.L., 2020. Evaluation of bioremediation strategies for treating recalcitrant halo-organic pollutants in soil environments. Ecotoxicol. Environ. Saf. 202, 110929. https://doi.org/10.1016/j.ecoenv.2020.110929

Sadia, M., Kunz, M., ter Laak, T., Jonge, M. De, Schriks, M., van Wezel, A.P., 2023. Forever legacies? Profiling historical PFAS contamination and current influence on groundwater used for drinking water. Sci. Total Environ. 890, 164420. https://doi.org/10.1016/J.SCITOTENV.2023.164420

Sander, R., 2015. Compilation of Henry's law constants (version 4.0) for water as solvent. Atmos. Chem. Phys. 15, 4399–4981. https://doi.org/10.5194/acp-15-4399-2015

Sarkar, J., Kazy, S.K., Gupta, A., Dutta, A., Mohapatra, B., Roy, A., Bera, P., Mitra, A., Sar, P., 2016. Biostimulation of indigenous microbial community for bioremediation of petroleum refinery sludge. Front. Microbiol. 7, 1–20. https://doi.org/10.3389/fmicb.2016.01407

Sasaki, K., Morita, M., Sasaki, D., Hirano, S. ichi, Matsumoto, N., Ohmura, N., Igarashi, Y., 2011. Methanogenic communities on the electrodes of bioelectrochemical reactors without membranes. J. Biosci. Bioeng. 111, 47–49. https://doi.org/10.1016/j.jbiosc.2010.08.010

Saxena, G., Thakur, I.S., Kumar, V., Shah, M.P., 2020. Electrobioremediation of Contaminants: Concepts, Mechanisms, Applications and Challenges. Comb. Appl. Physico-Chemical Microbiol. Process. Ind. Effl. Treat. Plant 291–313. https://doi.org/10.1007/978-981-15-0497-6_14/TABLES/2

Scarabotti, F., Rago, L., Bühler, K., Harnisch, F., 2021. The electrode potential determines the yield coefficients of early-stage Geobacter sulfurreducens biofilm anodes. Bioelectrochemistry 140, 107752. https://doi.org/10.1016/j.bioelechem.2021.107752

Siegert, M., Li, X.F., Yates, M.D., Logan, B.E., 2014. The presence of hydrogenotrophic methanogens in the inoculum improves methane gas production in microbial electrolysis cells. Front. Microbiol. 5, 1–12. https://doi.org/10.3389/fmicb.2014.00778

Singha, L.P., Pandey, P., 2020. Rhizobacterial community of Jatropha curcas associated with pyrene biodegradation by consortium of PAH-degrading bacteria. Appl. Soil Ecol. 155. https://doi.org/10.1016/j.apsoil.2020.103685

Sinha, D., Prasad, P., 2020. Health effects inflicted by chronic low-level arsenic contamination in groundwater: A global public health challenge. J. Appl. Toxicol. 40, 87–131. https://doi.org/10.1002/JAT.3823

Soder-Walz, J.M., Torrentó, C., Algora, C., Wasmund, K., Cortés, P., Soler, A., Vicent, T., Rosell, M., Marco-Urrea, E., 2022. Trichloromethane dechlorination by a novel Dehalobacter sp. strain 8M reveals a third contrasting C and Cl isotope fractionation pattern within this genus. Sci. Total Environ. 813. https://doi.org/10.1016/j.scitotenv.2021.152659

Sonone, S.S., Jadhav, S., Sankhla, M.S., Kumar, R., 2021. Water

Contamination by Heavy Metals and their Toxic Effect on Aquaculture and Human Health through Food Chain. Lett. Appl. NanoBioScience 10, 2148–2166. https://doi.org/10.33263/LIANBS102.21482166

Stams, A.J.M., Plugge, C.M., 2009. Electron transfer in syntrophic communities of anaerobic bacteria and archaea. Nat. Rev. Microbiol. 2009 78 7, 568–577. https://doi.org/10.1038/nrmicro2166

Suarez, M.P., Rifai, H.S., 2002. Evaluation of BTEX Remediation by Natural Attenuation at a Coastal Facility. Gr. Water Monit. Remediat. 22, 62–77.

Sui, Y., Fu, W., Yang, H., Zeng, Y., Zhang, Y., Zhao, Q., Li, Y., Zhou, X., Leng, Y., Li, M., Zou, G., 2010. Low temperature synthesis of Cu2O crystals: Shape evolution and growth mechanism. Cryst. Growth Des. 10, 99–108. https://doi.org/10.1021/cg900437x

Summers, Z.M., Fogarty, H.E., Leang, C., Franks, A.E., Malvankar, N.S., Lovley, D.R., 2010. Direct exchange of electrons within aggregates of an evolved syntrophic coculture of anaerobic bacteria. Science (80-.). 330, 1413–1415. https://doi.org/10.1126/SCIENCE.1196526/SUPPL_FILE/SUMMERS.SOM.PDF

Sun, M., Wang, X., Winter, L.R., Zhao, Y., Ma, W., Hedtke, T., Kim, J.H., Elimelech, M., 2021. Electrified Membranes for Water Treatment Applications. ACS ES T Eng. 1, 725–752. https://doi.org/10.1021/acsestengg.1c00015

Szydlowski, L., Ehlich, J., Szczerbiak, P., Shibata, N., Goryanin, I., 2022. Novel species identification and deep functional annotation of electrogenic biofilms, selectively enriched in a microbial fuel cell array. Front. Microbiol. 13. https://doi.org/10.3389/fmicb.2022.951044

Táncsics, A., Farkas, M., Horváth, B., Maróti, G., Bradford, L.M., Lueders, T., Kriszt, B., 2020. Genome analysis provides insights into microaerobic toluene-degradation pathway of Zoogloea oleivorans BucT. Arch. Microbiol. 202, 421–426. https://doi.org/10.1007/s00203-019-01743-8

Táncsics, A., Szalay, A.R., Farkas, M., Benedek, T., Szoboszlay, S., Szabó, I., Lueders, T., 2018. Stable isotope probing of hypoxic toluene degradation at the Siklós aquifer reveals prominent role of Rhodocyclaceae. FEMS Microbiol. Ecol. 94, 1–11. https://doi.org/10.1093/femsec/fiy088

Tang, J., Wang, M., Wang, F., Sun, Q., Zhou, Q., 2011. Eco-toxicity of petroleum hydrocarbon contaminated soil. J. Environ. Sci. 23, 845–851. https://doi.org/10.1016/S1001-0742(10)60517-7

Tang, S., Edwards, E.A., 2013. Identification of Dehalobacter reductive dehalogenases that catalyse dechlorination of chloroform, 1,1,1- trichloroethane and 1,1-dichloroethane. Philos. Trans. R. Soc. B Biol. Sci. 368. https://doi.org/10.1098/rstb.2012.0318

Teng, Y., Wang, X., Li, L., Li, Z., Luo, Y., 2015. Rhizobia and their bio-partners as novel drivers for functional remediation in contaminated soils. Front. Plant Sci. https://doi.org/10.3389/fpls.2015.00032

Thakur, I.S., Medhi, K., 2019. Nitrification and denitrification processes for mitigation of nitrous oxide from waste water treatment plants for biovalorization: Challenges and opportunities. Bioresour. Technol. 282, 502–513. https://doi.org/10.1016/j.biortech.2019.03.069

Toth, C.R.A., Luo, F., Bawa, N., Webb, J., Guo, S., Dworatzek, S., Edwards, E.A., 2021. Anaerobic benzene biodegradation linked to the growth of highly

specific bacterial clades. Environ. Sci. Technol. 55, 7970–7980. https://doi.org/10.1021/acs.est.1c00508

Trueba-Santiso, A., Fernández-Verdejo, D., Marco-Rius, I., Soder-Walz, J.M., Casabella, O., Vicent, T., Marco-Urrea, E., 2020. Interspecies interaction and effect of co-contaminants in an anaerobic dichloromethane-degrading culture. Chemosphere 240. https://doi.org/10.1016/j.chemosphere.2019.124877

Trueba-Santiso, A., Parladé, E., Rosell, M., Lliros, M., Mortan, S.H., Martínez-Alonso, M., Gaju, N., Martín-González, L., Vicent, T., Marco-Urrea, E., 2017. Molecular and carbon isotopic characterization of an anaerobic stable enrichment culture containing Dehalobacterium sp. during dichloromethane fermentation. Sci. Total Environ. 581–582, 640–648. https://doi.org/10.1016/j.scitotenv.2016.12.174

Tucci, M., Carolina, C.V., Resitano, M., Matturro, B., Crognale, S., Pietrini, I., Rossetti, S., Harnisch, F., Aulenta, F., 2021. Simultaneous removal of hydrocarbons and sulfate from groundwater using a “bioelectric well”. Electrochim. Acta 388, 138636. https://doi.org/10.1016/j.electacta.2021.138636

Tucci, M., Fernández-Verdejo, D., Resitano, M., Ciacia, P., Guisasola, A., Blánquez, P., Marco-Urrea, E., Viggi, C.C., Matturro, B., Crognale, S., Aulenta, F., 2023. Toluene-driven anaerobic biodegradation of chloroform in a continuous-flow bioelectrochemical reactor. Chemosphere 338, 139467. https://doi.org/10.1016/J.CHEMOSPHERE.2023.139467

Tucci, M., Milani, A., Resitano, M., Viggi, C.C., Giampaoli, O., Miccheli, A., Crognale, S., Matturro, B., Rossetti, S., Harnisch, F., Aulenta, F., 2022. Syntrophy drives the microbial electrochemical oxidation of toluene in a continuous-flow ‘bioelectric well’. J. Environ. Chem. Eng. 10, 107799.

https://doi.org/10.1016/j.jece.2022.107799

Tuxen, N., Reitzel, L.A., Albrechtsen, H.J., Bjerg, P.L., 2006. Oxygen-enhanced biodegradation of phenoxy acids in ground water at contaminated sites. Ground Water 44, 256–265. https://doi.org/10.1111/j.1745-6584.2005.00104.x

Tyagi, M., da Fonseca, M.M.R., de Carvalho, C.C.C.R., 2011. Bioaugmentation and biostimulation strategies to improve the effectiveness of bioremediation processes. Biodegradation 22, 231–241. https://doi.org/10.1007/s10532-010-9394-4

Ucar, D., Zhang, Y., Angelidaki, I., 2017. An overview of electron acceptors in microbial fuel cells. Front. Microbiol. 8, 248548. https://doi.org/10.3389/FMICB.2017.00643/BIBTEX

Vaiopoulou, E., Melidis, P., Aivasidis, A., 2005. Sulfide removal in wastewater from petrochemical industries by autotrophic denitrification. Water Res. 39, 4101–4109. https://doi.org/10.1016/j.watres.2005.07.022

Van Eerten-Jansen, M.C.A.A., Veldhoen, A.B., Plugge, C.M., Stams, A.J.M., Buisman, C.J.N., Ter Heijne, A., 2013. Microbial community analysis of a methane-producing biocathode in a bioelectrochemical system. Archaea 2013. https://doi.org/10.1155/2013/481784

Verdini, R., Aulenta, F., De Tora, F., Lai, A., Majone, M., 2015. Relative contribution of set cathode potential and external mass transport on TCE dechlorination in a continuous-flow bioelectrochemical reactor. Chemosphere 136. https://doi.org/10.1016/j.chemosphere.2015.03.092

Viggi, C.C., Rossetti, S., Fazi, S., Paiano, P., Majone, M., Aulenta, F., 2014.

Magnetite particles triggering a faster and more robust syntrophic pathway of methanogenic propionate degradation. Environ. Sci. Technol. 48, 7536–7543. https://doi.org/10.1021/ES5016789/SUPPL_FILE/ES5016789_SI_001.PDF

Villano, M., Monaco, G., Aulenta, F., Majone, M., 2011. Electrochemically assisted methane production in a biofilm reactor. J. Power Sources 196, 9467–9472. https://doi.org/10.1016/j.jpowsour.2011.07.016

Vogt, C., Dorer, C., Musat, F., Richnow, H.-H., 2016. Multi-element isotope fractionation concepts to characterize the biodegradation of hydrocarbons — from enzymes to the environment. Curr. Opin. Biotechnol. 41, 90–98. https://doi.org/10.1016/j.copbio.2016.04.027

Von Netzer, F., Kuntze, K., Vogt, C., Richnow, H.H., Boll, M., Lueders, T., 2016. Functional gene markers for fumarate-adding and dearomatizing key enzymes in anaerobic aromatic hydrocarbon degradation in terrestrial environments. J. Mol. Microbiol. Biotechnol. 26, 180–194. https://doi.org/10.1159/000441946

Wagner, R.C., Call, D.F., Logan, B.E., 2010. Optimal set anode potentials vary in bioelectrochemical systems. Environ. Sci. Technol. 44, 6036–6041. https://doi.org/10.1021/es101013e

Wang, H., Luo, H., Fallgren, P.H., Jin, S., Ren, Z.J., 2015. Bioelectrochemical system platform for sustainable environmental remediation and energy generation. Biotechnol. Adv. 33, 317–334. https://doi.org/10.1016/j.biotechadv.2015.04.003

Wang, H., Ren, Z.J., 2014. Bioelectrochemical metal recovery from wastewater: A review. Water Res. 66, 219–232. https://doi.org/10.1016/j.watres.2014.08.013

Wang, S., Adekunle, A., Raghavan, V., 2022. Bioelectrochemical systems-based metal removal and recovery from wastewater and polluted soil: Key factors, development, and perspective. J. Environ. Manage. 317, 115333. https://doi.org/10.1016/j.jenvman.2022.115333

Wang, X., Aulenta, F., Puig, S., Esteve-Núñez, A., He, Y., Mu, Y., Rabaey, K., 2020. Microbial electrochemistry for bioremediation. Environ. Sci. Ecotechnology 1, 100013. https://doi.org/10.1016/J.ESE.2020.100013

Wang, Y., Li, M., Gu, Y., Zhang, X., Wang, S., Li, Q., Zhang, Z., 2015. Tuning carbon nanotube assembly for flexible, strong and conductive films. Nanoscale 7, 3060–3066. https://doi.org/10.1039/c4nr06401a

Wartell, B., Boufadel, M., Rodriguez-Freire, L., 2021. An effort to understand and improve the anaerobic biodegradation of petroleum hydrocarbons: A literature review. Int. Biodeterior. Biodegrad. 157, 105156. https://doi.org/10.1016/j.ibiod.2020.105156

Weelink, S.A.B., Tan, N.C.G., Ten Broeke, H., Van Doesburg, W., Langenhoff, A.A.M., Gerritse, J., Stams, A.J.M., 2007. Physiological and phylogenetic characterization of a stable benzene-degrading, chlorate-reducing microbial community. FEMS Microbiol. Ecol. 60, 312–321. https://doi.org/10.1111/j.1574-6941.2007.00289.x

Weelink, S.A.B., van Eekert, M.H.A., Stams, A.J.M., 2010. Degradation of BTEX by anaerobic bacteria: physiology and application. Rev. Environ. Sci. Bio/Technology 2010 94 9, 359–385. https://doi.org/10.1007/S11157-010-9219-2

WHO, UNICEF, 2021. Progress on household drinking water, sanitation and

hygiene 2000-2020: five years into the SDGs, Joint Water Supply, & Sanitation Monitoring Programme.

Winderl, C., Schaefer, S., Lueders, T., 2007. Detection of anaerobic toluene and hydrocarbon degraders in contaminated aquifers using benzylsuccinate synthase (bssA) genes as a functional marker. Environ. Microbiol. 9, 1035–1046. https://doi.org/10.1111/j.1462-2920.2006.01230.x

Wu, M., Li, W., Dick, W.A., Ye, X., Chen, K., Kost, D., Chen, L., 2017. Bioremediation of hydrocarbon degradation in a petroleum-contaminated soil and microbial population and activity determination. Chemosphere 169, 124–130. https://doi.org/10.1016/j.chemosphere.2016.11.059

Xiao, Y., Zheng, Y., Wu, S., Zhang, E.H., Chen, Z., Liang, P., Huang, X., Yang, Z.H., Ng, I.S., Chen, B.Y., Zhao, F., 2015. Pyrosequencing reveals a core community of anodic bacterial biofilms in bioelectrochemical systems from China. Front. Microbiol. 6, 1–12. https://doi.org/10.3389/fmicb.2015.01410

Xie, M., Zhang, X., Jing, Y., Du, X., Zhang, Z., Tan, C., 2024. Review on Research and Application of Enhanced In-Situ Bioremediation Agents for Organic Pollution Remediation in Groundwater. Water (Switzerland) 16. https://doi.org/10.3390/W16030456

Xu, H., Wang, C., Yan, K., Wu, J., Zuo, J., Wang, K., 2016. Anaerobic granule-based biofilms formation reduces propionate accumulation under high H2 partial pressure using conductive carbon felt particles. Bioresour. Technol. 216, 677–683. https://doi.org/10.1016/j.biortech.2016.06.010

Xu, J., Yu, K., Zhu, Z., 2010. Synthesis and field emission properties of Cu dendritic nanostructures. Phys. E Low-Dimensional Syst. Nanostructures 42,

1451–1455. https://doi.org/10.1016/j.physe.2009.11.115

Ya, V., Martin, N., Chou, Y.H., Chen, Y.M., Choo, K.H., Chen, S.S., Li, C.W., 2018. Electrochemical treatment for simultaneous removal of heavy metals and organics from surface finishing wastewater using sacrificial iron anode. J. Taiwan Inst. Chem. Eng. 83, 107–114. https://doi.org/10.1016/j.jtice.2017.12.004

Yamamoto, S., Kasai, T., Matsumoto, M., Nishizawa, T., Arito, H., Nagano, K., Matsushima, T., 2002. Carcinogenicity and chronic toxicity in rats and mice exposed to chloroform by inhalation. J. Occup. Health 44, 283–293. https://doi.org/10.1539/joh.44.283

Yang, G., Tang, L., Zeng, G., Cai, Y., Tang, J., Pang, Y., Zhou, Y., Liu, Y., Wang, J., Zhang, S., Xiong, W., 2015. Simultaneous removal of lead and phenol contamination from water by nitrogen-functionalized magnetic ordered mesoporous carbon. Chem. Eng. J. 259, 854–864. https://doi.org/10.1016/j.cej.2014.08.081

Yang, K., Ji, M., Liang, B., Zhao, Y., Zhai, S., Ma, Z., Yang, Z., 2020. Bioelectrochemical degradation of monoaromatic compounds: Current advances and challenges. J. Hazard. Mater. 398, 122892. https://doi.org/10.1016/j.jhazmat.2020.122892

Yang, L.H., Cheng, H.Y., Zhu, T.T., Wang, H.C., Haider, M.R., Wang, A.J., 2021. Resorcinol as a highly efficient aromatic electron donor in bioelectrochemical system. J. Hazard. Mater. 408. https://doi.org/10.1016/j.jhazmat.2020.124416

Yang, S., Wen, X., Zhao, L., Shi, Y., Jin, H., 2014. Crude oil treatment leads to

shift of bacterial communities in soils from the deep active layer and upper permafrost along the China-Russia Crude Oil Pipeline route. PLoS One 9, 12–14. https://doi.org/10.1371/journal.pone.0096552

Yang, Y., McCarty, P.L., 2000. Biomass, oleate, and other possible substrates for chloroethene reductive dehalogenation. Bioremediat. J. 4, 125–133. https://doi.org/10.1080/10889860091114185

Yasri, N.G., Gunasekaran, S., 2017. Electrochemical Technologies for Environmental Remediation, in: Anjum, N.A., Gill, S.S., Tuteja, N. (Eds.), Enhancing Cleanup of Environmental Pollutants: Volume 2: Non-Biological Approaches. Springer International Publishing, Cham, pp. 5–73. https://doi.org/10.1007/978-3-319-55423-5_2

Yeshchenko, O.A., Dmitruk, I.M., Dmytruk, A.M., Alexeenko, A.A., 2007. Influence of annealing conditions on size and optical properties of copper nanoparticles embedded in silica matrix. Mater. Sci. Eng. B 137. https://doi.org/10.1016/j.mseb.2006.11.030

You, X., Liu, S., Dai, C., Guo, Y., Zhong, G., Duan, Y., 2020. Contaminant occurrence and migration between high- and low-permeability zones in groundwater systems: A review. Sci. Total Environ. 743, 140703. https://doi.org/10.1016/j.scitotenv.2020.140703

Yu, B., Tian, J., Feng, L., 2017. Remediation of PAH polluted soils using a soil microbial fuel cell: Influence of electrode interval and role of microbial community. J. Hazard. Mater. 336, 110–118. https://doi.org/10.1016/J.JHAZMAT.2017.04.066

Yu, Z., Smith, G.B., 2000. Inhibition of methanogenesis by C1- and C2-

polychlorinated aliphatic hydrocarbons. Environ. Toxicol. Chem. 19, 2212–2217. https://doi.org/10.1002/etc.5620190910

Yuan, Y., Zhou, S., Zhuang, L., 2010. A new approach to in situ sediment remediation based on air-cathode microbial fuel cells. J. Soils Sediments 10, 1427–1433. https://doi.org/10.1007/s11368-010-0276-5

Zanello, V., Scherger, L.E., Lexow, C., 2021. Assessment of groundwater contamination risk by BTEX from residual fuel soil phase. SN Appl. Sci. 3. https://doi.org/10.1007/s42452-021-04325-w

Zeikus, J.G., 1977. The biology of methanogenic bacteria. Bacteriol. Rev. 41, 514–541. https://doi.org/10.1128/MMBR.41.2.514-541.1977

Zhang, S., Leonhardt, B.E., Nguyen, N., Oluwalowo, A., Jolowsky, C., Hao, A., Liang, R., Park, J.G., 2018. Roll-to-roll continuous carbon nanotube sheets with high electrical conductivity. RSC Adv. 8, 12692–12700. https://doi.org/10.1039/c8ra01212a

Zhang, T., Gannon, S.M., Nevin, K.P., Franks, A.E., Lovley, D.R., 2010. Stimulating the anaerobic degradation of aromatic hydrocarbons in contaminated sediments by providing an electrode as the electron acceptor. Environ. Microbiol. 12, 1011–1020. https://doi.org/10.1111/J.1462-2920.2009.02145.X

Zhang, T., Tremblay, P.L., Chaurasia, A.K., Smith, J.A., Bain, T.S., Lovley, D.R., 2013. Anaerobic benzene oxidation via phenol in Geobacter metallireducens. Appl. Environ. Microbiol. 79, 7800–7806. https://doi.org/10.1128/AEM.03134-13

Zhang, X., Li, B., Wang, H., Sui, X., Ma, X., Hong, Q., Jiang, R., 2012. Rhizobium petrolearium sp. nov., isolated from oilcontaminated soil. Int. J. Syst. Evol. Microbiol. 62. https://doi.org/10.1099/ijs.0.026880-0

Zhang, Z., Li, J., Hao, X., Gu, Z., Xia, S., 2019. Electron donation characteristics and interplays of major volatile fatty acids from anaerobically fermented organic matters in bioelectrochemical systems. Environ. Technol. (United Kingdom) 40, 2337–2344. https://doi.org/10.1080/09593330.2018.1441334

Zhou, G.J., Ying, G.G., Liu, S., Zhou, L.J., Chen, Z.F., Peng, F.Q., 2014. Simultaneous removal of inorganic and organic compounds in wastewater by freshwater green microalgae. Environ. Sci. Process. Impacts 16, 2018–2027. https://doi.org/10.1039/c4em00094c

Zhu, K., Xu, Y., Yang, X., Fu, W., Dang, W., Yuan, J., Wang, Z., 2022. Sludge Derived Carbon Modified Anode in Microbial Fuel Cell for Performance Improvement and Microbial Community Dynamics. Membranes (Basel). 12. https://doi.org/10.3390/membranes12020120